Master's thesis

NTNU
Norwegian University of Science and Technology
Faculty of Information Technology and Electrical Engineering
Department of Electric Power Engineering

Rikke Enger Dihle
Marie Bakken

Flexibility in Solar and Battery Off-Grid Systems - Case Study Eco Moyo Education Centre in Kenya

Master's thesis in Energy and Environmental Engineering
Supervisor: Ida Fuchs
Co-supervisor: Jayaprakash Rajasekharan
June 2023

NTNU
Norwegian University of Science and Technology

Solar Energy Without Borders
Solenergi Uten Grenser

Rikke Enger Dihle
Marie Bakken

Flexibility in Solar and Battery Off-Grid Systems - Case Study Eco Moyo Education Centre in Kenya

Master's thesis in Energy and Environmental Engineering
Supervisor: Ida Fuchs
Co-supervisor: Jayaprakash Rajasekharan
June 2023

Norwegian University of Science and Technology
Faculty of Information Technology and Electrical Engineering
Department of Electric Power Engineering

NTNU
Norwegian University of
Science and Technology

Preface

This master's thesis is a conclusion of our Master in Science (MSc) in Energy and Environmental Engineering at the Department of Electric Energy at the Norwegian University of Science and Technology (NTNU).

We want to express our gratitude to the Department of Electric Energy for funding our field trips to Eco Moyo Education Centre. We also want to thank Solar Energy Without Borders for providing us with financial support for the field trip this spring. The field trips offered us valuable insights, learning opportunities, and input data for the thesis. Additionally, we would like to express our gratitude to our supervisor, Ida Fuchs, for her invaluable guidance and input throughout the entire semester. Further, we want to thank our co-supervisor, Jayaprakash Rajasekharan, for providing us with helpful feedback. We also want to thank the teachers at Eco Moyo for arranging meetings and helping us with our data acquisition. Further, we want to thank the entire staff and pupils for sharing their daily experiences with us. Your insights have been truly valuable.

Finally, we would like to thank all our friends and family for their support. Especially our fellow students. The past five years would not have been the same without EMIL'18.

Trondheim, June 2023

Marie Bakken

Rikke Enger Dihle

Abstract

Accelerating rural electrification is crucial to achieve Sustainable Development Goal (SDG) number 7 by 2030. While progress has been made in reducing the number of people without electricity, the COVID-19 pandemic and increased costs pose challenges. Kenya has made significant progress toward universal energy access, but rural areas still lag behind. Eco Moyo Education Centre is a Norwegian/Kenyan charity project offering free primary education to underprivileged children in the Dzunguni village in Kenya. The school has an off-grid solar and battery microgrid to supply basic electricity needs in the Staff Room. This thesis is based on a case study of the existing system at the school, with data collected during field trips in November 2022 and April/May 2023. The thesis addresses the expressed need of the school to provide electricity to additional buildings and focuses on how flexible operation of the loads can be used to extend the system.

The case study of Eco Moyo Education Centre highlights the potential of flexible solar and battery off-grid systems to optimize energy supply in rural areas. These systems are often based on unreliable Renewable Energy Sources (RESs), such as solar power, and Battery Energy Storage Systems (BESSs) are typically used to compensate for periods with limited power generation. Hence, user behavior patterns are the primary tool to increase flexibility in off-grid systems. The main objectives of the master's thesis are to develop an optimization model for scheduling flexible loads and a user-friendly early-stage Graphical User Interface (GUI) draft for end user communication. By minimizing the disutility cost of shifting loads, the potential of Demand Response (DR) in the shape of load shifting is investigated. The GUI incentivizes user flexibility and increases the end user knowledge of the system.

To obtain the objectives, load profiles generated in the Remote-Areas Multi-Energy Systems Load Profiles (RAMP) model and Photovoltaic (PV) production modeled in pvlib python serve as input to the optimization model developed in Python Optimization Modeling Objects (Pyomo). The purpose is to determine the optimal scheduling of flexible loads to minimize the disutility cost of load shifting. Additional appliances are introduced to assess the feasibility of powering other buildings using the existing system at the school. Three scenarios are considered; Scenario 0, Scenario 1, and Scenario 2, which involve implementing zero, one, and two additional batteries, respectively. The cost implications of different approaches are also analyzed, including a comparison with the price of a new system. To incentivize user flexibility, the surplus energy of the system must be visualized easily and understandably in a GUI. The GUI is an early-stage design including different functionalities to increase the consumers' understanding of the system and suggest flexible consumption behavior. An essential part of the research is to collect realistic input data and feedback from the end users at the school regarding flexible consumption behavior and GUI design.

This thesis demonstrates that DR is an effective strategy for addressing unmet demand in off-grid microgrids. By load shifting and adapting to seasonal variations, the existing system can supply additional buildings at the school, with a cost of only 7% of the price of a new system. Most of the year, the system can cover the additional demand with an extension of the system. However, the main challenge occurs when the generation is drastically reduced. When including additional batteries, the number of days when the optimization model is unable to fulfill the constraints and cover the demand is reduced. The initial uncovered demand is decreased with additional battery capacity, but the reduction in uncovered demand due to load shifting is persistent in all the scenarios. Hence, load shifting mainly affects the uncovered demand caused by load peaks exceeding the system's capacity. By including the additional batteries, the disutility of the users is decreased. However, the cost increases to 20% and 35% of implementing a new system, with one and two additional batteries, respectively. The user experience will be enhanced, but the lack of financial resources at Eco Moyo Education Centre plays a vital role in the decision. Furthermore, the GUI will contribute to cover the demand when extending the existing system at the school. The GUI design proposal is developed in Python and presented with different functionalities to incentivize user flexibility and increase the user's experience and overall engagement with the system. However, the GUI is only an early-stage draft, and further development is needed. App implementation and weather forecasts are among the ideas for further development.

Sammendrag

Elektrifiseringen av rurale områder må akselereres dersom FNs bærekraftsmål nummer 7 skal bli oppfylt innen 2030. Det er gjort fremskritt for å sikre at alle har tilgang på elektrisitet, men COVID-19 pandemien og økte kostnader skaper utfordringer. Kenya har gjort betydelige fremskritt for å sikre tilgang på elektrisitet for alle, men de rurale områdene henger fortsatt etter. Derfor er off-grid systemer avgjørende for å sikre at flere får tilgang til pålitelig strømkilder. Eco Moyo Education Centre er et norsk/kenyansk veldedighetsprosjekt som tilbyr gratis grunnskoleutdanning til barn i landsbyen Dzunguni i Kenya. Skolen har et off-grid sol- og batteri mikrogrid som dekker grunnleggende strømbehov på lærerværelset. Denne masteroppgaven er basert på en case-studie av det eksisterende systemet ved skolen, med data samlet under feltarbeid i november 2022 og april/mai 2023. Oppgaven tar for seg skolens behov for å tilby strøm til flere bygninger, ved å fokusere på hvordan fleksibel drift av laster kan brukes til å utvide det eksisterende systemet. Videre undersøkes kostnaden ved å implementere et nytt system som en alternativ løsning.

Case-studien av Eco Moyo Education Centre trekker frem potensialet for fleksibilitet i sol- og batteridrevne off-grid systemer til å optimere energiforsyningen i rurale områder. Disse systemene er ofte basert på ustabile fornybare energikilder, som solkraft, og batterilagringssystemer brukes vanligvis for å kompensere for perioder med begrenset produksjon. Derfor er bruksmønstre det viktigste verktøyet for å øke fleksibiliteten i off-grid-systemer. Hovedmålene for masteroppgaven er å utvikle en optimeringsmodell for planlegging av fleksible laster og et brukervennlig grafisk brukergrensesnitt i tidlig fase for kommunikasjon med sluttbrukere. Ved å minimere kostnaden ved å flytte laster, undersøkes potensialet for etterspørselsrespons i form av lastforskyvning. Det grafiske brukergrensesnittet oppfordrer til brukerfleksibilitet og øker brukernes kunnskap om systemet.

Lastprofiler generert ved hjelp av RAMP-modellen, og PV produksjon modellert i pvlib python er brukt som input til optimeringsmodellen. Denne modellen er utviklet i Pyomo. Målet er å bestemme den optimale planleggingen av fleksibile laster for å minimere reduksjonen i nytteverdien ved å flytte laster. Ytterligere laster introduseres for å vurdere om det eksisterende systemet kan forsyne flere bygninger. Tre ulike scenarioer er simulert, Scenario 0, Scenario 1 og Scenario 2, som innebærer implementering av null, ett og to ekstra batterier. I tillegg sammenlignes kostnadene ved å utvide systemet med kostnadene ved å implementere et nytt system. For å oppfordre til brukerfleksibilitet må overskuddsenergien i systemet visualiseres på en enkel og forståelig måte i et grafisk brukergrensesnitt. Brukergrensesinittet er en tidlig fase av designet som inkluderer ulike funksjonaliteter for å øke forbrukernes forståelse av systemet og foreslå fleksibel brukeradferd. En viktig del av studien er å samle realistiske data og tilbakemeldinger fra sluttbrukerne ved skolen angående fleksibel brukeradferd og brukergrensesnitt design.

Denne masteroppgaven viser at etterspørselsrespons er en effektiv strategi for å dekke øvrig forbruk. Ved flytting av last og tilpasning til sesongvariasjoner kan det eksisterende systemet forsyne ekstra bygninger på skolen, med en kostnad på kun 7% av prisen på et nytt anlegg. Utvidelsen av systemet kan dekke forbruket mesteparten av året. Den største utfordringen oppstår imidlertidig når produksjonen reduseres drastisk. Ved å inkludere ekstra batterier blir antall dager der optimeringsmodellen ikke klarer å oppfylle kravene og dekke forbruket redusert.

Den opprinnelige udekkede etterspørselen reduseres, men reduksjonen i udekket etterspørsel på grunn av lastforskyvning er vedvarende i alle scenariene. Lastforskyvning påvirker hovedsakelig den udekkede etterspørselen, som skyldes lasttopper som overskrider systemets kapasitet. Ved å inkludere ekstra batterier øker brukerens nytteverdi. Imidlertid øker kostnaden til 20% og 35% av implementeringen av et nytt system, med henholdsvis ett og to ekstra batterier. Brukeropplevelsen vil bli forbedret, men mangelen på økonomiske ressurser ved Eco Moyo Education Centre spiller en viktig rolle i beslutningen. Videre vil det grafiske brukergrensesnittet bidra til å dekke forbruket når det eksisterende systemet på skolen utvides. Designforslaget for det grafiske brukergrensesnittet er utviklet i Python og presenteres med ulike funksjonaliteter for å oppmuntre til brukerfleksibilitet og øke brukerens opplevelse og engasjement med systemet. Imidlertid er det grafiske brukergrensesnittet et tidlig utkast, og ytterligere utvikling er nødvendig. Implementering i en applikasjon og inkludering av værmeldinger er blant ideene for videreutvikling.

Table of Contents

List of Figures

List of Tables

Acronyms

AC Alternating Current. 1, 5, 7, 13

API Application Programming Interface. 13

BESS Battery Energy Storage System. ii, 1, 8, 13

DC Direct Current. 1, 5, 7, 13, 14

DoD Depth of Discharge. 6, 18, 49–51

DR Demand Response. ii, 7, 8, 10, 11, 54, 56–58

DSM Demand Side Management. 8, 10, 12, 13, 53

EMS Energy Management System. 10, 12, 13

GUI Graphical User Interface. ii, 2–4, 10, 12–14, 19, 20, 23, 30, 32, 39, 40, 51–53, 56–58

HEM Home Energy Management. 8

HVAC Heating, Ventilation, and Air-Conditioning. 7

IEA International Energy Agency. 1

IoT Internet-of-Things. 13

IP Integer Programming. 9

LED Light Emitting Diode. 7, 30

LP Linear Programming. 9, 10

MILP Mixed-integer Linear Programming. 9, 16

MINLP Mixed-integer Non-linear Programming. 9

MIP Mixed-integer Programming. 9

MPPT Maximum Power Point Tracker. 7, 24

NLP Non-linear Programming. 9

PV Photovoltaic. ii, 1–4, 6–8, 12–14, 16–18, 21–25, 29, 32, 33, 38–41, 44, 45, 48, 50, 52–58

Pyomo Python Optimization Modeling Objects. ii, 2, 14, 16, 57

RAMP Remote-Areas Multi-Energy Systems Load Profiles. ii, 4, 14–16, 18, 29, 32–34, 52, 54, 57

RES Renewable Energy Source. ii, 1, 5, 7

SDG Sustainable Development Goal. ii, 1

SHS Solar Home System. 1, 6, 7, 23, 26, 55

SoC State of Charge. x, 4, 6, 12, 13, 18, 21, 22, 29, 38–42, 44–48, 52–58, 71–73

SSA Sub-Saharan Africa. 1

TCL Thermostatically Controlled Load. 8

TMY Typical Meteorological Year. 3, 14, 21, 33, 54

Nomenclature

Sets

$a \in A$	Appliances
$t \in T$	Time steps

Parameters

β_t	Non-flexible load in time step t [W]
η_{bat}	Efficiency of the battery [%]
η_{inv}	Efficiency of the inverter [%]
τ_a^{start}	Initial start time of appliance a
τ_a^{user}	User time of appliance a [min]
$D_{a,t}$	Original demand before optimization for appliance a in time step t [W]
E_{max}^{bat}	Max capacity of the batteries [kWh]
E_{max}^{inv}	Max capacity of the inverter [kWh]
n_a	Number of appliance a
P_t^{pv}	PV production in time step t [kWh]
P_a	Rated power of appliance a [W]
SOC_{start}	State of Charge of the batteries in time step $t = 0$ [kWh]
X_a	Disutility cost of moving appliance a one time step
k	Conversion parameter from W to kWh

Variables

$\delta_{a,t}$	Binary decision variable for appliance a in time step t
$\tau_{a,t}^{move}$	Time difference from original load profile for appliance a in time step t
$inv2load_t$	Power flow from the inverter to the load in time step t [kWh]
$L_{a,t}$	Load profile after optimization for appliance a in time step t [W]
$pv2inv_t$	Power flow from the PV system to the inverter in time step t [kWh]
$pv2store_t$	Power flow from the PV system to the batteries in time step t [kWh]
res_pv_t	Residual power from the PV system in time step t [kWh]
SOC_t	State of Charge of the batteries in time step t [kWh]
$store2inv_t$	Power flow from the batteries to the inverter in time step t [kWh]

1 Introduction

1.1 Background

To achieve Sustainable Development Goal (SDG) number 7 of universal access to affordable, reliable, sustainable, and modern energy by 2030, the pace of rural electrification needs to be accelerated [1]. The number of people without electricity dropped from 1.2 billion in 2010 to 733 million by 2020, and the majority of these people live in rural areas in Sub-Saharan Africa (SSA). However, due to the COVID-19 pandemic, the pace of progress is decreased, and the increased price of energy and shipping has caused higher costs of transporting and production of renewable energy resources, such as Photovoltaic (PV) modules and wind turbines. Hence, a major mobilization of private and public capital is required to reach the people living in the least developed countries to achieve global energy access [2].

Kenya is a leading country of economic growth in SSA, and the energy access rate has increased from 32% to 75% of households from 2013 to 2022 [3]. Renewable energy sources constitute over 80% of the generated electricity in Kenya, and geothermal energy is the most significant source. Due to the country's location close to the equator, Kenya also has a huge potential for solar power, and several solar projects are planned for 2023. However, in 2022, while the urban access rate was 100%, the rate of electricity access in rural areas was only at 65%. Nevertheless, the usage of stand-alone Solar Home Systems (SHSs) has rapidly increased, and this segment plays a significant role in the electrification of rural Kenya [4]. SHSs provides the most cost-effective electrification solution, particularly for households in rural areas. These communities, often comprised of the poorest and most vulnerable individuals, heavily rely on affordable options. Hence, the price of the electrification solutions plays a crucial role [5].

1.2 Motivation

Eco Moyo Education Centre is a Norwegian/Kenyan charity project that, as of 2022, provides free primary education to 240 underprivileged children. The school is located in the Dzunguni village, close to Kilifi on the Kenyan coast. Primarily, the village's residents live in mud houses without electricity or running water [6]. In March 2022, the school received a new solar and battery off-grid system to meet the school's basic electricity needs. The microgrid consists of seven solar panels of 450 Wp, four batteries of 200 Ah, and an inverter for Direct Current (DC) to Alternating Current (AC) power conversion with a capacity of 3.50 kW. It powers various appliances such as lights, PCs, tablets, phones, a printer, a fan, a TV, and smaller units in the Staff Room. However, the electricity supply in the other buildings at the school is limited to SHSs for lighting. The school received an offer from a local company to build a new microgrid to supply the Staff Court with electricity. However, the costs were too high, and it was decided not to move forward with the project. The preliminary project was written as a part of the course TET4510 Electrical Energy and Power Systems at NTNU in the autumn of 2022, and the results revealed that the existing system has the potential to supply additional buildings. This thesis investigates how user flexibility enables the existing microgrid at Eco Moyo Education Centre to supply additional buildings. Hereby, Eco Moyo Education Centre is referred to as Eco Moyo.

The International Energy Agency (IEA) states that demand-side activities should be prioritized when it comes to creating more reliable and sustainable energy systems. To include demand side activities with smart grid technologies are beneficial for both stakeholders in the energy value chain and the society as a whole [7]. Based on the case study of Eco Moyo, it is possible to discuss how flexibility in solar and battery off-grid systems can be utilized to optimize the energy supply in rural areas. Off-grid systems have proved to be challenging due to high service costs and low affordability [7]. These systems are often based on unreliable Renewable Energy Sources (RESs) like solar power. Battery Energy Storage Systems (BESSs) are typically used to compensate for periods with limited power generation. Hence, user behavior patterns are the primary tool to increase flexibility in off-grid systems. The possibility to flexibly operate loads also enhances the utilization of the installed capacity. Hence, flexibility in off-grid systems is essential to secure

reliable energy access in rural areas. An optimization model to minimize the disutility cost of load shifting can be used for the users to align their consumption with the available power generation. A Graphical User Interface (GUI) that communicates optimal behavior to the end user will help the user flexibly operate loads and enable them to make the most efficient use of their limited energy resources. In rural areas, limited understanding and access to technology is a major challenge. The digital divide between urban and rural communities has rapidly increased in the past few years. Hence, the lack of adequate technological knowledge in rural areas limits the individuals' ability to fully benefit from the potential that technology offers.

In November 2022 and April/May 2023, field trips to Eco Moyo were conducted. Figure 1 shows the installed PV system at the school. The first field trip revealed that the limited technological knowledge was a challenge considering the microgrid installed at the site. The system parameters visible on the inverter display are not understandable, and the users have limited to no knowledge about the system. Hence, one of the contributions in this thesis is to develop an early-stage draft of a GUI for end user communication. This GUI design proposal presents the system parameters in a user-friendly way to incentivize user flexibility by suggesting optimal user behavior. Additionally, The primary purpose of the second field trip was to collect data and examine the possibility of including more buildings in the existing system, including obtaining a price estimate for the extension. Additionally, the developed GUI draft was tested, and end user consumption behavior and operation of the system were observed. Meetings with the teachers revealed valuable insight into their flexibility regarding electricity and their willingness to adapt suggestions on flexible user behavior.

Figure 1: The PV panels of the existing system at Eco Moyo in November 2022.

1.3 Objective

The objective of this master's thesis is to investigate flexibility in rural off-grid microgrids based on a case study of the solar and battery off-grid system at Eco Moyo Education Centre in Kenya. The main objectives of the thesis are listed below:

- Create an optimization model in Python Optimization Modeling Objects (Pyomo) to decide the optimal scheduling of flexible loads by minimizing the total disutility cost of load shifting to maintain the end user experience.
- Develop an early-stage draft GUI for end user communication in Python to incentivize user flexibility based on optimal consumption behavior patterns.

The goal of the thesis is to use the optimization model to investigate how user flexibility in the form of load shifting can be used to extend the existing system to provide electricity to the Staff

Court, the Office Building, and the Staff Room. The costs are high for implementing a new system, and a more affordable solution, including user flexibility, is investigated. Additionally, this thesis develops a first sketch of a GUI for end user communication to increase the system's flexibility. An essential part of the research is to test the interface on the specific system and optimize the platform's functionality based on feedback from the users at the school.

1.4 Scope

To achieve the contributions stated in Chapter 1.3, a scope is defined for this master's thesis. The scope is presented below:

- Model realistic load profiles with additional loads using the RAMP model and data collected during the field trips to Eco Moyo.
- Model the production of the PV system at Eco Moyo using pvlib and input data from a Typical Meteorological Year (TMY) from PVGIS.
- Simulate the system dispatch of the microgrid at Eco Moyo with the optimized load profiles in Prosumpy with the modeled PV production from pvlib for three different scenarios;
  - Scenario 0 considers the existing system in the Staff Room with the additional load in the Staff Court and Office Building. This scenario investigates if the existing system is able to supply the additional buildings when flexible user behavior is implemented.
  - In Scenario 1, an additional battery is included in the existing system in the Staff Room. This scenario investigates how the additional battery capacity affects the flexibility and disutility of the consumers.
  - Scenario 2 includes two additional batteries. The scenario investigates further how the increased battery capacity affects the flexibility and disutility of the consumers.
- Use the optimized load profiles to propose optimal consumption behavior patterns for weather, climate, and seasonal variations for optimal utilization of the microgrid to cover more of the needs at the school.
- Optimize the early-stage GUI draft based on feedback from the users at the school to incentivize user flexibility and suggest functionalities for off-grid microgrids.
- Compare the costs between different approaches of electrifying the Office Building and the Staff Court to find the most suitable solution.

1.5 Outline

In this chapter, the outline of the master's thesis is presented.

Chapter 1: Introduction

The background, motivation, objective, and scope of this master's thesis are presented in this chapter.

Chapter 2: Theory

In this chapter, the essential theoretical background for analyzing the existing solar and battery off-grid system at Eco Moyo is presented. It covers microgrids, batteries, solar energy, converters and controllers, energy system flexibility, utility, and optimization.

Chapter 3: Related Research and Contributions in the Field

This chapter presents related research regarding the modeling of load profiles in rural areas, energy flexibility on the demand side, off-grid flexibility, and GUI development and design.

Chapter 4: Methodology

This chapter presents the methodology of this master's thesis. The methodology includes modeling of PV production in pvlib python and load profiles in Remote-Areas Multi-Energy Systems Load Profiles (RAMP). Further, an optimization model to decide the optimal scheduling of flexible loads, system dispatch in Prosumpy, and the development of an early stage GUI draft for end user communication are presented.

Chapter 5: Case Study: Eco Moyo Education Centre in Kenya

In this chapter, the case study of the thesis is presented. Relevant information about the existing system, buildings, and seasonal variations is described. Further, the results of the preliminary project are presented, which establishes an essential foundation for the master's thesis. Following, the fieldwork is presented, with price estimates for a new system and an extension of the existing system, flexibility ranking of appliances, availability of appliances in the area, additional findings related to user consumption, and evaluation of the GUI design proposal. Finally, the input data for the methodology and simulations are presented for the case study of Eco Moyo.

Chapter 6: Results

This chapter presents the results of the master's thesis. The modeled PV production and demand are described. Further, the results of the optimization model and annual system dispatch in Prosumpy are analyzed. The batteries' State of Charge (SoC) and the system's surplus energy are analyzed on dates when loads are shifted, or the system is unable to fulfill the constraints of the optimization model. Further, the costs of the different approaches for electrification of the Staff Court are presented. Finally, the design proposal of an early-stage GUI for end user communication is presented, and the functionalities are visualized.

Chapter 7: Discussion

The results presented in Chapter 6 are discussed in this chapter. Additionally, the results are compared to related research, presented in Chapter 3.

Chapter 8: Conclusion

In this chapter, a summary of the findings is provided, and concluding remarks are presented. Furthermore, improvements and further work are stated.

2 Theory

This chapter presents relevant theory for analyzing off-grid solar- and battery microgrids. Further, energy system flexibility, the basics of optimization, and utility theory are presented. Chapter 2.1, 2.2, 2.3, and 2.4 are directly extracted from the preliminary project [8, p.5-9].

2.1 Microgrids

Microgrids are small-scale energy systems with loads and energy generation resources [9]. These systems can be based on RESs, such as solar and wind, and they can also include devices for energy storage. The main advantage of using microgrids is the opportunity to operate independently of the grid, often referred to as "autonomous" or "off-grid" microgrids [9]. Nevertheless, microgrids based on RES can also be connected to the grid, and it becomes more common to customize the systems with applications to enable grid connection. This will increase the reliability of energy access for consumers. Based on the power structure, microgrids can be classified into three categories; DC, AC, and hybrid microgrids [10]. An overview of the different microgrids is presented in Figure 2.

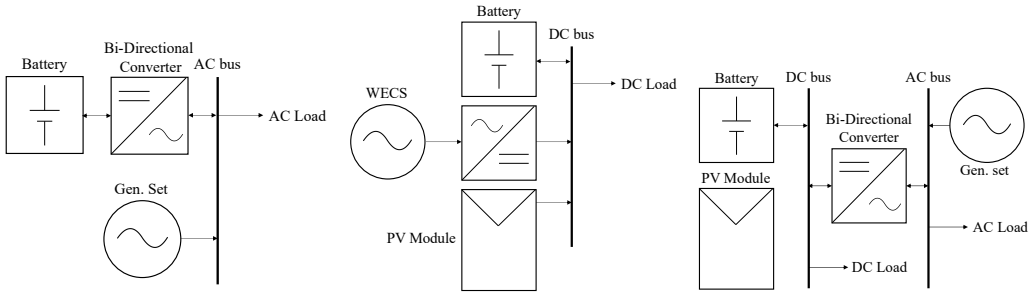

(a) AC Microgrid (b) DC Microgrid (c) Hybrid Microgrid

Figure 2: Examples of AC, DC, and Hybrid Microgrids [11].

2.2 Batteries

Storage systems such as batteries play a significant role regarding the effectiveness of renewable microgrids [9]. Because of the intermittency of RESs, it is evident to include battery storage in the systems to compensate for periods with reduced energy generation [12]. Batteries improve the stability, flexibility, reliability, and power quality of microgrids [13].

Historically, the batteries used in microgrids are lead-acid because of their low costs, technical maturity, and wide availability [11]. Gel batteries are valve-regulated, maintenance-free, lead-acid batteries. They are highly robust and versatile and can be used in places without much ventilation [14]. However, due to advanced research regarding lithium-ion batteries, there are substantial cost reductions in this technology. Advanced lead-acid batteries have an increasing capability to operate with higher efficiency and handle more cycles [15].

2.2.1 Capacity

The capacity of a battery is a measure of the charge stored in the battery and is generally expressed in ampere-hours (Ah). For example, a constant discharge current of 10 A can be drawn from a 10 Ah battery for one hour. The rated capacity of a battery represents the maximum capacity under certain specified conditions. However, the actual capacity of a battery depends strongly on the age, past charging and discharging regimes, and temperature of the battery [16].

2.2.2 State of Charge

SoC of batteries is described as "a restraint presenting the linkage between energy storage in the battery and the process of discharging and charging" [10, p.38]. Further, the battery must not be overcharged or over-discharged because this will affect the efficiency and the battery's lifetime. The battery operation is often between the minimum and maximum capacity [12].

2.2.3 Depth of Discharge

Depth of Discharge (DoD) of a battery is expressed as a percentage and represents the removed capacity from a battery divided by its real capacity [17]. The relation between DoD and SoC is represented in Equation 1.

$$DoD = 1 - SoC \tag{1}$$

2.3 Solar Energy

Solar energy is energy from the sun's radiation and is the most abundant of all energy resources. The solar energy intercepted by the earth is more than 10,000 times greater than the total energy consumption by humankind [18]. The energy is received as heat and light and can be converted to various usable forms, such as electricity and heat [19]. PV units generate electrical energy by transforming the radiance energy from the sun directly into electrical power.

2.3.1 Solar Radiation

The solar radiation exposed to the PV panels is highly affected by the tilt and azimuth angles. Maximizing the radiation the PV panels receive is essential to optimize the production. The tilt angle is the angle of the PV modules from the horizontal plane. Hence, the optimal tilt is dependent on the latitude of the location.

In countries near the equator, a low tilt angle is optimal. However, tilt angles below 10° are unsuitable because they will make the natural rainwater run-off less effective. This will lead to increased debris collection and losses in the production [20]. The azimuth of the PV panel is the east-west orientation in degrees. It is most common to refer to an azimuth value of zero when the PV panel faces the equator in both the northern and the southern hemispheres [21]. Further references to the term will consider a site position in the southern hemisphere. This means that an azimuth of 0° is towards the north, and 180° is towards the south.

2.3.2 PV Systems

Multiple PV panels can be combined into a PV system. They can be connected in series or parallel to supply sufficient current and voltage to a system. When PV modules are connected in series, it is referred to as a PV string. The voltage output of a PV string is increased while the current is constant. However, when connected in parallel, the total output current of the PV module is increased while the voltage is kept constant [22]. Some PV systems also include batteries to store electricity for future use.

2.3.3 Solar Home Systems

Solar Home Systems (SHSs) are stand-alone PV systems to cover the demand of rural areas where households are not connected to the grid. These systems cover basic electricity needs, such as lighting and other low-power devices. SHSs are the only electricity available for thousands of

people living in remote areas. Typically, a SHS consists of a PV panel, a storage technology, and a charge controller. It provides electricity for lighting when the solar irradiation is low [23]. The systems with the lowest installation cost are DC SHSs, which provide energy for Light Emitting Diode (LED) lights and USB for charging. AC systems are more expensive because it requires an inverter. However, the AC systems provide a wider range of electricity, and the storage system usually has a higher level of capacity [24].

2.4 Converters and Controllers

Microgrids require converters and controllers to ensure high-quality power to consumers. Converters regulate the discharging and charging of the battery as well as facilitate the power flow in AC, and DC systems [11]. Inverters convert the generating DC voltage to usable AC voltage to consumers. Other converters are rectifiers, which convert from AC to DC, and DC-DC converters, which regulate the output DC voltage.

2.4.1 Maximum Power Point Tracker

Maximum Power Point Trackers (MPPTs) are generally used to increase the produced power of PV systems. The basic premise is to decouple the voltage from the load and the PV array in order to let the PV array operate at the voltage corresponding to the maximum power point. The PV array is connected to a DC-DC converter, and the output is connected to a battery or a load through a charge controller. The converter's duty cycle is monitored to track the maximum power point of the PV array as the array's temperature, irradiance, and shading changes [11].

2.5 Energy System Flexibility

To operate properly, energy systems must continuously balance the power supply and demand. The term energy system flexibility describes an energy system's ability to adjust the supply and demand to maintain the energy balance [25]. Balance in the system is essential to avoid blackouts and keep the system frequency and -voltage stable. To succeed with the energy transition from fossil-based production to RESs, the flexibility of power systems is crucial to secure reliable energy access. With the integration of large-scale intermittent RESs, like hydro, solar, and wind, the need for flexibility is increased. Conventional power systems achieve sufficient flexibility using dispatchable power plants, such as gas turbines, that can easily connect and disconnect when needed [26]. However, flexibility must be attained from other sources in the future energy system. Flexibility can be divided into supply- and demand-side flexibility [27]. The supply side includes the generation of the system, such as RESs, while the demand side is the energy consumption by the end users, such as electrical appliances and Heating, Ventilation, and Air-Conditioning (HVAC) systems [27].

2.5.1 Grid Ancillary Services

Grid Ancillary Services are necessary to operate a transmission or distribution system and are a part of the supply-side flexibility. It includes power quality and regulation to secure the system's stability [28]. These services are also essential in the conventional power system and not necessarily bound to integrating renewable energy sources [26].

2.5.2 Demand Side Management and Demand Response

Flexible operation of loads allows the energy demand to be adjusted according to the supply of a system. This power adjustment by the users is known as Demand Response (DR) [29]. It can be categorized as reducing, increasing, or rescheduling the energy demand [30] to balance the

energy system. Figure 3 illustrates three different categories of Demand Side Management (DSM); conservation and peak shaving, valley filling and load growth, and load shifting. Peak shaving refers to leveling out peaks by reducing the load during peak periods, while valley filling refers to increasing the load during off-peak periods. Load shifting combines these two and refers to rescheduling the load from peak to off-peak periods. An example of load shifting is households charging their electric vehicles at night. Load shifting is often beneficial compared to the two other categories, as it allows users to utilize the same amount of power in the period and hence, the user's utility is maintained. For the consumers to contribute to DR, the appliances need to be categorized. The classification of appliances is determined by whether their energy consumption can be deferred within a certain limit to prevent inconvenience for consumers [31]. If there are Thermostatically Controlled Loads (TCLs), this is also included in the classification, as they can contribute to the DR.

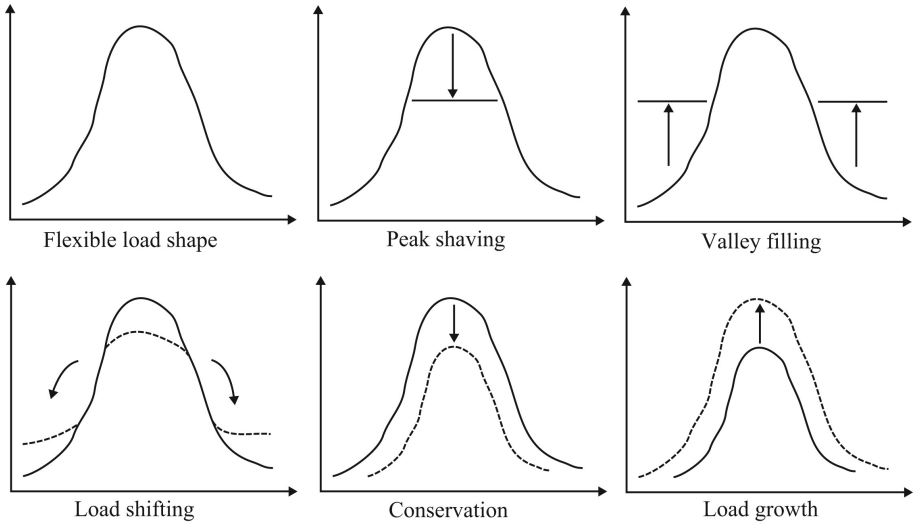

Figure 3: Categories of DSM [30].

2.5.3 Off-Grid Flexibility

Sustainable off-grid systems, meaning off-grid systems without a diesel generator or other conventional power sources, are often based on intermittent energy sources such as wind and solar power. Hence, uncertain and uncontrollable power generation are the main drivers of flexibility, as dispatchable power plants can be connected and disconnected rapidly to the grid are irrelevant in off-grid systems [26]. In off-grid systems reliant only on solar power, it is optimal for the users to use more energy during the daytime when the PV panels produce energy due to limited storage capacity. It is necessary to examine whether there are any high consumption patterns and whether the patterns are evenly distributed in the off-grid system to ensure reliability [32]. This is especially important in rural areas, as developed areas tend to have Home Energy Management (HEM) systems, ensuring more efficient use of the available energy [33]. Alternative energy technologies in a home system will increase flexibility, such as fuel-based generators, BESSs, flywheel- and fuel cell systems [33]. User behavior patterns and BESSs are crucial elements that serve as the main tools for enhancing flexibility in such systems.

2.6 Utility

Utility is a term used in economics to describe the satisfaction or benefit from consuming a good or service. In practice, the utility of a consumer is impossible to measure or quantify [34]. However, utility theory is postulated in economics to explain consumer behavior based on the premise that individuals can always rank their choices depending upon their preferences [35]. Various models are used to indirectly estimate the utility of an economic good [34]. After observing the choices of

individuals, assumptions about their preferences can be drawn. This can be represented analytically by a utility function, which is a mathematical formulation that ranks the preferences of the individual in terms of the satisfaction different consumption bundles provide. The utility theory makes the following assumptions [35]:

- Completeness: Individuals can always rank different combinations of consumption bundles based on preferences.
- More-is-better: If an individual prefers consumption of bundle A off goods to bundle B, and is offered a bundle with more of everything in bundle A, he will choose the last bundle.
- Mix-is-better: The mix of several goods is always preferred compared to stand-alone goods. Suppose an individual is indifferent to two goods, meaning either choice by itself is not preferred over the other. Then, the mix-is-better assumption says that a mix of the two will always be preferred.
- Rationality: If bundle A is preferred to B, and bundle B is preferred to C, then A is also preferred to C. Meaning that the rank ordering of goods is fixed, regardless of the context and time.

2.7 Optimization

Optimization is a tool to find the best solution among other possible solutions. The objective function quantifies the solution's value and is either maximized or minimized, subject to a number of constraints. The solution of an optimization problem may be found using graphical, algebraic, or computer-aided tools. Recently, the use of computer-aided tools is becoming a common practice, as it is effective for solving large-scale problems [36]. An example of an optimization problem is minimizing the electricity cost subject to a given demand and energy system constraints. An optimization model where the objective function is minimized can mathematically be formulated as presented below. The objective function to be minimized is formulated in Equation 2a. Equation 2b and 2c are inequality and equality constraints, respectively. The variables $x_1, x_2, \ldots, x_N$ are decision variables and are the unknown variables to be optimized.

$$\underset{x_1,\ldots,x_N}{\text{minimize}} \quad f(x_1, x_2, \ldots, x_N) \tag{2a}$$

subject to

$$g(x_1, x_2, \ldots, x_N) \leq 0, \tag{2b}$$

$$h(x_1, x_2, \ldots, x_N = 0 \tag{2c}$$

If the objective function and all the constraints are linear, it is called a Linear Programming (LP) optimization problem. Otherwise, the term Non-linear Programming (NLP) is used. The classification of the optimization problem also depends on the optimization variables. If all the variables are integers, whole numbers, the optimization problem is classified as a Integer Programming (IP) optimization problem. Moreover, an optimization problem involving continuous optimization variables is referred to as a Mixed-integer Programming (MIP) optimization problem. Depending on the linearity or non-linearity of a MIP problem, it is classified as a Mixed-integer Linear Programming (MILP) or a Mixed-integer Non-linear Programming (MINLP) problem [36].

3 Related Research and Contributions in the Field

In this chapter, related research regarding the modeling of load profiles in rural areas, energy flexibility, off-grid flexibility, and GUI development are presented. These topics are highly relevant for investigating flexibility in off-grid solar and battery systems and incentivizing flexible consumption behavior by the end users.

3.1 Modeling of Load Profiles in Rural Areas

This chapter is directly extracted from the preliminary project, as modeling load profiles is an essential part of simulating microgrids in rural areas [8, p.16].

> Stochastic approaches are often used to model residential load profiles to include random consumer behavior [37]. These models are often conceived for on-grid systems in industrialized countries where the detail level and availability are higher [38]. In remote areas, the input data for these models are unavailable; if they are, the accuracy is usually not acceptable. The systems in rural areas are generally off-grid, and the load profiles are generated based on interview-based information without any measured data [39]. Models for generating load profiles in rural areas need to be customized for energy planning instead of forecasting the loads [40]. This means that systems in rural areas need to be adaptable to appliances unavailable in the community when the surveys and interviews are held [38]. Even if the surveys were more detailed, it is impossible to catch possibilities and user behavior for non-yet-existing devices.
>
> In [40], a bottom-up stochastic approach in order to include the information based on interviews is developed. In the model, the uncertainties were considered by using a parameter (randomly varying) to the self-declared activity patterns from the interviews. Despite this, this model does not allow for extending of non-electric loads, such as cooking and heating of water. Hence, in [38], the authors propose an open-source bottom-up stochastic model to generate load profiles located in remote areas. Their model is based on the approach in [40] with interview-based data, but the model has an expanded approach where the degree of stochasticity is increased [38].

3.2 Modeling of Energy Flexibility on the Demand Side

In recent research, flexibility in terms of DSM is gaining considerable attention. Due to new technology and political goals, traditional electricity systems are undergoing significant changes. Hence, a more active demand side will be crucial for future energy systems [7]. With the development of smart grids, the communication between the consumer and power supplier is expected to increase due to the availability of technology enabling bidirectional communication [41]. DR aims to adapt the consumption in response to signals controlled by the utility company. Often in the form of variability in electricity prices. This is beneficial for both parties. Consumers can reduce their electricity bills, and utility companies benefit from smoothing out the peak demand, resulting in increased system reliability and reduced generation costs.

In [7], the authors aim to decide the optimal plan for utilizing flexible loads in a building. The authors use an integrated energy carrier approach based on the energy hub concept. The goal is to capture multiple energy carriers, converters, and storages to increase the flexibility potential. An energy hub is an integrated system where the inputs are multiple energy carriers, like natural gas and electricity. The output of the energy hub is services to meet loads like electricity, heating, and cooling [7]. [41] describes an optimization model to adjust the hourly load level in response to hourly electricity prices. The objective is to maximize consumer utility based on a simple bidirectional communication device between the consumer and producer. Such bidirectional communication allows the consumer to receive hourly price information and adjust the consumption to minimize the electricity price and maximize the consumer utility. The simple LP algorithm can easily be implemented in the Energy Management System (EMS) of a household [41]. [42] aims to achieve

optimal energy scheduling for DR across several residences and develop an algorithm for the smart meters to attain optimal schedules. It is based on the fact that each residence has a smart meter communicating with the various electric devices and the utility company.

There are multiple ways of modeling flexibility on the demand side. A price elastic inverse curve can be used. However, this is a simplification and is insufficient to describe the dynamic flexibility on the demand side. It does not consider that changing the load in one period also affects the demand and decision-making in later periods [7]. In [41], the authors propose a real-time electricity demand response model with minimum daily energy consumption constrained by minimum and maximum hourly load levels. Another solution is used in [42], where the total load is divided into three components to model the demand side flexibility. The first component is the "must-run" load, which is inflexible and must be covered. The second component is the adjustable load, where the total demand must be met over the scheduling horizon but can be rescheduled. Finally, the third component is the load that can be cut to the dissatisfaction of the end user [42].

In [7], the authors base the model on a combination of the methods used in [41] and [42]. The loads are split into inflexible, shiftable, and curtailable load types. The inflexible loads are the loads where the demand must always be met. Moreover, shiftable loads are the loads where the demand must be met but can be moved within a given time interval. Within the shiftable loads [7] further distinguish between shiftable profile load units, where the whole load profile must be shifted, and shiftable volume load units, where the load profile can be changed within limits as long as the total volume is met. Finally, the curtailable loads can be reduced at the cost of the consumer's utility. Reducible load units are curtailable loads where the demand can be reduced to a certain level, while disconnectable load units are loads that are either turned on or off [7]. Figure 4 depicts the different load classes used to describe the flexibility in [7]. To model the curtailable loads [7] introduce binary decision variables. The first variable δ^{start} gets the value 1 in the period where the load is started. Followingly, the variable δ^{end} gets the value 1 when the curtailable load is stopped. Finally, the variable δ^{run} gets the value 1 in periods when the load is turned on and not started or stopped in the same period [7].

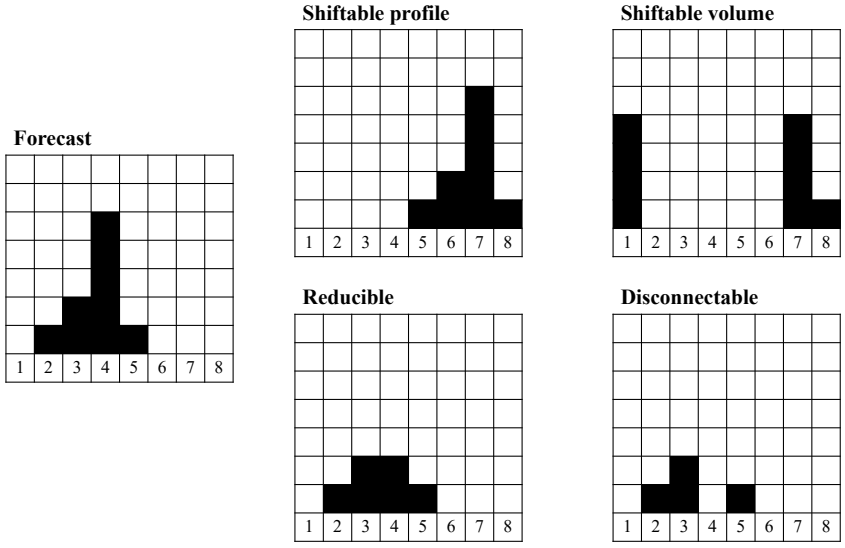

Figure 4: Illustration of the different load flexibility classes used in [7, p.366].

In [41], the consumer utility is initially assumed to be constant throughout the hours of the day. Hence, the consumer obtains a positive profit if the energy prices are lower than a certain limit. This results in an average weekly utility that is 13.20% higher than without a smart grid that enables bidirectional communication and increased DR. However, a simplified constant utility function is not generally the case. In another case study, to obtain more realistic results, [41] model the consumer hourly utility function by four blocks. Each block is 75 MWh, with a decreasing utility for each block. As a consequence of the adjusted utility function, the increased utility caused by using a smart grid is decreased. The resulting weekly average utility is 4.99% higher than

the result obtained without bidirectional communication when modeling the consumer utility in different blocks [41]. In [42], the authors aim to maximize social welfare, defined as the consumer's utility from power consumption minus the total cost of electricity from all the residences. To model the consumer's utility, a convex disutility function $V_t(p_t)$ is used. The function is decreasing in the power consumption p_t by the considered device, presumably with $V_t(p_t^{max}) = 0$. The disutility function varies in time to reflect how the importance of operating a device depends on the time. [7] consider the consumer's utility by including the disutility cost for curtailment of loads in the objective function. The cost is measured in [NOK/kWh], but the specific values are not discussed in the paper [7]. In [31], a technique for combining residential demand utilizing a multi-class queueing system is presented. The demand is divided into blocks, and the cost of the aggregated appliances' power consumption is minimized. As a consequence of the demand aggregation, the complexity of the model is reduced.

This master's thesis includes an optimization model with several similarities to the previously discussed models. The flexibility on the demand side is modeled by dividing the total load into different components, similar to what is done in [7] and [42]. However, the model only separates the loads into must-run and curtailable load types. Equal to [7], binary decision variables are introduced to model the curtailable loads. Another big difference is that the model in this project considers an off-grid system, and the electricity prices are irrelevant. However, the utility function also plays a vital role in this model. Similarly to [7], a disutility cost for curtailment of loads is considered in the objective function. Nonetheless, in our case, it is modeled to be linear with respect to the curtailment. Further, the load profiles in this model is implemented for each appliance, unlike the load profiles in [31]. The difference is the number of residences, as [31] collects demand data for several residents while in this case, only data for Eco Moyo is included. However, an aggregated load profile would have decreased the complexity of the optimization model. The mathematical formulation of the optimization model is further discussed in Chapter 4.3.

3.3 Energy Flexibility in Off-Grid Systems

A case study regarding DSM of off-grid PV microgrids in Tanzania is presented in [32]. The microgrid consists of PV panels, a charge controller, batteries, and an inverter and serves electricity to a village. The presented work proposes a machine-learning-based DSM system which guides effective power usage. The proposed method in [32] analyzes the dominant consumption pattern, detects anomalies, and power usage guidance. In [43], a prioritization technique to secure a continuous supply of essential loads in rural areas is presented. The proposed strategy improves the hours of energy served to the system by improving the SoC of the battery. Several studies investigate DSM strategies with different optimization processes. However, these methods require high programming skills which can be challenging to achieve with the basic EMS systems commonly found in rural areas [43]. Off-grid systems in rural areas are limited by the absence of economic incentives and household responsibility [32]. Although the methods in [32] and [43], there is a lack of research regarding DSM of off-grid systems in rural areas. Nevertheless, optimal power user guidelines can be provided and visualized to encourage user flexibility, and in this way, the user will understand the importance of the DSM.

3.4 Design of Graphical User Interfaces

To allow the users to interact with developed systems, a GUIs is essential. Interface design plays a significant role in user engagement, as a complicated interface adversely affects the user's experience [44]. According to [45], a practical interface design has several factors considered, such as the motivation and intention of the users and the user's cultural background. The "digital divide" is a common term for people from deprived socioeconomic backgrounds with limited technology access, and developing countries are particularly affected by this digital exclusion gap [46]. As each GUI needs to adapt both the system's technology and the end user, the development of an interface is an iterative process. Hence, no standardized development procedures ensure completely satisfied users and a successful interface [44].

Computers have become more integrated into people's everyday lives, which may be problematic for older people. For people accustomed to growing up with technology, this interaction will be more of a routine [44]. In [47], a GUI for an intelligent alerting system at the bedside is developed with an early user-engaged design. The median age of the participants is 35 years, and the purpose of this work is to "elicit iterative design feedback from clinical end users on an early GUI prototype display" [47, p.1]. As a result of the early user feedback, the design of the interface was fundamentally changed both in the display and functionality. Additionally, the end users gave feedback regarding colors, fonts, and size to improve the readability [47].

Traditionally, end user knowledge of doing changes in interactive systems has been limited to manual changes to the system settings [48]. Software personnel is needed to develop or modify new applications in an existing system. The difference in needs of people makes software development cycles time-consuming, expensive, and slow with software professionals [49]. Hence, the aim of end user development is described in [49] as "empowering end users to develop and adapt systems themselves" [49, p.2] without any programming skills. This will make the evolution of GUIs more customized to each user and increase the user's experience.

Several studies have investigated EMS for microgrids. [50] proposes a system-level EMS for AC/DC microgrids in residents tested in real-time in a laboratory environment. In [51], an advanced DSM for an effective EMS is developed for smart microgrids, and [52] proposes an optimized EMS grid-interactive hybrid microgrid based on a smart Internet-of-Things (IoT) platform. Nevertheless, none of these studies incorporate a GUI, which limits the level of human interaction with the systems. Hence, [53] proposes an EMS based on IoT for microgrids, including a web-based GUI and an Application Programming Interface (API). The user-friendly GUI allows the user to be interactive, configure internal settings, and view graphics in the web application. Further, the home screen visualizes the SoC of the BESS and the active PV generation in real time. The PV production is based on the average power PV generation profile, including $\pm$ 5% forecasting error [53]. At the bottom of the page, the total generation, operation cost, and daily consumption are presented. Despite this, there is a lack of GUI for microgrids, especially for off-grid systems in rural areas. In these areas, the availability of appliances is limited. To increase the interaction between the microgrid and the users, this thesis proposes a GUI design draft for end user communication to visualize essential data from the system and encourage flexible user behavior. Additionally, the visualization of the PV production in the GUI draft in this thesis is motivated by [53].

4 Methodology

To investigate flexibility in off-grid solar and battery systems, an optimization model to minimize the disutility cost of shifting loads is created in Pyomo. The model is based on system parameters, load profiles, and solar production. Modeling of solar production is done using pvlib, an open-source tool in Python with weather data from PVGIS, and the load profiles are simulated using the RAMP model. Further, the simulated load profiles are modified to reflect the simplifications in the optimization model. The resulting load profiles from the optimization model are used to simulate the system dispatch in Prosumpy. Finally, an early-stage GUI is developed to access real-time data from the inverter, propose optimal consumption behavior, and present theoretical trends from the optimization model. Figure 5 illustrates the different stages of the modeling.

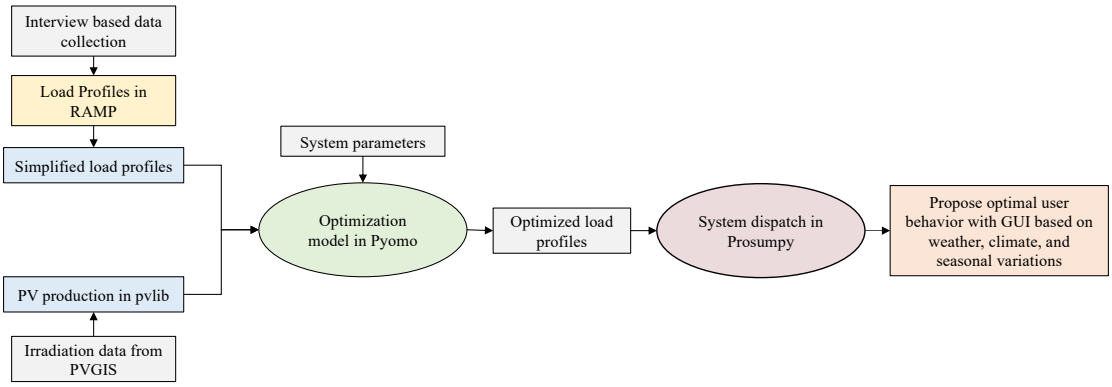

Figure 5: Flow chart of methodology and simulations.

4.1 PV Production in pvlib python

PV production in the system is modeled using the open-source tool pvlib python. The tool is developed on GitHub with contributors from academia, national laboratories, and private industry. It provides core functions based on algorithms from peer-reviewed publications [54]. Multiple solar resource datasets can be included in pvlib, and in this project, the dataset PVGIS-SARAH2 is used. It is a solar radiation dataset from the free PVGIS database. The data are based on geostationary satellites covering Europe, Africa, and Asia [55]. The data resolution is hourly, and the dataset includes radiation data, sun height, air temperature, and wind speed. To create a representative dataset, TMY for the given geographical location of the system is utilized.

To calculate the DC output from the PV system, two core functions in pvlib are used. The function `temperature.faiman()` is used to calculate the temperature of the PV module based on the Faiman model. The model calculates the temperature based on the total incident irradiance, air temperature, and wind speed, using an empirical heat loss factor [56]. Finally, the core function `pvwatts_dc()` is used to calculate the DC output power P_{dc}, based on the cell temperature T_{cell}, transmitted plane array irradiance I_{tr} and rated power P_{dc0}, as shown in Equation 3. The parameters I_{ref} and T_{ref} represent the reference irradiance and temperature and are set to $1000\frac{W}{m^2}$ and $25°C$, respectively. γ_{pdc} is the temperature coefficient and is used to model how the efficiency of the PV module decreases at a linear rate of the temperature rise [57].

$$P_{dc} = \frac{I_{tr}}{I_{ref}} P_{dc0}(1 + \gamma_{pdc}(T_{cell} - T_{ref})) \tag{3}$$

4.2 Load Profiles in RAMP

Load profiles for the different appliances are modeled using the open-source stochastic RAMP model described in [38] and presented in Chapter 3.1. The model is implemented in Python and designed to generate load profiles in remote areas. It consists of three main layers; *User Type*, *User*, and *Appliance*, as illustrated in Figure 6. Due to the stochastic model, each *User* has a unique load profile consisting of independent *Appliances* with different behaviors [38]. The generated load profiles will differ from each model run and represent the unpredictable behavior of the users.

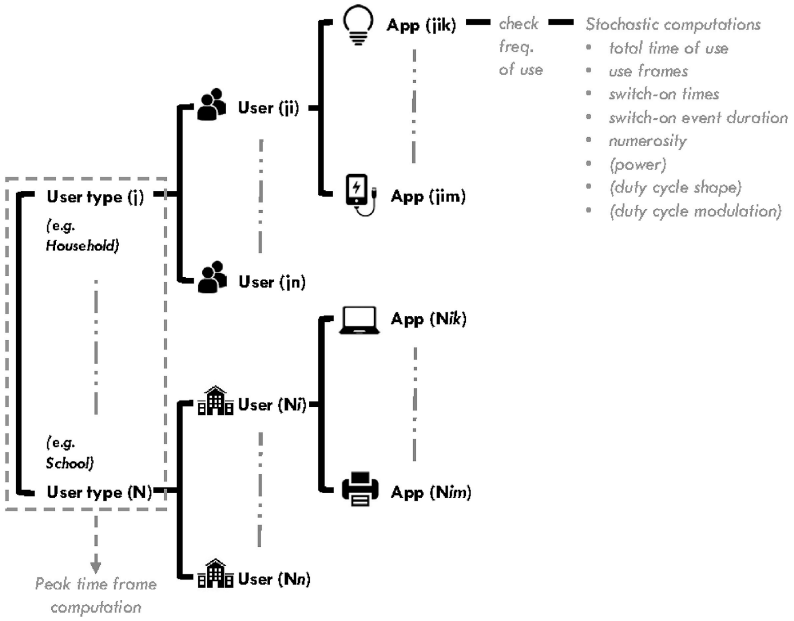

Figure 6: Graphical sketch of the modeling layers in RAMP [38, p.435].

Table 1 provides a short description of the input parameters used for the appliances when generating load profiles with the RAMP model. The appliance belongs to a *User*. Each appliance is also associated with a time window where it is likely to be switched on during the day. To be used as an input in the optimization model described in Chapter 4.3, the load profiles are modified to match the simplifications. To identify the specific behavior of each load, a unique load profile is generated for each appliance. Each appliance is also only used once during the day and always as long as the defined user time tot_use. Hence, the stochastic parameter r_t, and the total user time are not subject to random variability. The parameter $func\_time$ is also set to be equal to the user time, as the appliance always will be switched on for the duration of the user time. The parameter $freq.$ describes the occurrence of an appliance during a week. The frequency of an appliance is given by the number of days during the week divided by five if the device is only used during the weekdays and by seven otherwise.

Table 1: Input parameters for each appliance in the RAMP model.

Parameter	**Description**
$user$	User to which the appliance is bounded.
m	Number of appliances of the specified kind.
$P[W]$	Power of the specified appliance.
$freq.[\%]$	Weekly frequency for use of the specified appliance.
$tot\_use[min]$	Total time the appliance is on during the day.
$Window$	Time frames in which a random switch-on of the appliance can occur.
$r_t[\%]$	Percentage of total use that is subject to random variability.
$fixed$	If 'True' all the n appliances are kept on after the switch-on event.
wd_we_type	Defines if the appliance is associated with weekdays or weekends.
$func\_time$	Minimum time the appliance is kept on after the switch-on event.

An important feature in the RAMP model is the attribute to model duty cycles, which makes it possible to simulate the behavior of a fridge [38]. The operating cycle of a fridge consists of cooling and standby mode, which repeats itself throughout the day. During the cooling period, the fridge consumes the rated peak power until the temperature inside the fridge is sufficiently low. Then the power consumption is drastically decreased in standby mode until the temperature has risen through a given threshold and the cooling mode is repeated [58]. The operation cycle of the fridge depends on several factors, like size, efficiency, outside temperature, isolation, and user patterns. The warming process during the standby mode will be sped up if the fridge is opened regularly or the isolation is insufficient. To include the variations in the duty cycles the RAMP model includes the attribute to model different cycles that can be associated with different time frames during the day [38]. Figure 7 illustrates three default duty cycles modeled for a fridge in the RAMP model. The duty cycles are categorized into standard, intermediate, and intensive, depending on user behavior and ambient temperature.

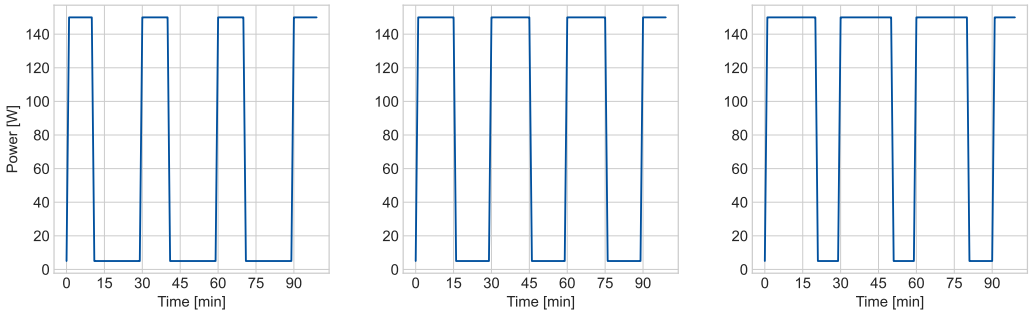

(a) Standard Cycle (b) Intermediate Cycle (c) Intensive Cycle

Figure 7: Default duty cycles of a fridge modeled in RAMP [38].

4.3 Mathematical Formulation of the Optimization Model

The optimization model is created using the Pyomo software. It is a Python-based, open-source optimization modeling language [59]. The goal is to decide the optimal scheduling of flexible loads in off-grid solar and battery microgrids, by minimizing the disutility cost of shifting loads. It is formulated as a MILP problem. Load profiles for all the appliances generated in RAMP and PV production from pvlib are used as input to the model. Appliances are classified into two categories; shiftable loads and non-shiftable loads. The shiftable loads are deferrable and can be rescheduled to reduce the peak demand. These loads are typically charging of appliances. Non-shiftable loads can not be modified and are typically lighting and cooking. This chapter describes the mathematical formulation of the optimization model presented below. The Python script for the optimization model is included in Appendix F.

$$\underset{\tau_{a,t}^{move},\, res\_pv_t}{\text{minimize}} \quad \sum_{t=0}^{T}\sum_{a=0}^{A} X_a \cdot \tau_{a,t}^{move} + \sum_{t=0}^{T} res\_pv_t \qquad a \in A, \quad t \in T \tag{4a}$$

subject to

$$\sum_{i=0}^{T-\tau_a} \delta_{a,i} - 1 = 0, \quad a \in A, \tag{4b}$$

$$L_{a,t} - \sum_{i=0}^{t} P_a \cdot \delta_{a,i} \cdot n_a = 0, \quad t = 0, \ldots, \tau_a - 2, \quad a \in A, \tag{4c}$$

$$L_{a,t} - \sum_{i=t-\tau_a+1}^{t} P_a \cdot \delta_{a,i} \cdot n_a = 0, \quad t = \tau_a - 1, \ldots, T, \quad a \in A, \tag{4d}$$

$$\tau_{a,t}^{move} - \delta_{a,t} \cdot |\tau_a^{start} - t| \cdot n_a = 0, \quad t \in T, \quad a \in A, \tag{4e}$$

$$\sum_{i=0}^{A}\sum_{j=0}^{T} D_{i,j} - \sum_{k=0}^{A}\sum_{l=0}^{T} L_{k,l} = 0, \tag{4f}$$

$$inv2load_t - (store2inv_t + pv2inv_t) \cdot \eta_{inv} = 0, \quad t \in T, \tag{4g}$$

$$pv2store_t + pv2inv_t + res\_pv_t - pv_t = 0, \quad t \in T, \tag{4h}$$

$$inv2load_t - (\beta_t + \sum_{i=0}^{A} L_{i,t}) \cdot k = 0, \quad t \in T, \tag{4i}$$

$$inv2load_t - E_{max}^{inv} \cdot \eta_{inv} \leq 0, \quad t \in T, \tag{4j}$$

$$pv2store_t - E_{max}^{bat} \leq 0, \quad t \in T, \tag{4k}$$

$$SOC_t - SOC_{start} = 0, \quad t = 0, \tag{4l}$$

$$SOC_t - SOC_{t-1} - pv2store_t \cdot \eta_{bat} + store2inv_t = 0, \quad t \in T, \tag{4m}$$

$$SOC_t - E_{max}^{bat} \leq 0, \quad t = 0, \ldots, T-1, \tag{4n}$$

$$SOC_t - 0.2 \cdot E_{max}^{bat} \geq 0, \quad t = T \tag{4o}$$

4.3.1 Objective Function

Equation 4a formulates the objective function that minimizes the total disutility cost of shifting loads, in addition to the residual PV production. X_a is the disutility cost of moving the appliance with index a one time step. $\tau_{a,t}^{move}$ is a decision variable and describes how many time steps appliance a has been moved. Hence, the disutility function is assumed to be linear and increasing in the curtailment time. The residual PV production is minimized to ensure that the system dispatch corresponds to the Prosumpy model described in Chapter 4.4, where the dispatch of the system is performed in such a way that the self-consumption is maximized.

4.3.2 Shiftable Load Units

$\delta_{a,t}$ is a binary variable that controls the shiftable loads. The variable gets the value 1 in time step t when appliance a is switched on. Equation 4b controls that each load only starts once during the modeled time horizon. The limit $T - \tau_a$ is set so that the load always will be able to run for the whole user time. Equation 4c and 4d set the optimized load profile for appliance a in time step t to be equal to the rated power of the appliance from the starting time when $\delta_{a,t}$ has the value 1, and for the whole user time. The decision variable $\tau_{a,t}^{move}$ is calculated in Equation 4e, based on the binary decision variable and the initial start time of appliance a. Note that the variable is assigned a value only during the time step when the appliance a is switched on. For all other time steps, it is assigned the value 0. The decision variable $\tau_{a,t}^{move}$ also considers the quantity of appliance a. The constraint defined in Equation 4f ensures that the shiftable load is moved and never cut. After optimizing, the total shiftable load is equal to the initial shiftable demand.

4.3.3 Power Balances

The power input and output of the internal systems must be balanced. Equation 4g is used to balance the power input from the PV module and the batteries with the output from the inverter to the load. The efficiency of the inverter is also considered. Equation 4h balance the input to the PV module with the output to the batteries, inverter, and the residual energy. The power balance for the load is formulated in Equation 4i, and controls that the output from the inverter is equal to the non-shiftable load and the total shiftable load for all the appliances. k is a conversion parameter that converts the values from W to kWh.

4.3.4 Capacity Constraints

The constraints formulated in Equation 4j and 4k ensure that the energy flows in the system are within the capacity of the components. Equation 4j limits the output from the inverter to the load by the rated maximum output, including the efficiency of the inverter. The input to the batteries from the PV module is limited by the capacity of the batteries in Equation 4k.

4.3.5 Battery Constraints

The initial SoC of the battery in time step $t = 0$ is given by the parameter SOC_{start}, as formulated in Equation 4l. For the rest of the time steps, the SoC is given by the SoC in the previous time step, and the input from the PV module, and batteries, formulated in Equation 4m. Equation 4n limits the maximum SoC of battery by the maximal capacity. The constraint formulated in Equation 4o ensures that the SoC of the battery is greater than, or equal to 20% at the end of the time horizon of the optimization. It is added in order to prevent insufficient battery capacity for the next day.

4.4 System Dispatch in Prosumpy

This chapter describes the system dispatch simulated in Prosumpy. The initial SoC is given as an input parameter to the model. The simulations will be used to analyze the annual dispatch of the system. The total covered demand, uncovered demand, energy surplus, amount of energy provided by the battery, and the average DoD will be investigated for the system before and after optimization. If the optimization model fails to fulfill the constraints for a day, the initial load profile will be considered when analyzing the system dispatch after optimization. The same model is used in the preliminary project, and the following paragraph is rewritten from the project [8, p.25-26].

The system is simulated in Prosumpy using annual PV data from pvlib and demand data from load profiles generated in RAMP. Further, the PV data and the demand are interpolated to have 15-minute time steps. The initial system in the model is grid-connected, and the variables are changed to simulate an off-grid system. Figure 8 visualizes the system and the corresponding variables in the model. "energySurplus" and "notCoveredDemand" are changed variables and were initially related to import and export to the grid. Additionally, the storage dispatch model aims to maximize self-consumption. When the PV power is insufficient to meet the load, the battery is fully discharged, and when the PV power exceeds the load, the battery is fully charged [60]. Furthermore, the total surplus energy of the system is calculated as the remaining energy from the PV production after subtracting the self-consumed energy. The demand that is not covered by either PV or storage is calculated as the remaining energy of the total demand minus the energy provided by the inverter.

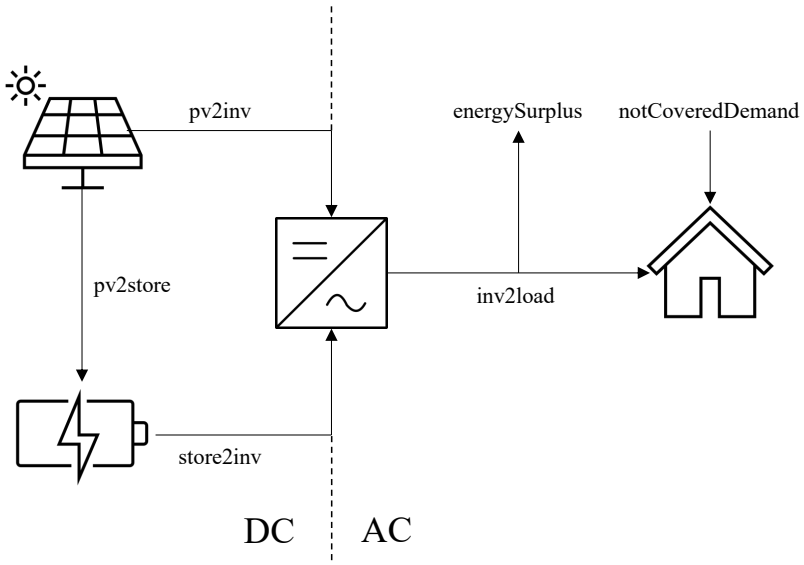

Figure 8: Overview of the system with corresponding variable names in Prosumpy.

Additionally, the maximum capacity of the inverter is implemented in the model. The power supplied to the load is not limited by the maximum capacity of the inverter. To comply with the limit, if the power exceeds the inverter's capacity, the energy from the storage is now reduced.

4.5 Development of the Graphical User Interface

To incentivize user flexibility, the surplus energy of the system has to be visualized in an easily understandable way in a GUI. Usually, inverter displays are hard to understand for non-technical staff. Therefore, the interface will include several features to increase the consumers' understanding of the energy available and suggest flexible behavior. The GUI is a first-stage proposal developed in Python. An essential part of the development is optimize the platform's functionalities based on feedback from the end users. The development of the GUI is divided into two parts; the backend and the frontend of the interface. Automatic download of the real-time data is included in the backend and the design of the platform represents the frontend. Chapter 4.5.1 and 4.5.2 presents the backend and the frontend development, respectively. Figure 9 visualizes the different interface development stages. It is essential to acknowledge that the GUI is currently an initial draft, and future improvements are necessary before the interface is usable for the end users.

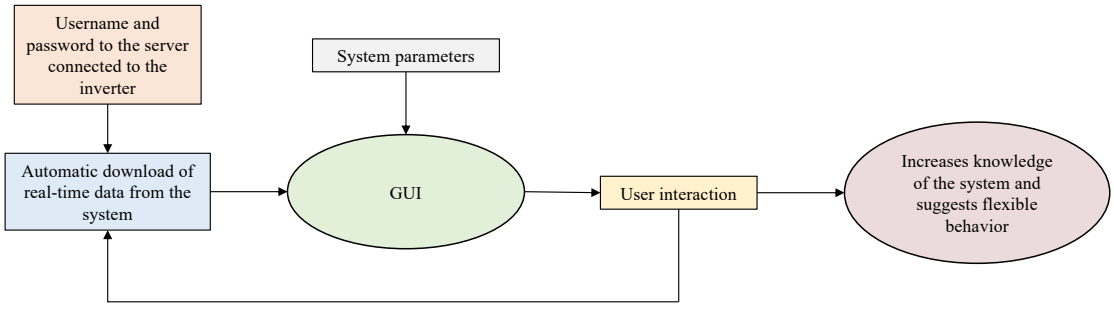

Figure 9: The different stages of GUI development.

4.5.1 Backend

A setup for automatically downloading real-time data from the system is presented in this chapter. To access the system's data, the inverter is assumed to be connected to an online server. It is necessary for the GUI to automatically download real-time data to ensure accurate results.

Selenium is a Python package that interacts with a web browser in Python scripts automatically [61]. Using Selenium, the script of the GUI automatically signs in and finds the correct elements for downloading real-time data by using the html code of the server. The utilized web driver is Google Chrome, where the driver allows one to choose the file path of the downloaded file as well as delete files with similar names to prevent the GUI from using outdated data. Additionally, the automation script for downloading real-time data can be run in "headless" mode, where the automation is invisible to the user. In the need for a validation code before signing in, a while loop is used to continue reading the validation code until it is correct to prevent incorrect code insertion. In order to keep the username and password confidential, the credentials are stored in a configuration file, and the Python module "configparser" is used to read the file. The Python script is presented in Appendix G.

4.5.2 Frontend

The overall design of the GUI is developed in Tkinter, a standard interface package in Python. In Tkinter, a main window, "the root", is created, and additional features, such as pictures, text, and buttons, are added to the root. In this case, different buttons are made with corresponding functionality. The act of clicking a button results in the closure of any concurrently open buttons, thereby enhancing the user-friendliness of the platform. As a main rule, high-power appliances are not allowed to be used simultaneously, as this most likely will exceed the maximum capacity of the inverter. Hence, the GUI do not take care of previously requested appliances when presenting the percentage of used capacity when an appliance is requested. Theoretical trends are also included to incorporate the results from the optimization model from Chapter 4.3. Both the questions to the end users and the theoretical trends will enhance user flexibility in the system. Figure 10 visualizes the buttons described in the following paragraphs. The provided buttons offer suggestions for different functionalities that can be incorporated into a GUI designed for off-grid systems in rural areas. In Appendix H, the Python script for the frontend is presented.

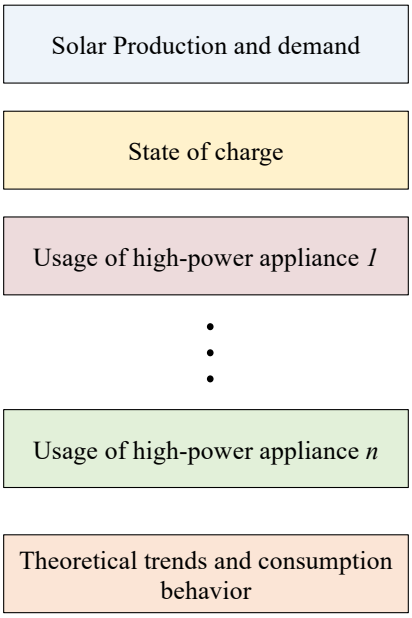

Figure 10: Visualization of the different functionalities in the GUI draft.

Solar Production and Demand

The first button visualizes today's solar production and demand, and shows the percentage of capacity used at the current time. As the real-time PV production is curtailed, the production of the current day is based on the production modeled in pvlib based on a TMY, including a forecasting error of ± 5%. However, the demand is real-time data from the online server. An example of the visualization of the PV production and the demand with fictive values is given in Figure 11.

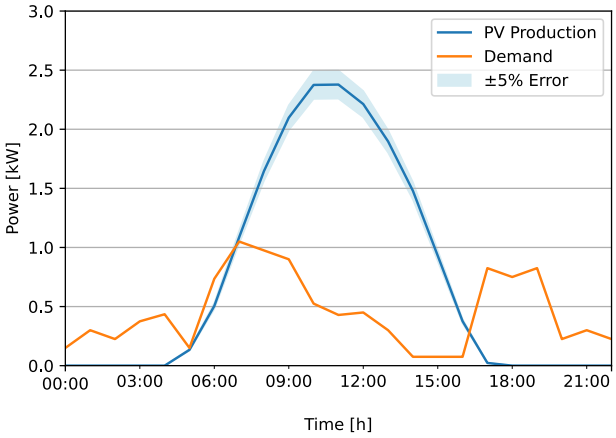

Figure 11: An example of visualization of PV production and demand in the GUI.

State of Charge

The second button visualizes a graph of the SoC of the day, and the current SoC is presented.

Usage of High-Power Appliances

The functionality of the third button focuses on assessing the possibility of utilizing a high-power appliance, such as an iron, a kettle, or a drill, at the given time. Each appliance will have its own button. The system retrieves the latest tracked SoC and demand to accomplish this. Equation 5 calculates the available energy in the battery and Equation 6 calculates the energy of using the specific appliance for time t.

$$E_{bat} = C_{bat} \cdot \eta_{bat} \cdot SOC_{now} \tag{5}$$

$$E_{appliance} = P_{appliance} \cdot t \tag{6}$$

If Equation 7 is true, the text: "You can use the appliance without any problem right now!" is printed, and the percentage of energy used, including the appliance performed, is presented. If not, the text: "Sorry, but there is not enough capacity to use the appliance now... Try again in 15 minutes!" is printed.

$$E_{bat} > E_{appliance} \;\; \& \;\; (D_{now} + P_{appliance} < C_{inv} \cdot \eta_{inv}) \tag{7}$$

Theoretical Trends and Consumption Behavior

Based on the optimization model outlined in Chapter 4.3, the sixth button will display the theoretical trends of the current period. Together with the real-time data from the system, the end

users will be given a comparison of the real-time data and the theoretical trend, and the input to the optimization model will be the current date and the battery's SoC at the beginning of the day. This feature will be useful for the end users, especially during the seasons when the PV production is limited.

5 Case Study: Eco Moyo Education Centre in Kenya

Eco Moyo is a Norwegian/Kenyan charity project offering free primary education to 240 children in the Dzunguni village and is the case study of this master's thesis. The Dzunguni village is located close to Kilifi on the coast of Kenya and is small and impoverished. Most of the inhabitants live in mud houses without access to electricity or running water. Eco Moyo is crucial in order to provide primary education to the underprivileged children in the village and help the inhabitant out of poverty. In March 2022, the school received a new solar and battery off-grid system to supply basic electricity needs in the teacher's area, the Staff Room. As a part of the master's thesis, a field trip to Eco Moyo was conducted in April/May 2023. This fieldwork was a continuation of the previous field trip to Eco Moyo in November 2022, which was carried out in conjunction with the preliminary project. In this chapter, relevant information about the existing system, relevant buildings, and seasonal variations are presented. Further, the preliminary project is presented, which establishes an essential foundation for the thesis. Following, the fieldwork is presented, with price estimates for a new system and an extension of the system, flexibility ranking of appliances, availability of appliances in the area, additional findings related to user consumption, and evaluation of the GUI. Finally, the input data for the methodology described in Chapter 4 are presented for this specific case study. Three different scenarios are based on this input; Scenario 0, Scenario 1, and Scenario 2, which involve implementing zero, one, and two additional batteries in the existing system, respectively.

5.1 Existing Solar and Battery Off-Grid System

The microgrid at Eco Moyo consists of seven solar panels of 450 Wp, four batteries of 200 Ah, and an inverter with a capacity of 3.50 kW. Today, the system provides the Staff Room with electricity and powers a fridge, lighting, PCs, tablets, phones, a printer, a fan, and a TV. Figure 12 offers an overview of the school area at Eco Moyo. The Staff Room is in the bottom right corner, with the old PV system on the roof. This is now moved to the kitchen area and power lights. However, the old system is unreliable, and the remaining lifetime is unknown. Table 2 presents the component parameters of the new system installed in the Staff Room. The remaining buildings use SHSs to provide electricity for lighting. However, the battery capacity is limited to charging a few phones and providing lighting during the evening.

Figure 12: Overview of The Staff Room and Classrooms at Eco Moyo [62, p.44].

Table 2: Components of the PV system installed at Eco Moyo in March 2022 [63].

Description	**Qty.**	**Capacity**
PV Panels	7	450 Wp
Hybrid PV Off-Grid Inverter	1	3.50 kW
Tubular Gel Battery	4	200 Ah/12.0 V

The new PV system is placed on the roof of Class 5, on the right side of the Staff Room in Figure 12. It was decided to place the panels on the roof of Class 5 due to the suitable tilt angle, azimuth, and location close to the Staff Room. The system consists of seven panels with a peak power of 450 Wp connected in series. Resulting in a total peak power of $3,150$ W. The tilt angle and azimuth of the panels are $6.2°$ and $-50°$, respectively [63]. Figure 13 show the PV panels on the roof of Class 5, and the datasheet is included in Appendix A.

Figure 13: The PV panels located on the roof of Class 5 at Eco Moyo.

A battery pack of four tubular gel batteries is installed in the Staff Room. Each battery has an output voltage of 12 V and a capacity of 200 Ah. They are connected in series, resulting in a total output voltage of 48 V and a capacity of 800 Ah. Appendix C includes the datasheet of the batteries. Figure 14 show the inverter installed in the Staff Room. It is a hybrid PV off-grid inverter from the brand Growatt. It has an integrated MPPT controller and a rated output of 3.50 kW. The datasheet of the inverter is included in Appendix B.

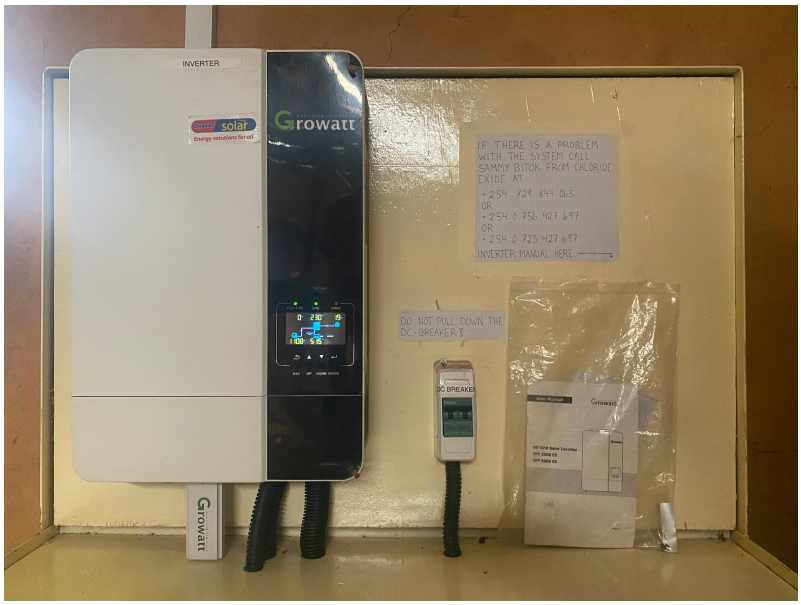

Figure 14: The inverter located in the Staff Room at Eco Moyo.

Growatt also offers an online server called ShineDesign, with real-time data from the inverter. It displays battery percentage, PV production, and consumption, among other system parameters. A screenshot of the online server is provided in Figure 15.

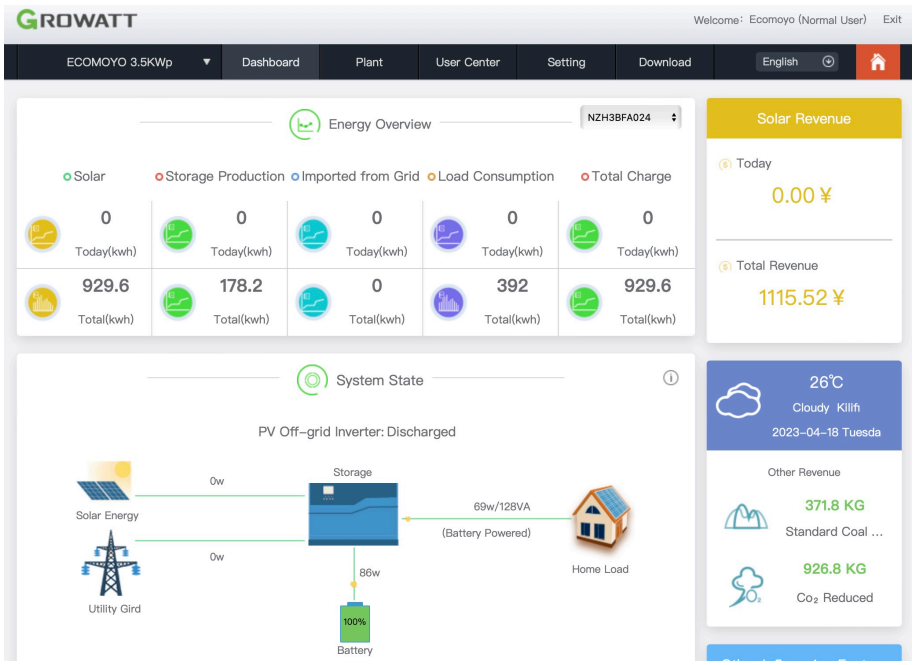

Figure 15: A screenshot of the online server, ShineDesign, connected to the inverter.

5.2 Overview of Relevant Buildings

This chapter provides an overview of the relevant buildings at Eco Moyo. In order to investigate the possibility of incentivizing user flexibility, the system is extended to provide electricity to the Staff Court and Office Building. Chapter 5.2.1, 5.2.2, and 5.2.3 outline the buildings and their designated areas of use.

5.2.1 Staff Room

As previously mentioned, the microgrid at Eco Moyo is located in the Staff Room. The building is located close to the classrooms and is frequently used by the teachers during the day. There are currently 12 teachers working at Eco Moyo, and six of them are living at the school. Until the afternoon, the building is used as an office, where the teachers charge their computers and phones. During the evening, the building is used as a hangout area by the teachers living at the property. They often gather in the Staff Room to watch TV or charge their belongings during the evening. The building is also used during the weekends. However, some of the teachers leave the property during the weekends, resulting in reduced activity. During the longer vacations, the teachers usually leave the property, and the activity in the Staff Room is limited. Figure 16 shows the outside of the Staff Room building.

Figure 16: The outside of the Staff Room at Eco Moyo.

5.2.2 Staff Court

The Staff Court accommodates the six teachers living on the property. It is located close to the Staff Room and consists of six simple bedrooms and an outside hangout area. Currently, the only electricity supply in the building is SHSs providing lighting. However, by installing a cable from the Staff Room to the Staff Court, it would be possible to provide electricity in this building as well. Conversations with the founder during the field trip in November 2022 revealed that it is desired to increase the standard of living for the teachers. This will make the teacher positions alluring and attract talented and motivated teachers. Today there is an issue that the teachers quit if they are offered a position at a public school where the terms are better. Hence, increasing the living standard at the Staff Court will help to increase the quality of education at Eco Moyo. Figure 17 shows the outside of the Staff Court.

Figure 17: The outside of the Staff Court at Eco Moyo.

5.2.3 Office Building

The Office Building is located straight across from the Staff Room and contains two offices. There is no electricity supply in the building, but due to the short distance from the Staff Room, an extension cord is sometimes used to power a printer. However, this solution is not sustainable due to the fire risk. A possible solution is to install a cable from the Staff Room to the Office Building. During the field trip in November 2022, the School Director expressed the need for a fan and lighting in the office. Figure 18 shows the outside of the Office Building.

Figure 18: The outside of the Office Building at Eco Moyo.

5.3 Seasonal Variations

Eco Moyo is situated in Kilifi, a coastal county characterized by a tropical climate that experiences distinct wet and dry seasons. Primarily, the rainfall seasons are divided into two; "long rains" and "short rains" season. The long rain season is the period from March through May, while the

short rain season occurs from October through December. During January and February, Kenya experiences the dry season, with dry weather and sunny conditions. The major rainfall season is the long rain season which extends across large parts of Kenya [64]. Figure 19 shows the rainfall averages and precipitation in Kilifi, displaying the different seasons clearly.

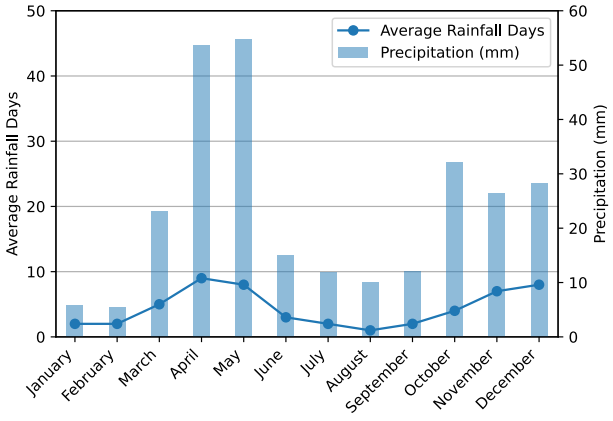

Figure 19: Historical rainfall averages for Kilifi [65].

5.4 Preliminary Project

Simulating the existing off-grid system at Eco Moyo was a crucial aspect of the preliminary project. Realistic load profiles for the Staff Room were modeled using the RAMP model and data collected during a field trip to Eco Moyo in November 2022. The production of the PV system was modeled using pvlib and input data from PVGIS. Different scenarios were simulated using Prosumpy to test the behavior of the microgrid and its ability to sustain additional loads.

The initial scenario in the preliminary project describes the appliances present in the Staff Room when the project was conducted. The aim of the scenario was to analyze how much of the system's capacity was utilized with the current loads. The loads present at the time were indoor and outdoor lighting, charging of phones, tablets, and laptops, a TV, and a fan. Figure 20 depicts the weekly results in Prosumpy from the simulation of week 23 in June 2019. This is during the cold season, as described in Chapter 4.2, where the PV production is at the lowest during the year. The weekly PV production, power consumption, SoC, and surplus energy are illustrated. The yellow graph presents PV production; the black presents power consumption; the grey present SoC, and the green presents energy surplus. It can be seen that the peak loads are generally seen during the day and that the battery discharge level is insignificant. The energy surplus is large during the day when the PV production is high.

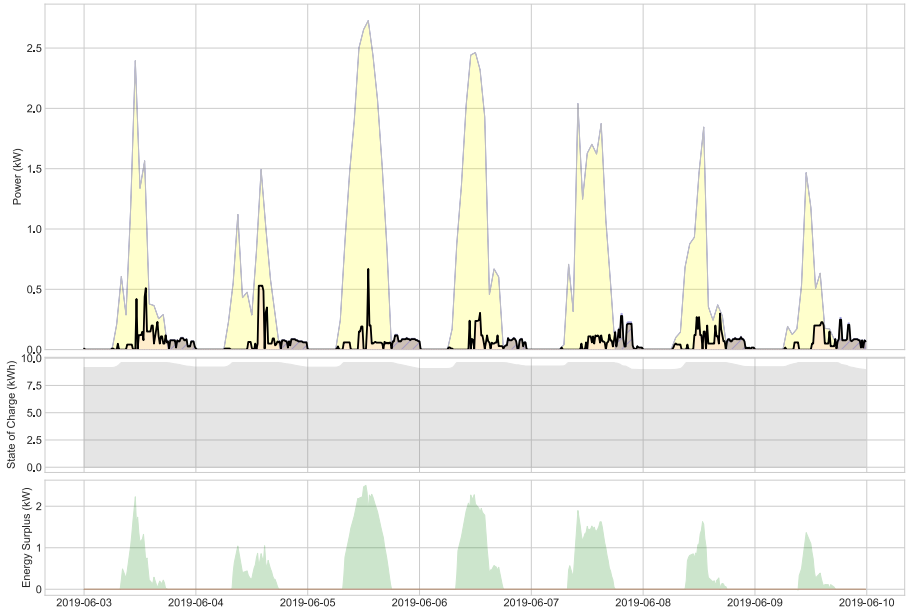

Figure 20: Weekly results in Prosumpy for the cold season (week 23) from the base case the preliminary project.

The simulations from the preliminary project show the immense potential for implementing additional loads without any difficulties in the existing microgrid at Eco Moyo. Based on the results from the project, a fridge was implemented. Today there is only electricity in the Staff Room, and there is a lot of surplus energy being wasted.

5.5 Fieldwork

The fieldwork in November involved data collection, observations of user behavior, and the operation of the existing system. The second field trip in April/May 2023 focused on obtaining price estimates for extending the existing system and implementing a new system for electrifying other buildings at the school. Additionally, meetings with the teachers were performed to get end users' opinions about flexible behavior proposals, flexibility ranking of appliances, and feedback on the GUI proposal. The availability of different appliances close to Eco Moyo was also examined to get a reasonable insight into appliances to include in the extension of the system. Different peaks in ShineDesign corresponding to high-power appliances were observed.

5.5.1 Extension of the Existing System

The existing microgrid at Eco Moyo is capable of providing electricity to several buildings at the school due to its capacity. Several teachers have expressed a desire for outside lights for the school's outdoor area and the toilets in the Staff Court. Hence, a price estimate for extending the system from the Staff Room to the Staff Court is provided. The price estimate includes all the essential supplies required for installing sockets, indoor-, and outdoor LED in the teachers' rooms, and the result is presented in Table 3. The price is converted from KES to USD with a conversion rate of 0.0072, and the total cost of the extension is approximately 600 USD. A more detailed list of supplies is provided with local valuta in Appendix D.

Table 3: Description of the price estimate for the extension of the system.

Description	**Qty.**	**Total Price [USD]**
Single sockets	6	10.80
Twin sockets	6	18.14
Cables	-	257.8
LED bulbs 7 W	12	17.28
Light switch	6	10.37
Distribution board	1	38.16
Other necessary supplies	-	238.8

5.5.2 New System in the Staff Court

An alternative approach to electrify the Staff Court is to introduce a new off-grid system designed for similar loads as the existing system in the Staff Room. However, the new system is designed for a user time for fans of 10 hours per day, which is significantly higher than observed during the fieldwork. As a result, the number of batteries is doubled compared to the system in the Staff Room. Further description of the new system is presented in Table 4, with an estimated total cost of approximately 8500 USD. In addition, the cost of an extra battery is estimated to cost approximately 600 USD, covering installation labor and transportation. The system is proposed by a local company.

Table 4: Description of the price estimate for the new system.

Description	**Qty.**
PV module	6
Battery	8
Inverter and associated equipment	1
MPPT charge controller	1
Installation materials	1
Installation labor	1
Transport and logistics	-
Other necessary supplies	-

5.5.3 Flexibility Ranking of Appliances

To better understand which appliances the end users of the system value the most, a scheme of all the appliances was given to the teachers. This scheme aimed to get a ranking of the importance of the appliances, where 1 is the most important, and 11 is the least important. This ranking list is essential to establish the flexibility of the appliances, where the least flexible appliance will have the highest disutility cost. The ranking is presented in Table 5.

Table 5: Ranking of the importance of the appliances from the teachers.

Appliance	**Ranking of Importance**
Phone	1
Laptop	3
TV	2
Printer	9
Tablet	4
Iron	5
Kettle	7
Drill	11
Speaker	6
Radio	8
Fan	10

5.5.4 Availability of Appliances in Kilifi

As part of the fieldwork, an investigation was conducted into various appliances' availability and power ratings. The examination involved assessing the appliances found at the nearest supermarket in Kilifi, which featured a range of appliances with different power ratings, such as fridges, kettles, irons, and speakers, presented in Table 6. An iron is currently present at the school, but the power rating is 2000 W. However, an iron with a lower power rating is found at the supermarket. The teachers also wished for new speakers, as the old ones are broken. Unfortunately, the speakers found at the supermarket are of bad quality, but the power rating is used as a reference.

Table 6: Appliances with corresponding power ratings found in Kilifi.

Appliance	**Power Rating [W]**
Fridge	90
Iron	1200
Kettle	2200
Speaker	100

5.5.5 Additional Findings Related to User Consumption

When examining the existing appliances in the Staff Room, the iron was tested on the system. The objective was to detect the result in the online server, ShineDesign, and the result is presented in Figure 21a. In the figure, a distinct peak around 10:00 indicates the usage of the iron. The following observation is provided in Figure 21b where a peak is observed around 7:00. This peak aligns with the power rating of a drill. Notably, the drill has a power rating of 500 W, whereas the fridge operates at 90 W, which corresponds to the peak. Furthermore, the demand curves depicted in both figures clearly illustrate the duty cycles of the installed fridge. Due to the continuous recording of real-time data when loads consume energy, the horizontal axis of Figure 21a and 21b shows different time steps.

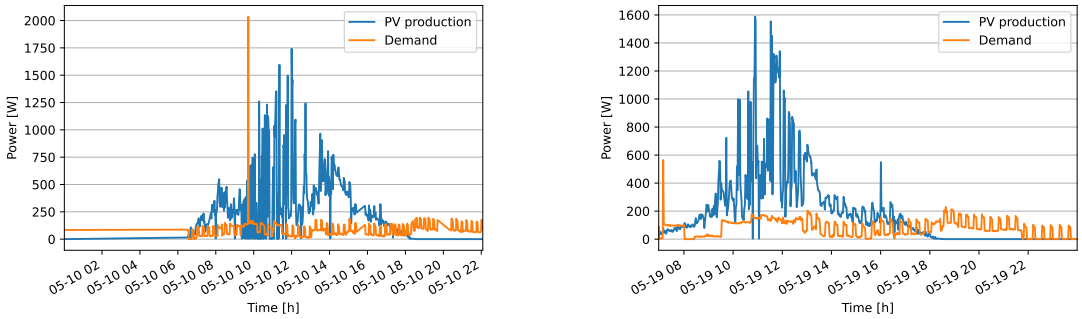

(a) PV production and demand from May 10th.

(b) PV production and demand from May 19th.

Figure 21: Observations of different energy peaks at Eco Moyo with data from ShineDesign.

5.5.6 Evaluation of the Graphical User Interface

According to the teachers, the inverter display is hard to understand, and they were favorable to a user-friendly GUI. The inverter's display, visualized in Figure 22, presents different parameters regarding PV production, load, and storage, and the end users do not consider these parameters as crucial. Thus, the developed GUI draft should present the information in an understandable way. The teachers emphasized the importance of presenting inverter data in percentage form, and they responded positively to the proposal regarding optimal user behavior. Hence, the GUI is designed to include various buttons that allow end users to inquire about the current feasibility of using appliances such as a kettle, an iron, or a drill. They can then receive a simple yes or no response. The developed GUI draft is more interactive than the ShineDesign server, which they do not have access to.

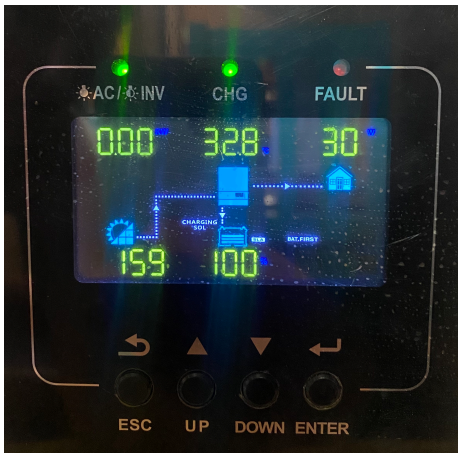

Figure 22: Display of the inverter at Eco Moyo.

5.6 Input Data

The input data for Eco Moyo for the methodology, described in Chapter 4, is presented in this chapter. This includes the site parameters for PV production in pvlib, input data for generating load profiles in RAMP, system parameters for the dispatch in Prosumpy, and input to the optimization model. Furthermore, three different scenarios are simulated, and the load profiles are optimized. Scenario 0 considers the existing system at Eco Moyo, presented in Chapter 5.1. Scenarios 1 and 2 consider the system with one and two additional batteries of 200 Ah, respectively. The effect of the increased battery capacity is investigated in order to see how it affects the flexibility in the system, and the possibility to reduce uncovered demand.

5.6.1 PV Production in pvlib python

To create a representative dataset for the PV production modeled in Chapter 4.1, a TMY based on data from 2005-2020 is generated. Table 7 presents the years the data for each month in the TMY is collected from. The location and site parameters of Eco Moyo are listed in Table 8.

Table 7: Data used for a TMY based on data from 2005-2020.

Month	**Year**
January	2005
February	2015
March	2007
April	2006
May	2014
June	2010
July	2006
August	2012
September	2013
October	2014
November	2015
December	2008

Table 8: Location input parameters for Eco Moyo in pvlib.

Parameter	**Value**
Latitude	3.5°S
Longitude	39.8°E
Altitude	58 m
Timezone	GMT+3
Slope	6.8°
Azimuth	-50°

5.6.2 Load Profiles in RAMP

When generating load profiles at Eco Moyo, only the *User* and *Appliance* layers in RAMP are used. The buildings at the school are considered different *Users* while the appliances in each building are a part of the *Appliance* layer. Table 9 shows the rated power of the different appliances modeled at Eco Moyo. As discussed in Chapter 4.2, a unique load profile is generated for each appliance in order to identify the specific behavior of each appliance. However, some of the appliances in the Staff Room and Staff Court are combined to reduce the run time of the optimization model. The power ratings of the different appliances are based on the fieldwork.

Table 9: Power rating of the appliances modeled at Eco Moyo.

Appliance	**Power Rating [W]**
TV	70
Phone	7
Laptop	60
Fan	50
Indoor LED	9
Outdoor LED	9
Tablet	15
Fridge	90
Iron	1200
Printer	200
Kettle	2200

In [63], an annual load profile for Eco Moyo is generated for the entire school with additional appliances. Different seasons are established to include variations in user behavior due to the change in temperature. The year is divided into three seasons dependent on the monthly average temperature, presented in Table 10. In addition to the variations in temperature, the user behavior at the school also depends on the school and visitor activity. Table 11 presents the different periods during a year based on the seasons, school, and visitor activity. By associating different parameters with the appliances in each period, annual load profiles can be generated using the RAMP model.

Table 10: Climate seasons defined by monthly average temperatures [63].

Season Type	**Temperature [°C]**
Hot	27.1 - 28.5
Warm	25.1 - 26.3
Cold	24.1 - 24.9

Table 11: Time periods for the RAMP model input to establish annual load profiles [63].

Start date	**End date**	**Climate Season**	**School Activity**	**Visitor Activity**
January 1	January 31	Hot	Regular	High
February 1	February 7	Hot	Mid-term vacation	High
February 8	March 31	Hot	Regular	High
April 1	April 30	Hot	Vacation	High
May 1	May 31	Warm	Regular	Low
June 1	July 31	Cold	Regular	Low
August 1	August 31	Cold	Vacation	Low
September 1	September 23	Warm	Regular	Low
September 24	October 31	Warm	Regular	High
November 1	November 15	Hot	Regular	High
November 15	December 31	Hot	Vacation	High

The input parameters for the fridges at Eco Moyo are based on a specific fridge from a retailer in Kilifi, as mentioned in Chapter 5.5.4. It has a peak power of 90 W and a yearly consumption of 231 kWh. A similar fridge is now installed at the school. In order to achieve the rated annual energy consumption, the default duty cycles in the RAMP model are modified, as illustrated in Figure 23. The duration of the standby mode is increased compared to the default cycles in Figure 7. Further, the power consumption is increased to 7 W, compared to 5 W [38]. Table 12 shows the duration of the different duty cycles, and Table 13 shows what timeframes the different cycles' are associated with, varying with the hot, warm, and cold seasons. All the modeled fridges at Eco Moyo are based on the same input parameters and duty cycles.

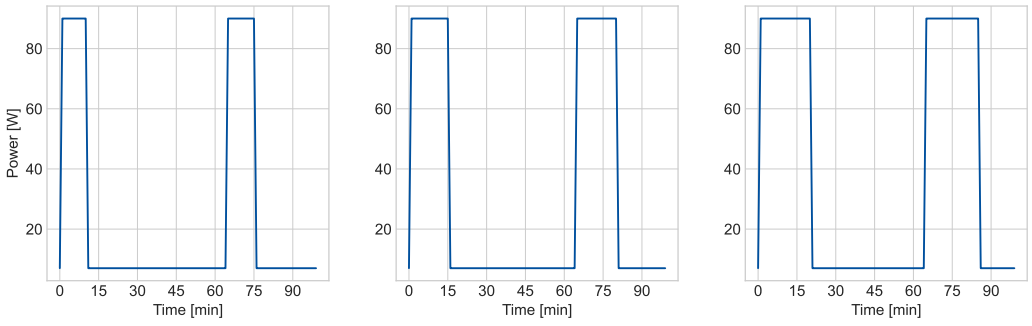

(a) Standard Cycle (b) Intermediate Cycle (c) Intensive Cycle

Figure 23: Duty cycles of the fridges modeled at Eco Moyo.

Table 12: Duration of the duty cycles of the fridges modeled at Eco Moyo.

Cycle	Standby [min]	Cooling [min]
Standard	55	10
Intermediate	50	15
Intensive	45	20

Table 13: Seasonal variations in the duty cycles of the fridges modeled at Eco Moyo.

Season Type	Standard Cycle	Intermediate Cycle	Intensive Cycle
Hot	00:00 - 05:59	06:00 - 07:59	08:00 - 19:00
	19:01 - 23:59	-	-
Warm	00:00 - 06:59	07:00 - 10:39	10:40 - 16:00
	16:01 - 23:59	-	-
Cold	00:00 - 04:00	06:00 - 18:00	-
	18:01 - 23:59	-	-

The appliances with belonging parameters for the Staff Room, Staff Court, and Office Building are presented below.

Staff Room

The seasonal variations of the loads are mainly considered in the Staff Room. This is the only building with access to electricity today, and where there are observations of variations during the different periods. The Staff Room is also the only building where the demand is affected by visitor activity. Hence, the number of phones and laptops varies with the different time periods. The Indoor LED, outdoor LED, and fridge are fixed loads, which means that the appliances are always switched on during the entire time window each day. The load profiles of the phones and laptops in the Staff Room are simplified to include several appliances in each load profile. It is modeled four different load profiles for the phones, where one includes four phones and the others include two phones each. For the laptops three different load profiles are modeled. Two of them include two laptops, and the third include four. Table 14, 15, and 16 present the input data for the appliances in the Staff Room during the hot and warm season with high visitor activity, vacations, and the cold and warm season with low visitor activity, respectively.

Table 14: Input data for the Staff Room - hot and warm season - high visitor activity.

				Weekdays			Weekends		
Appliance	**P**	**freq.**	**tot_use**	**m**	**Window 1**	**Window 2**	**m**	**Window 1**	**Window 2**
Indoor LED	9	100	-	2	06:00 - 07:00	18:00 - 23:59	2	06:00 - 07:00	18:00 - 23:59
Outdoor LED	9	100	-	2	06:00 - 07:00	18:00 - 23:59	2	06:00 - 07:00	18:00 - 23:59
Fridge	90	100	-	1	00:00 - 23:59	-	1	00:00 - 23:59	-
Phone	7	100	120	10	07:00 - 19:00	-	6	07:00 - 19:00	-
Laptop	60	100	120	8	07:00 - 19:00	-	4	09:00 - 20:00	-
TV	70	100	240	1	16:00 - 23:59	-	1	10:00 - 23:59	-
Printer	200	43	30	1	07:00 - 19:00	-	1	07:00 - 19:00	-
Tablet	15	40	120	10	10:00 - 16:00	-	-	-	-
Iron	1200	43	30	1	12:00 - 15:00	-	1	12:00 - 15:00	-
Kettle	2200	100	15	1	10:00 - 12:00	14:00 - 17:00	1	10:00 - 12:00	14:00 - 17:00
Drill	500	60	120	1	07:00 - 16:00	-	1	-	-
Speaker	100	100	120	1	15:00 - 18:00	-	1	12:00 - 18:00	-
Radio	36	100	120	1	16:00 - 22:00	-	1	12:00 - 22:00	-

Table 15: Input data for the Staff Room - vacation and mid-term vacation.

Appliance	P	freq.	tot_use	m	Window 1	Window 2
Indoor LED	9	100	-	2	06:00 - 07:00	18:00 - 23:59
Outdoor LED	9	100	-	2	06:00 - 07:00	18:00 - 23:59
Fridge	90	100	-	1	00:00 - 23:59	-
Phone	7	100	120	6	07:00 - 19:00	-
Laptop	60	100	120	2	07:00 - 19:00	-
TV	70	100	240	1	10:00 - 23:59	-
Printer	200	43	30	1	07:00 - 19:00	-
Tablet	-	-	-	-	-	-
Iron	1200	43	30	1	12:00 - 15:00	-
Kettle	2200	100	15	1	10:00 - 12:00	14:00 - 17:00
Drill	-	-	-	-	-	-
Speaker	100	100	120	1	12:00 - 18:00	-
Radio	36	100	120	1	12:00 - 22:00	-

Table 16: Input data for the Staff Room - cold and warm season - low visitor activity.

				Weekdays			Weekends		
Appliance	P	freq.	tot_use	m	Window 1	Window 2	m	Window 1	Window 2
Indoor LED	9	100	-	2	06:00 - 07:00	18:00 - 23:59	2	06:00 - 07:00	18:00-23:59
Outdoor LED	9	100	-	2	06:00 - 07:00	18:00 - 23:59	2	06:00 - 07:00	18:00-23:59
Fridge	90	100	-	1	00:00 - 23:59	-	1	00:00 - 23:59	-
Phone	7	100	120	8	07:00 - 19:00	-	4	07:00 - 19:00	-
Laptop	60	100	120	8	07:00 - 19:00	-	4	09:00 - 20:00	-
TV	70	100	240	1	16:00 - 23:59	-	1	10:00 - 23:59	-
Printer	200	43	30	1	07:00 - 19:00	-	1	07:00 - 19:00	-
Tablet	15	40	120	10	10:00 - 16:00	-	-	-	-
Iron	1200	43	30	1	12:00 - 15:00	-	1	12:00 - 15:00	-
Kettle	2200	100	15	1	10:00 - 12:00	14:00 - 17:00	1	10:00 - 12:00	14:00 - 17:00
Drill	500	60	120	1	07:00 - 16:00	-	1	-	-
Speaker	100	100	120	1	15:00 - 18:00	-	1	12:00 - 18:00	-
Radio	36	100	120	1	16:00 - 22:00	-	1	12:00 - 22:00	-

Table 17: Input data for the fans in the Staff Room.

					Window		
Appliance	P	freq.	m	tot_use	Hot season	Warm season	Cold season
Fan	50	100	2	360	12:00 - 23:59	12:00 - 23:59	12:00 - 20:00

Staff Court

In the Staff Court, the indoor LED and outdoor LED are fixed loads. All of the appliances are used every day of the week, but the number of appliances is reduced during the weekends. Input data for the appliances in the Staff Court is presented in Table 18. To simplify the model, the load profiles of the phones, laptops, TVs, and radios in the Staff Court are aggregated to include three appliances in each profile. Hence, there are two load profiles for each of the appliances mentioned above.

Table 18: Input data for the Staff Court.

				Weekdays			Weekends		
Appliance	**P**	**freq.**	**tot_use**	**m**	**Window 1**	**Window 2**	**m**	**Window 1**	**Window 2**
Indoor LED	9	100	-	12	06:00 - 07:00	18:00 - 23:59	6	06:00 - 07:00	18:00 - 23:59
Outdoor LED	9	100	-	6	00:00 - 07:00	18:00 - 23:59	6	00:00 - 07:00	18:00 - 23:59
Phone	7	100	120	6	17:00 - 23:59	-	3	18:00 - 23:59	-
Laptop	60	100	120	6	17:00 - 23:59	-	3	18:00 - 23:59	-
TV	70	100	240	6	16:00 - 23:59	-	3	10:00 - 23:59	-
Speaker	100	100	120	1	17:00 - 20:00	-	1	09:00 - 20:00	-
Radio	36	100	120	6	17:00 - 22:00	-	3	09:00 - 22:00	-

Table 19: Input data for the fans in the Staff Court.

				Weekdays		Weekends	
Appliance	**P**	**freq.**	**tot_use**	**m**	**Window 1**	**m**	**Window 1**
Fan	50	100	360	6	16:00 - 23:59	3	12:00 - 23:59

Office Building

The Office Building is only used during weekdays with regular school activity. All of the appliances are used every day during weekdays. The input data for the appliances in the Office Building is presented in Table 20.

Table 20: Input data for the Office Building.

				Weekdays			Vacations		
Appliance	**P**	**freq.**	**tot_use**	**m**	**Window 1**	**Window 2**	**m**	**Window 1**	**Window 2**
Indoor LED	9	100	-	2	07:00 - 17:00	-	-	-	-
Outdoor LED	9	100	-	2	19:00 - 22:00	-	-	-	-
Fridge	90	100	-	1	00:00 - 23:59	-	1	00:00 - 23:59	-
Phone	7	100	120	2	07:00 - 17:00	-	-	-	-
Laptop	60	100	120	2	07:00 - 17:00	-	-	-	-
Printer	200	100	30	2	07:00 - 17:00	-	-	-	-
Radio	36	100	120	2	12:00 - 18:00	-	-	-	-

Table 21: Input data for the fans in the Office Building.

				Weekdays	
Appliance	**P**	**freq.**	**tot_use**	**m**	**Window 1**
Fan	50	100	360	2	10:00 - 17:00

5.6.3 Optimization Model

The appliances in the system at Eco Moyo are divided into three categories; shiftable loads, non-shiftable loads, and other controllable loads. The classification of the appliances are presented in Table 22. Appliances where the purpose of load shifting is preventing overload, are classified as high-power appliances. However, these categories are slightly modified to fit in the optimization model, presented in Chapter 4.3. The fridges are considered non-shiftable loads, and the fans are shiftable loads.

Table 22: Classification, flexibility scale and purpose of load shifting for all the appliances.

Classification		Flexibility Scale		Purpose of Load Shifting	
Load Category	**Appliance**	**Low Flexibility Capacity**	**High Flexibility Capacity**	**Energy Saving**	**Prevent Overload**
Shiftable loads	Phone		x	x	
	Laptop		x	x	
	TV		x	x	
	Printer		x	x	
	Tablet		x	x	
	Iron		x		x
	Kettle		x		x
	Drill		x		x
	Speaker		x	x	
	Radio		x	x	
Non-shiftable loads	Indoor LED	x		x	
	Outdoor LED	x		x	
Other controllable loads	Fan		x	x	
	Fridge	x		x	

To decide the optimal scheduling of the flexible loads at Eco Moyo by minimizing the disutility cost of shifting loads, the optimization model considers a time horizon from 00:00 to 23:45 for a given day with time steps of 15 minutes. To simulate a whole year, the model is run 365 times. Table 23 presents the disutility cost of shifting the different appliances at Eco Moyo. The values are based on the ranking in Table 5 from the fieldwork. Moreover, the disutility cost has no unit as the essential factor is the ratio between the values. When the model is run for a whole year, the initial SoC is given as the SoC in the last time step of the previously modeled day. If the optimization model fails, meaning it is unable to fulfill the constraints, the SoC for the next day is set to 20%.

Table 23: Disutility cost of moving the appliances one time step.

Appliance	**Disutility Cost**
Phone	100
TV	90
Laptop	85
Tablet	65
Iron	60
Speaker	50
Kettle	30
Radio	25
Printer	20
Fan	15
Drill	10

Results from the optimization model will be used to analyze how load shifting affects end user consumption at Eco Moyo. The SoC and surplus energy will be analyzed on dates when loads are shifted, or the system is unable to fulfill the constraints.

5.6.4 System Dispatch in Prosumpy

Table 24 presents the technical parameters for the existing system at Eco Moyo, used as input data to the system dispatch in Prosumpy. The parameters regarding the PV system, inverter, and batteries are found in the datasheets in Appendix A, B, and C, respectively.

Parameter	Value
PV Size	3.15 kW
Battery Capacity	9.60 kWh
Battery Efficiency	90.0%
Inverter Efficiency	93.0%
Time step	0.25
Max Power	3.50 kW

Table 24: Technical input parameters for the system at Eco Moyo in Prosumpy.

5.6.5 Development of the Graphical User Interface

As mentioned in Chapter 5.5.6, the surplus energy of the system has to be visualized in an easily understandable way in a GUI. Real-time data is automatically downloaded from ShineDesign. The SoC available in the server is presented in four levels from 0-100%. Hence, the accurate SoC is not available. Additionally, the end user does not have access to ShineDesign. The inverter's display at Eco Moyo is hard to understand for the users, and the field trip revealed that the teachers preferred the data in percentage. The proposed user behavior is given as questions to the end users. As described in Chapter 4.5, different buttons for the usage of high-power appliances are included in the GUI. At Eco Moyo, three buttons are implemented for the usage of the kettle, the iron, and the Drill in the Staff Room.

6 Results

This chapter presents the results of the master's thesis. The modeled PV production and demand are described. Further, the results of the optimization model and annual system dispatch in Prosumpy are analyzed. Three different scenarios are considered. Scenario 0 considers the existing system in the Staff Room with the additional load in the Staff Court and Office Building. This scenario investigates if the existing system is able to supply the additional buildings when flexible consumption behavior is implemented. In Scenario 1, an additional battery is included. This scenario investigates how the additional battery capacity affects the flexibility and disutility of the consumers when supplying the additional buildings. Scenario 2 includes two additional batteries and investigates how a further increase in battery capacity affects the system. The batteries' SoC and the system's surplus energy are analyzed on dates when loads are shifted, or the system is unable to fulfill the constraints of the optimization model. Further, the costs of the different approaches to the electrification of the Staff Court are presented. Finally, the design proposal of an early-stage GUI for end user communication is presented, and the functionalities are visualized.

6.1 PV Production and Demand

Figure 24 depicts the monthly PV production and demand for the modeled year in kWh. The production is consistently higher than the demand. As expected, the results show that the PV production is significantly decreased from April through July. This includes the long rain season from March through May, as described in Chapter 5.3. However, in the short rain season from October through December, the reduction in production is not as remarkable. On the other hand, the demand is more consistent. There is a range of about 50 kWh throughout the year. Despite the small range, the result shows that the demand reaches its maximum during the short rain season when the production is at the minimum. The total annual demand and PV production are 3916 kWh and 6605 kWh, respectively.

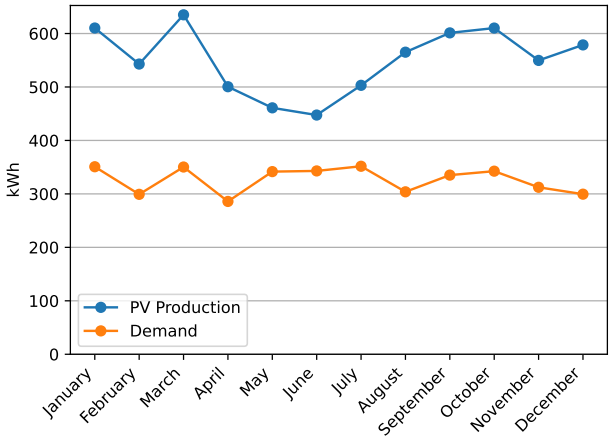

Figure 24: Modeled monthly PV production and demand for the modeled year.

In Figure 25, the comparison between the real-time and modeled PV production is presented. The real-time data obtained from the inverter does not represent the total PV production accurately due to the curtailment by the inverter controller. In an off-grid system, the inverter does not accurately measure the total PV production, as any excess energy beyond what is required to power the load and charge the storage is not accounted for. As a result, the modeled production is considerably higher than the recorded real-time production obtained by the inverter.

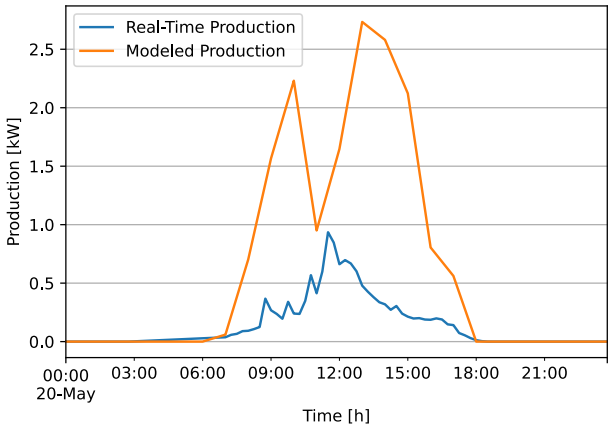

Figure 25: Real-time and modeled PV production of May 20th, 2023.

6.2 Optimization Model

6.2.1 Scenario 0

The detailed results of the optimization of Scenario 0 are presented in Table E.38 in Appendix E.1. There are 27 days throughout the year when the optimization model moves shiftable loads and ensures that the demand is covered. It is mainly the kettle in the Staff Room that is moved. However, the drill, printer, and fans are also shifted occasionally. With the exception of three dates, only one load is shifted for a few time steps. On May 24th and July 6th, two and three fans are shifted. Table 25 shows initial and new time windows on July 7th, where eight loads are shifted.

Table 25: Initial and new time windows after optimization July 7th in Scenario 0.

Appliance	Number	Building	Initial Window	New Window
Fan	1	Staff Room	12:15 - 18:15	11:30 - 17:30
Fan	1	Staff Room	12:45 - 18:45	11:30 - 17:30
Kettle	1	Staff Room	16:15 - 16:30	12:45 - 13:00
Drill	1	Staff Room	07:30 - 09:30	07:45 - 09:45
Fan	1	Office Building	10:45 - 16:45	09:30 - 15:30
Fan	1	Office Building	11:15 - 17:15	13:30 - 19:30
Fan	3	Staff Court	16:15 - 22:15	11:30 - 17:30
Fan	3	Staff Court	16:15 - 22:15	13:30 - 19:30

Figure 26 and 27 show the system dispatch of July 7th before and after optimization. In Figure 26 it can be seen that there are three different load peaks. Two of them are during the day when there are PV production, and one is after the sun has set. The total demand increase severely during the evening and the battery is discharged. Even though there is no uncovered demand with the initial load profiles, the SoC is below 20% at the end of the day, and eight loads are shifted by the optimization model. The highest peak before the optimization is caused by the kettle. Hence, the kettle is shifted for three and a half hours to get the highest peak during the day. The drill also has a relatively high power consumption of 500 W in the morning. However, it is only shifted 15 minutes when the PV production is slightly higher. Additionally, all the fans are shifted. The fans in the Staff Room and Office Building are shifted for a few time steps. However, the fans in the Staff Court are shifted for a longer time period. These load profiles include several fans, and the time windows are during the evening. This results in lower power consumption during the evening, and the SoC is 20% at the end of the day after optimization.

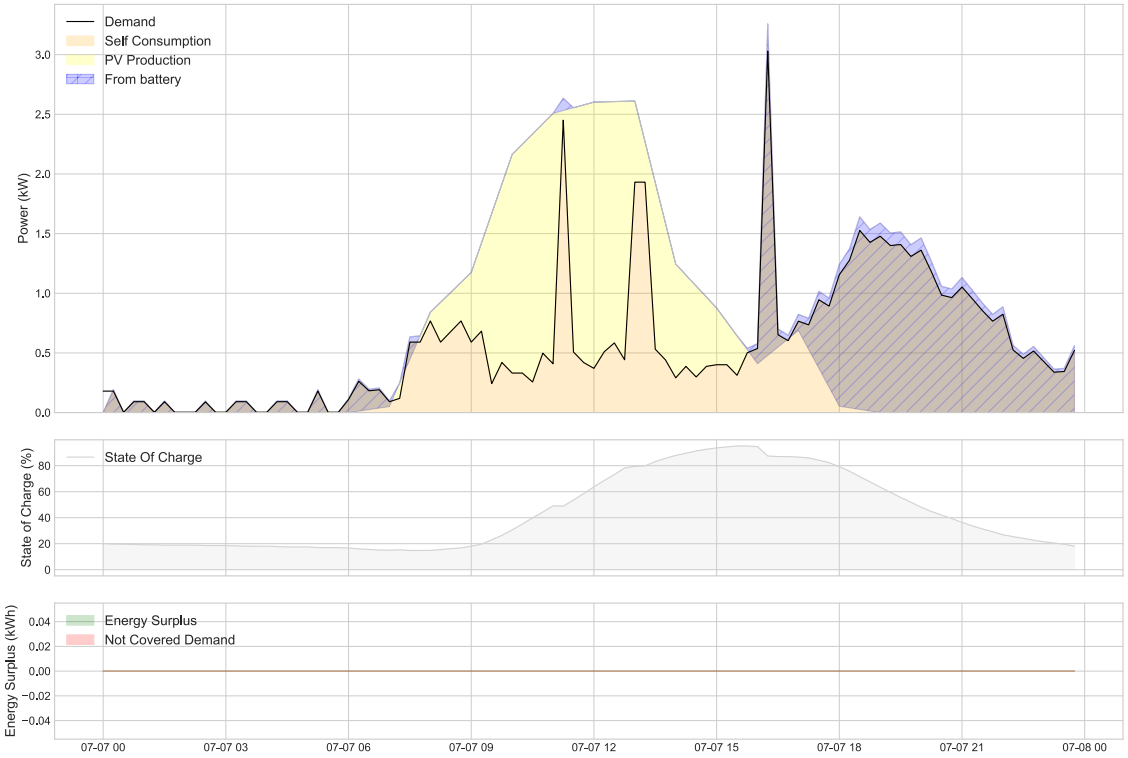

Figure 26: System dispatch in Prosumpy July 7th before optimization in Scenario 0.

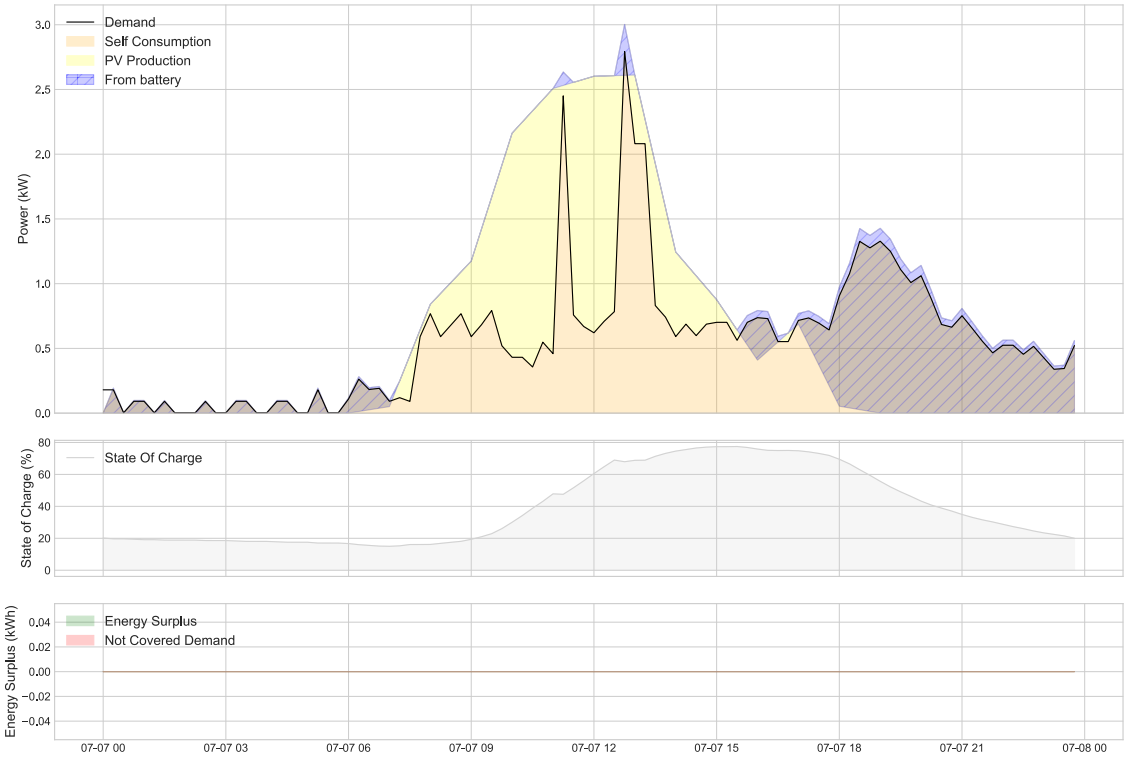

Figure 27: System dispatch in Prosumpy July 7th after optimization in Scenario 0.

Table 26 shows the results after optimization for October 20th. The uncovered demand is 247.3 Wh before optimization. Hence, the kettle is shifted for 15 minutes. Figure 28 and 29 depict the system dispatch for 20th of October before and after optimization. Even though the battery's SoC

is adequate, the peak caused by the kettle exceeds the capacity of the inverter, resulting in unmet demand. The system dispatch after optimization in Figure 29 demonstrates that by shifting the kettle for 15 minutes, the peak is sufficiently reduced, resulting in no uncovered demand.

Table 26: Initial and new time windows after optimization October 20th in Scenario 0.

Uncovered demand	**Appliance**	**Building**	**Initial Window**	**New Window**
247.3 Wh	Kettle	Staff Room	14:15 - 14:30	14:00 - 14:15

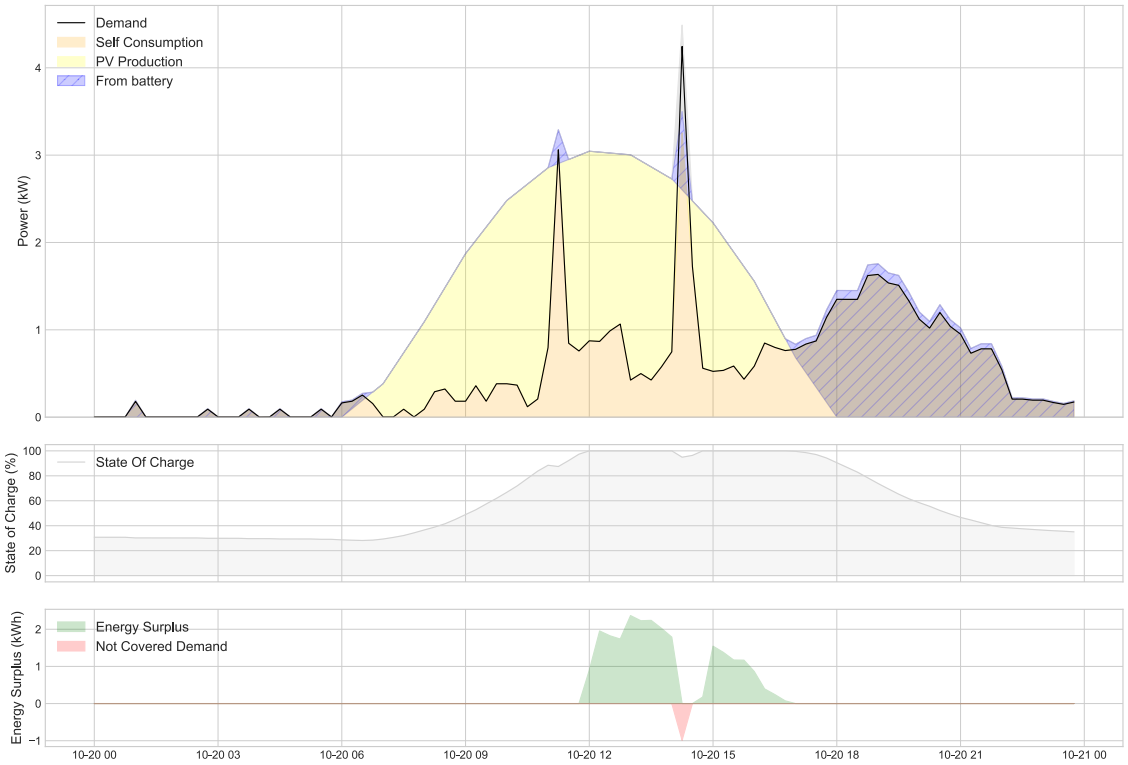

Figure 28: System dispatch in Prosumpy October 20th before optimization in Scenario 0.

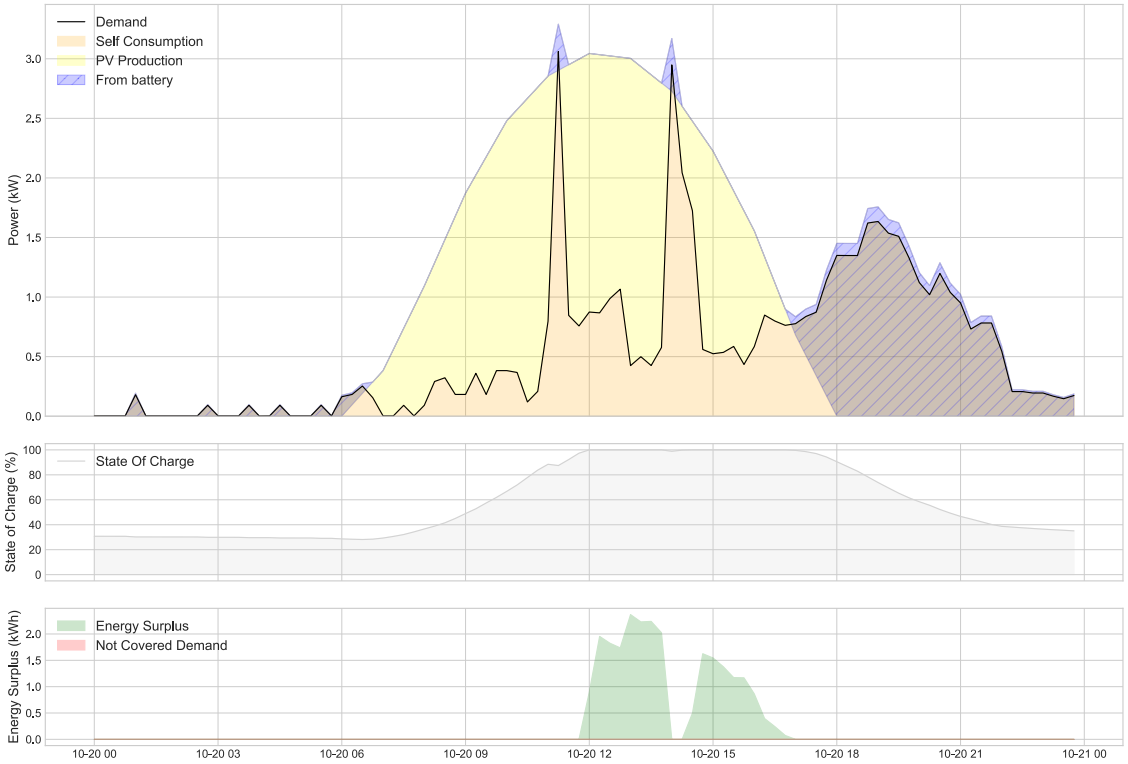

Figure 29: System dispatch in Prosumpy October 20th after optimization in Scenario 0.

Table E.39 and E.40 in Appendix E.1 show the days in Scenario 0 when the optimization model fails to fulfill the constraints. In Scenario 0, there are 22 days when there is uncovered demand with the initial load profiles, and the SoC is 0% at the end of the day. As the battery is depleted at the end of the time horizon considered in the optimization model with the original load profiles, the model is not able to move any of the shiftable loads to fulfill the constraints. February 3rd, the SoC is 43.75% at the beginning of the day, but the total uncovered demand is 33.84 Wh, and the battery is depleted by the end of the day. Figure 30 depicts the system dispatch in Prosumpy, and it can be seen that the uncovered demand appears at the end of the day. The battery is discharged, and the system is not able to cover the demand, as there are no PV production.

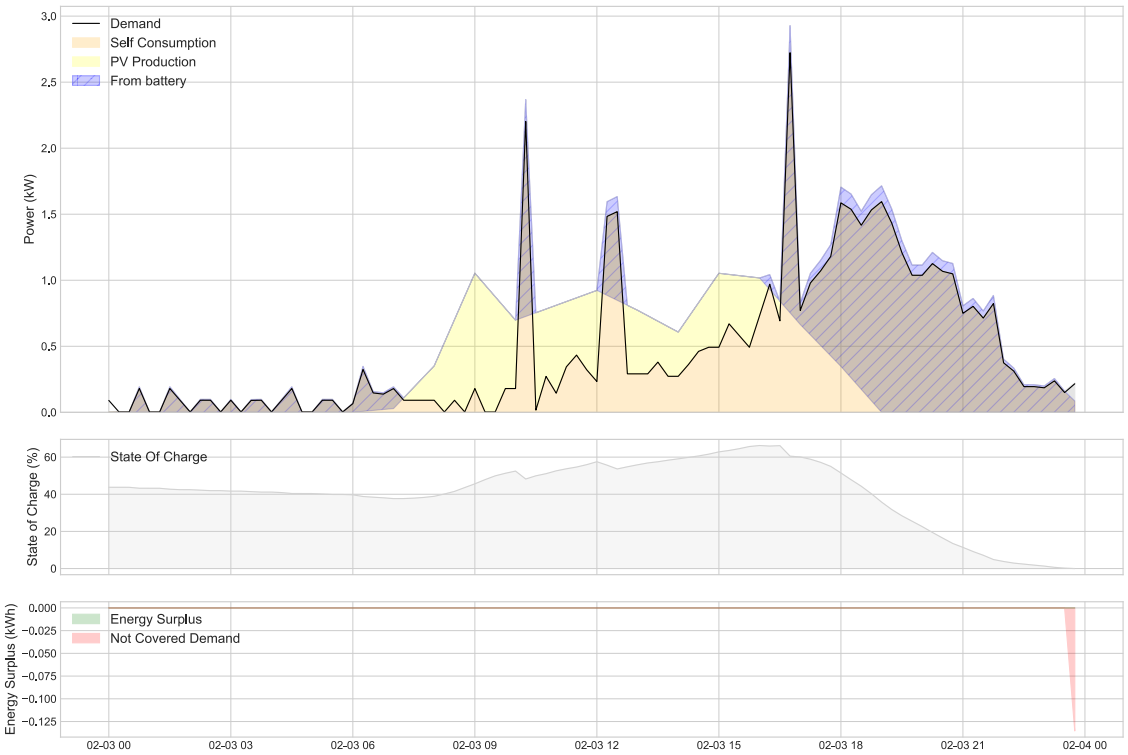

Figure 30: System dispatch in Prosumpy February 3rd in Scenario 0.

There are 12 days in Scenario 0 where the model fails, even though there is no uncovered demand with the original load profiles. The battery's SoC is greater than or equal to 20% at the start of the day on all the dates. Despite this, the battery capacity at the end of the day is insufficient. Hence, the constraint to ensure that the SoC is greater than, or equal to 20% is impossible to fulfill, and the model fails. Most of the model failures occur during the period when the PV production is drastically reduced, as described in Chapter 6.1. The model successfully meets the model's constraints throughout January, March, and December without any failures.

6.2.2 Scenario 1

Table E.41 in Appendix E.2 presents the detailed results of the optimization of Scenario 1. This scenario includes an additional battery compared to Scenario 0. In Scenario 1, there are 22 days where the optimization model moves shiftable loads to cover the demand. Similar to Scenario 0, the kettle in the Staff Room is often shifted. However, the drill, printer, and fans are shifted in Scenario 1 as well. Loads are shifted for more than half an hour only on February 3rd. In Scenario 1, no loads are shifted on the July 7th. The system dispatch from Prosumpy in Figure 31 shows that the additional battery capacity ensures that the SoC is greater than 20% with the initial load profiles. Hence, the kettle is not shifted in Scenario 1.

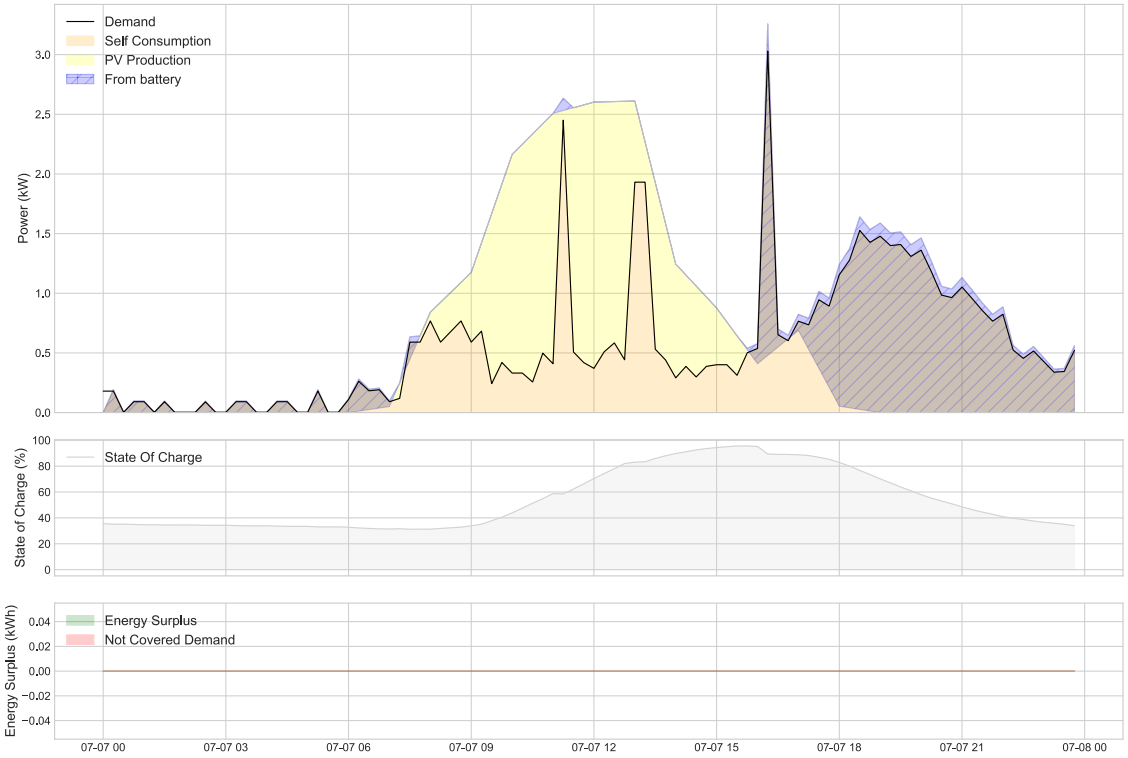

Figure 31: System dispatch in Prosumpy July 7th in Scenario 1.

Despite the additional battery, the kettle is still moved October 20th in Scenario 1. Table 27 show that the uncovered demand is persistently 247.3 Wh, and the kettle is shifted 15 minutes. As the peak caused by the kettle is higher than the capacity of the inverter, the additional battery will not be able to cover the demand.

Table 27: Initial and new time windows after optimization October 20th in Scenario 1.

Uncovered demand	Appliance	Building	Initial Window	New Window
247.3 Wh	Kettle	Staff Room	14:15 - 14:30	14:00 - 14:15

Table E.43 and E.42 in Appendix E.2 presents the days in Scenario 1 where the optimization model fails. In this scenario, there are 14 days where there is uncovered demand, and the battery is depleted at the end of the day before optimization. However, in Scenario 1, the model successfully covers the loads on February 3rd, resulting in no uncovered demand. Table 28 shows that the fans in the Staff Court are shifted. Three of the fans are only shifted for 15 minutes, while the three others are moved two hours forward. The system dispatch in Figure 32 shows that as a result of the shifted loads and additional battery, the SoC of the battery is greater than 20%, and the constraints of the optimization model are fulfilled.

Table 28: Initial and new time windows after optimization February 3rd in Scenario 1.

Appliance	Number	Building	Initial Window	New Window
Fan	3	Staff Court	16:00 - 22:00	14:00 - 20:00
Fan	3	Staff Court	16:15 - 22:15	16:00 - 22:00

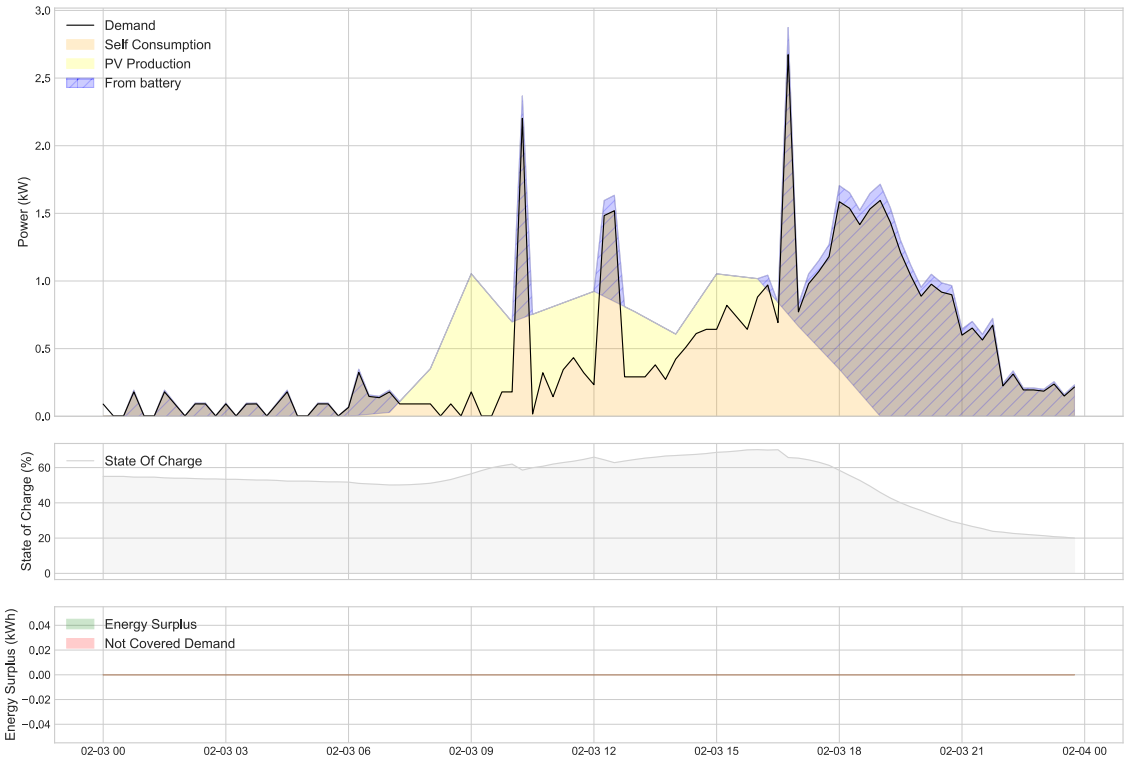

Figure 32: System dispatch in Prosumpy February 3rd after optimization in Scenario 1.

In Scenario 1, there are 9 days when the model fails due to insufficient battery capacity at the end of the day. The days of failure are reduced in this scenario, but the failures still mainly occur from March through July.

6.2.3 Scenario 2

The detailed results of the optimization of Scenario 2 are presented in Table E.44 in Appendix E.3. Scenario 2 includes two additional batteries, compared to the existing system in the Staff Room. Similar to Scenario 1, there are 22 days throughout the year when the optimization shift loads to cover the demand in this scenario. It is still mainly the kettle that is shifted, with a few exceptions of the drill, printers, and fans. Despite the additional batteries, the uncovered demand is persistently 247.3 Wh October 20th, and the kettle is shifted. The system dispatch in Prosumpy before optimization in Figure 33 shows that the system is incapable of covering the peak caused by the kettle, even though the SoC is close to 100%.

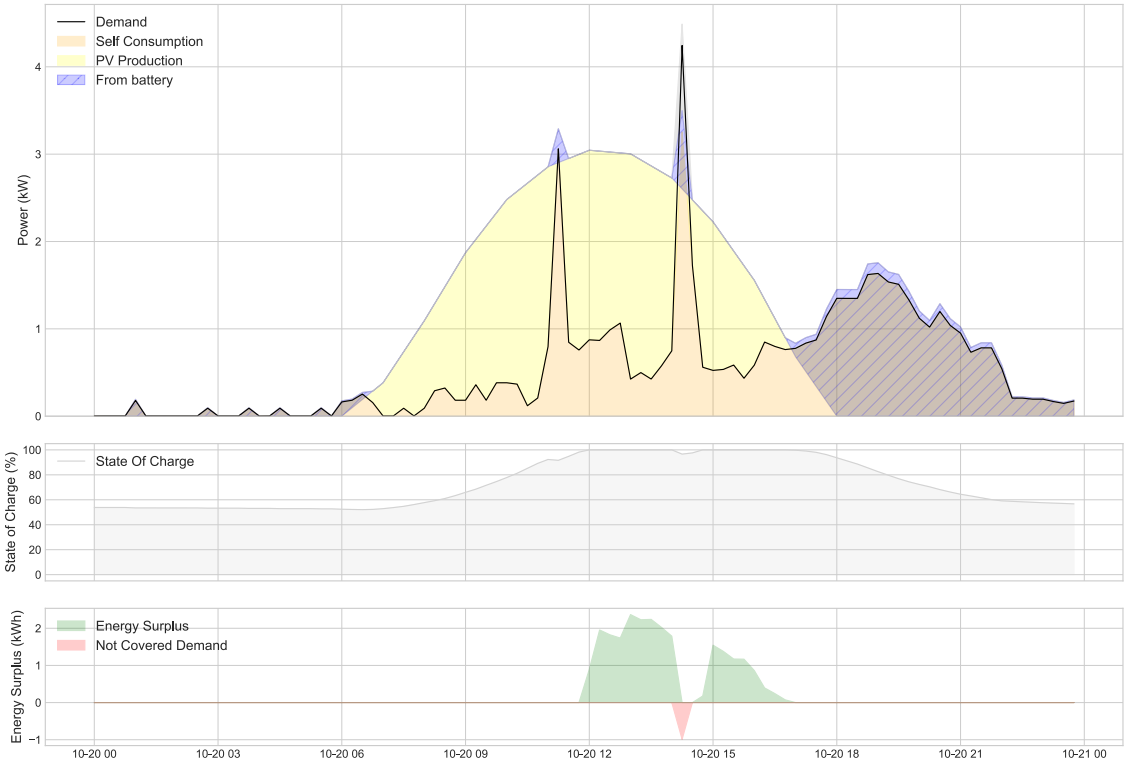

Figure 33: System dispatch in Prosumpy October 20th before optimization in Scenario 2.

Due to the additional batteries, there are no loads shifted on July 7th or February 3rd in this Scenario. The SoC is greater than or equal to 20% at the end of the day with the initial load profiles. However, there are still days in Scenario 2 when the optimization model fails. The dates are listed in Table E.45 and E.46 in Appendix E.3. There are eight days in this scenario when there is uncovered demand, and the model fails due to the depletion of the battery with the initial load profiles. The date with the highest uncovered demand is June 9th. The uncovered demand is 2093 Wh, and the battery at the start of the day is 46.76%. The system dispatch in Figure 34 shows that the uncovered demand occurs during the evening. In Table 29, the time windows of the fans on June 9th are listed. The table shows that the fans in the Staff Room and Office Building are mainly on during the time period with PV production. However, all the fans in the Staff Court are on during the evening when there is uncovered demand.

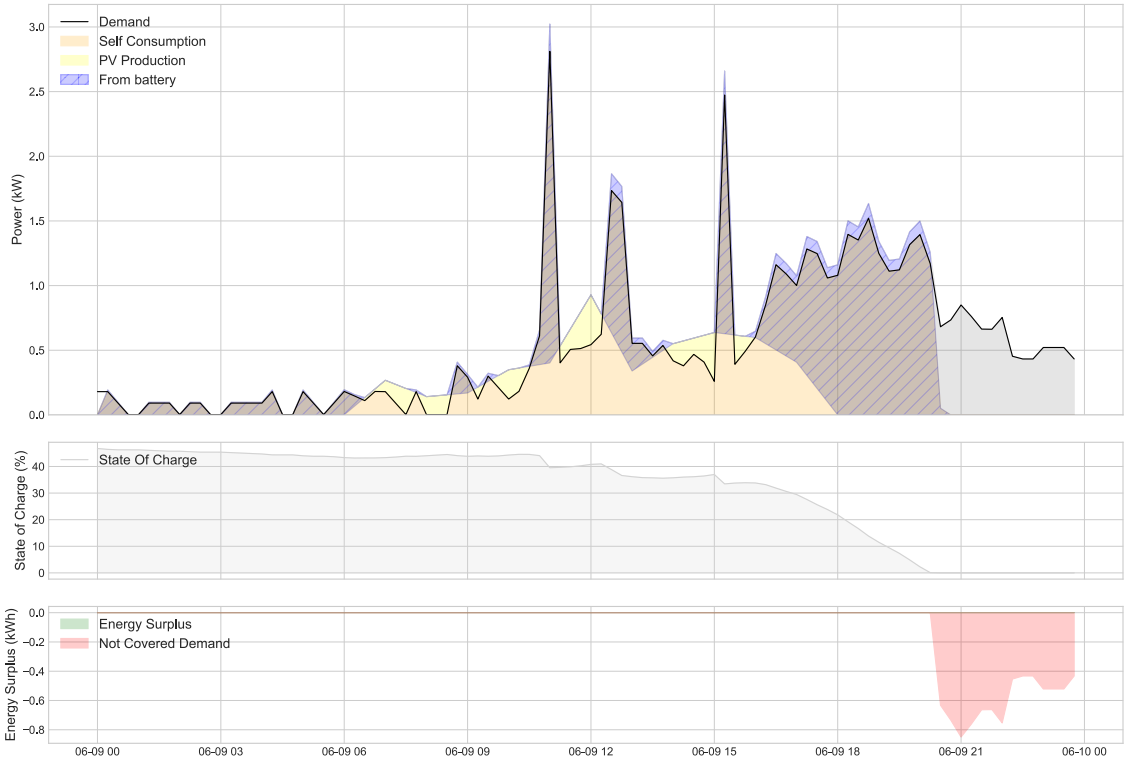

Figure 34: System dispatch in Prosumpy June 9th in Scenario 2.

Table 29: Time windows for the fans June 9th in Scenario 2.

Building	Number	Window
Staff Room	1	13:00 - 19:00
Staff Room	1	12:15 - 18:15
Office Building	2	10:45 - 16:45
Staff Court	6	16:15 - 22:15

In Scenario 2, the model fails due to insufficient battery capacity at the end of the day on 10 dates, even though there is no unmet demand. Compared to 12 days in Scenario 1, the reduction due to an additional battery is not remarkable in this scenario. However, the days of failure in this scenario are still mainly from March through July.

6.3 Annual System Dispatch in Prosumpy

6.3.1 Scenario 0

Table 30 presents the results from the system dispatch for Scenario 0 in Prosumpy with the initial load profiles before optimization. The results show that 3842 kWh of the total demand is covered, resulting in a total uncovered demand of 73.49 kWh. As the results presented are before optimization, no load is shifted. The total energy surplus is 2075 kWh, and 2200 kWh of the total annual consumption is provided by the battery. Further, the average DoD is 0.6278.

Table 30: Output data from Prosumpy for the initial system dispatch in Scenario 0.

Total Covered Demand	3842 kWh
Total Uncovered Demand	73.49 kWh
Total Shifted Load	0.000 kWh
Total Energy Surplus	2075 kWh
Amount of Energy Provided by the Battery	2200 kWh
Average Depth of Discharge	0.6278

In Table 31, the results from the system dispatch in Prosumpy for Scenario 0 after optimization are listed. The results show that 20.24 kWh of the total demand is shifted by the optimization model. As expected, the covered demand is increased, and the uncovered demand is decreased. However, after optimization, the uncovered demand is only reduced by approximately 2 kWh. The total energy surplus is persistent before and after optimization, as the loads only are shifted for a few time steps. As a result, the consumption is not remarkably increased during the time periods when the PV production is high. Followingly, the decrease in the amount of energy provided by the battery and the DoD is not remarkable.

Table 31: Output data from Prosumpy for the system dispatch after optimization in Scenario 0.

Total Covered Demand	3844 kWh
Total Uncovered Demand	71.30 kWh
Total Shifted Load	20.24 kWh
Total Energy Surplus	2075 kWh
Amount of Energy Provided by the Battery	2196 kWh
Average Depth of Discharge	0.6267

6.3.2 Scenario 1

The results from the system dispatch in Prosumpy for Scenario 1 before optimization are listed in Table 32. As a result of the additional battery, the covered demand and energy provided by the battery are increased compared to the initial system dispatch in Scenario 0. Followingly, the uncovered demand, energy surplus, and average DoD are decreased.

Table 32: Output data from Prosumpy for the initial system dispatch in Scenario 1.

Total Covered Demand	3877 kWh
Total Uncovered Demand	38.75 kWh
Total Shifted Load	0.000 kWh
Total Energy Surplus	2036 kWh
Amount of Energy Provided by the Battery	2237 kWh
Average Depth of Discharge	0.5108

Table 33 presents the results from the system dispatch in Prosumpy after optimization for Scenario 1. The results show that 9.013 kWh of the load is shifted. Similar to Scenario 0, the uncovered demand is reduced by approximately 2 kWh. The surplus energy is also constant in this scenario, while the amount of energy provided by the battery and the average DoD is slightly reduced.

Table 33: Output data from Prosumpy for the system dispatch after optimization in Scenario 1.

Total Covered Demand	3879 kWh
Total Uncovered Demand	36.92 kWh
Total Shifted Load	9.013 kWh
Total Energy Surplus	2036 kWh
Amount of Energy Provided by the Battery	2235 kWh
Average Depth of Discharge	0.5102

6.3.3 Scenario 2

Table 34 lists the results from the system dispatch in Prosumpy with the initial load profiles for Scenario 2. As expected, the uncovered demand is remarkably reduced with two additional batteries. Followingly, the covered demand and the amount of energy provided by the battery are increased compared to the other scenarios. The energy surplus and the average DoD are decreased.

Table 34: Output data from Prosumpy for the initial system dispatch in Scenario 2.

Total Covered Demand	3899 kWh
Total Uncovered Demand	16.70 kWh
Total Shifted Load	0.000 kWh
Total Energy Surplus	2011 kWh
Amount of Energy Provided by the Battery	2261 kWh
Average Depth of Discharge	0.4302

The results from the system dispatch in Prosumpy after optimization for Scenario 2 are listed in Table 35. The amount of total shifted load is slightly reduced compared to Scenario 1. Similar to the other scenarios, the uncovered demand is reduced by approximately 2 kWh. The total energy surplus is persistently constant, while the amount of energy provided by the battery and the average DoD is slightly reduced.

Table 35: Output data from Prosumpy for the system dispatch after optimization in Scenario 2.

Total Covered Demand	3901 kWh
Total Uncovered Demand	14.88 kWh
Total Shifted Load	9.225 kWh
Total Energy Surplus	2011 kWh
Amount of Energy Provided by the Battery	2259 kWh
Average Depth of Discharge	0.4298

6.4 Cost Comparison for Staff Court Electrification Approaches

The costs of the different approaches for electrification of the Staff Court are presented in Table 36. It reveals that the cost of extending the existing system corresponds to approximately 7% of the costs of a new system. However, adding additional batteries of 200 Ah increase the cost by approximately 600 USD per battery. Hence, the cost of Scenario 1 and 2 are 14% and 21% of the costs of the new system, respectively.

Table 36: Approximately costs of different electrification approaches for the Staff Court.

Approach	**Total Cost [USD]**
Scenario 0	600
Scenario 1	1200
Scenario 2	1800
New system	8500

6.5 Graphical User Interface

The design proposal of the GUI is presented in Figure 35, and the platform's features are implemented as different buttons with different functionality. Real-time data from the inverter is automatically downloaded each time the interface is started. Both the design, features, and download of real-time data are implemented as described in Chapter 4.5, based on the feedback from the users. The current data from ShineDesign does not include the additional appliances. However, a

daily load profile with additional appliances from RAMP and the modeled PV production is used as input to the GUI to describe the importance of flexibility in the extended system.

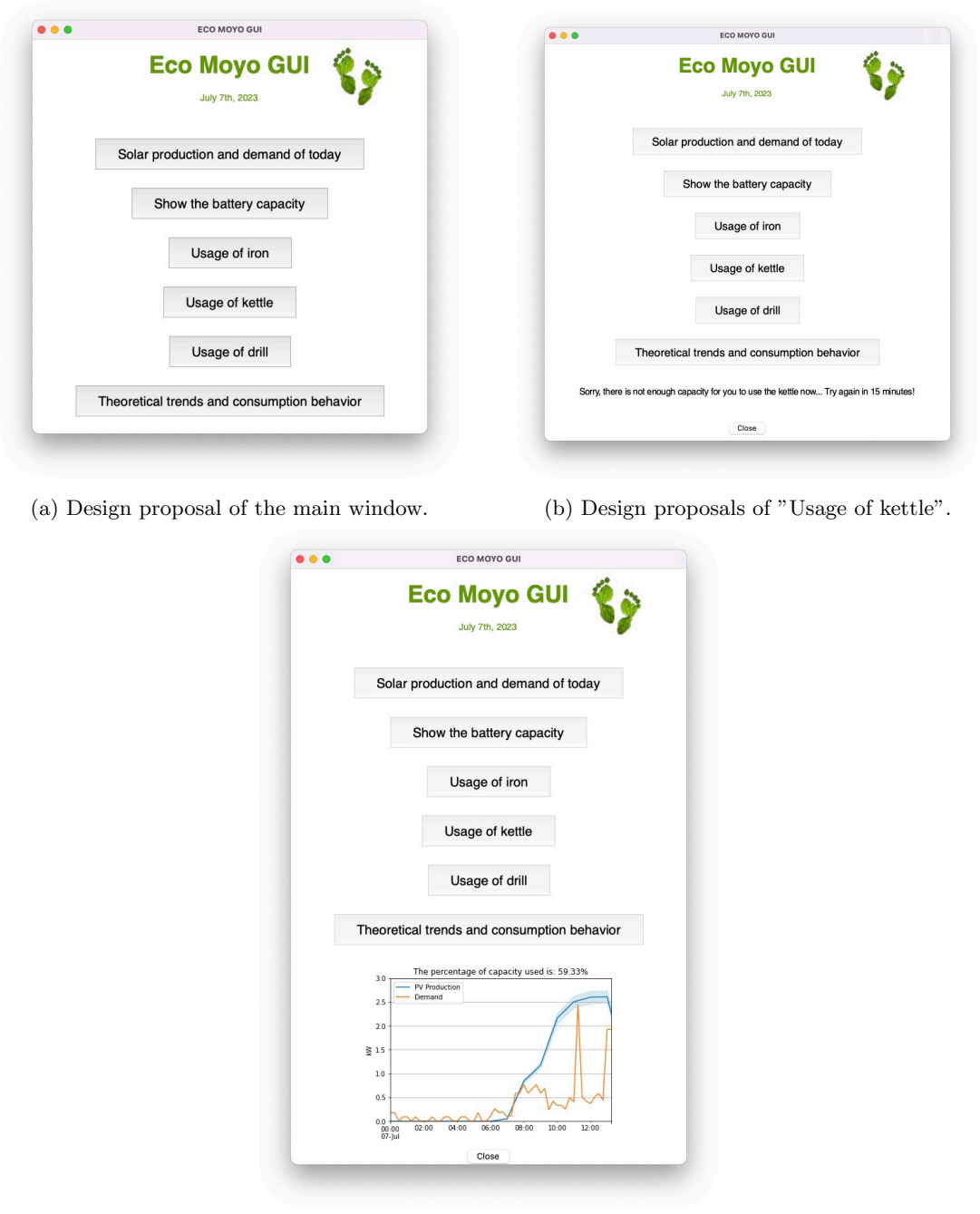

(a) Design proposal of the main window.

(b) Design proposals of "Usage of kettle".

(c) Design proposal of "Solar production and demand".

Figure 35: Design proposals of the GUI.

The structure of the main dashboard of the GUI is divided into two; the header and the functionality menu. The header is "ECO MOYO GUI", including the current date and the logo of Eco Moyo. Following, the menu is presented with six buttons with different functionalities. The first button displays the graph of PV production and demand of the current day, as displayed in Figure 35. The next button displays the battery's SoC. As the ShinDesign server only provides the SoC in four levels between 0 and 100%, the accurate SoC is not available at this time. Following, the next three buttons investigates the possibility of using an iron, a kettle, and a drill, respectively. These

buttons also present the percentage of energy use when using one of the mentioned appliances. The last button is supposed to present energy consumption and production trends but is not currently implemented in the early-stage design proposal. However, the energy trends will be based on the optimization model presented in 6.2, where the real-time SoC and demand will be input to the model.

If the GUI returns "no" when a button of a specific appliance is clicked, the SoC is lower than the energy usage of the appliance, or the total demand is greater than the inverter's capacity. This is visualized in Figure 35b. The GUI gives feedback to the user to try again in 15 minutes. By waiting 15 minutes, the appliance is shifted one time step as modeled in the optimization model. The appliance is now rescheduled, and hence, DSM is implemented in the system. Additionally, the interface should give feedback on energy trends of the period, including recommending which appliances to use. This feedback will be especially useful during the periods when the PV production is significantly decreased.

The user-friendly presentation of daily solar production, demand, and usage of the different appliances, both in percentage and graphically, enhances the end user's knowledge of the system. The possibility of observing energy trends of the period and comparing them to the current day allows the users to stay informed about their energy consumption. With the manual load shifting provided by the GUI when the capacity is at its limit or the SoC are low, the flexibility in the system is increased. The GUI plays a crucial role in preventing users from exceeding the system's limit. Without a GUI, the users would lack the necessary information to determine if it is safe to connect the appliances.

7 Discussion

This chapter presents the discussion of the results obtained in this thesis. The discussion includes the modeled PV production and demand, optimization model, annual system dispatch, cost comparison between different approaches for the electrification of the Staff Court, and GUI design. Furthermore, the results are compared to relevant research findings in the field.

7.1 PV Production and Demand

There are several methods for generating meteorological data, which may result in different annual solar irradiation. Hence, the total PV production throughout a year may differ when using TMY compared to other methods. Furthermore, the PV production presented in Chapter 6.1 does not account for shading. Due to this, the overall production is not precise and may be lower than expected in reality. Further, the results reveal that the modeled PV production is remarkably decreased in the months of April through July. Hence, the modeling using TMY corresponds with the seasonal variations in Kilifi, described in Chapter 5.3.

The high degree of stochasticity in the RAMP model makes the model capable of reproducing load profiles of both the typical daily consumption as well as the day-to-day variations. Nonetheless, it is essential to acknowledge that the input parameters used in the model are derived from conversations with the staff during the field trips. As a result, the actual load profiles may deviate from the simulated load profiles. Additionally, appliances not currently presented at the school are implemented in RAMP based on the teachers' weekly activities and observed energy consumption behavior. Hence, the input parameters for the additional appliances may differ from reality, and the total modeled demand is significantly increased compared to the demand of today.

7.2 Optimization Model

As expected, the results from the optimization reveal that mainly the kettle is shifted in all the scenarios. This is expected as the kettle is the appliance with the highest power consumption and often is used in the afternoon when the PV production is limited. It is also expected that the drill, printer, and fans are shifted occasionally, based on the disutility costs associated with shifting appliances by one time step, outlined in Table 23. The drill, printer, and fans have relatively high power consumption and low disutility cost. Hence, the appliances are shifted in order to fulfill the constraints in the optimization model. The disutility cost is crucial for prioritizing which appliances to shift in the model. However, the price variation between the appliances is minimal. Consequently, the kettle is shifted several times due to the small variations in disutility cost and its high power rating. Nevertheless, for the end users, shifting the kettle rather than several appliances with a lower disutility cost is a more convenient approach.

The kettle is shifted on October 20th in all the scenarios. Even though the batteries' SoC is sufficient, the unmet demand is persistent. The total peak, when the kettle is used, exceeds the capacity of the inverter, resulting in uncovered demand. Hence, the kettle is shifted for 15 minutes. The demand is reduced, and the new peak is within the limit. This is also observed in Scenario 1 and 2, where additional batteries are included. The capacity of the inverter is still limiting the system, and the uncovered demand is persistent. Hence, increasing the number of batteries will not cover the unmet demand caused by such load peaks. However, in these cases, DR in the form of load shifting is a great tool to utilize the capacity of the system. By shifting the kettle for 15 minutes, the peak is severely decreased without remarkable inconvenience for the consumers.

In Scenario 0, eight loads are shifted on July 7th, even though there is no uncovered demand. However, the loads are shifted to ensure that the SoC is greater than or equal to 20% at the end of the day. In Scenario 1 and 2, the additional batteries ensure that all the constraints are fulfilled, and no appliances are shifted. Due to a higher battery capacity at the start of the day, the battery is not discharged below 20% in the evening. The constraint concerning the SoC at the end of the day is added to prevent insufficient battery capacity for the next day. The limit of 20% is

chosen to ensure that the system is able to cover the non-shiftable load the following day until the PV production is sufficient. The non-shiftable load consists of indoor and outdoor lighting in all the buildings, and fridges in both the Staff Room and Office Building. However, the constraint causes failure on days where the initial load profile prevents the model from shifting loads to ensure sufficient SoC at the end of the day. By implementing load cutting in the optimization model, this problem can be avoided, and the total annual uncovered demand would be severely decreased after optimization. However, the run-time of the optimization model would be significantly increased due to non-linearity. Therefore, only the shifting of appliances is implemented in this thesis to prevent excessive run time. The run time and the complexity of the optimization model could have been further decreased by aggregating the load profiles. As discussed in Chapter 3.2, [31] divide the demand into blocks to reduce the complexity of the model. However, further aggregation of the demand would result in the shifting of several appliances at the same time. This results in increased disutility for the end user.

On February 3rd, the model fails in Scenario 0 due to the depletion of the battery. However, in Scenario 1, the additional battery prevents the model from failing. There is no uncovered demand, and the fans in the Staff Court are shifted forward in order to ensure sufficient SoC at the end of the day. As the load profiles of the fans in the Staff Court include three fans in each load profile, it is expected that these are shifted compared to the fans in the other buildings. The fans in the Staff Court are also more likely to be used late in the evening. Table 19 shows that the time window is set to 16:00 - 23:59. Table 17 and 21 show that the fans in the Staff Room and Office Building are set to 12:00 - 23:59 and 10:00 - 17:00, respectively. As the window of the fans in the Staff Court is shorter, they are more likely to be used during the evening, than the fans in the Staff Room. This is a reasonable assumption, as the Staff Court accommodates six teachers. However, the only electricity supply in the Staff Court is SHSs providing lighting. As highlighted in Chapter 3.1, a well-known challenge when modeling load profiles in rural areas is capturing detailed user behavior for non-yet-existing devices. However, it is a reasonable assumption that the usage of the fans in the Staff Court will be reduced when the PV production is limited.

The additional batteries in Scenario 1 and 2 lead to a reduction in the occurrence of model failure. In Scenario 1, the model fails for a total of 23 days, which is a significant improvement compared to the 34 days observed in Scenario 0. In Scenario 2, the model experiences failure for a total of 18 days. The results show that the reduction is mainly on the dates when there is unmet demand and the battery is depleted with the initial load profiles. By adding additional battery capacity, the system is able to cover the demand for additional days. However, the number of days when the system is able to cover the demand but the battery is depleted is not significantly reduced. The findings in Scenario 2 demonstrate that two additional batteries do not necessarily cover the demand when the PV production is drastically reduced. As depicted in Figure 24, the PV production reaches its lowest point in June, while the demand remains relatively stable throughout the year. Hence, most of the days when the model fails to fulfill the constraints are during the period when the PV production is drastically reduced. Despite a relatively high SoC in the morning on June 9th, there is a remarkable amount of unmet demand. Additionally, Table 29 reveals that all the fans in the Staff Court are used during the evening. By restricting fan usage in the evening, it would be possible to mitigate the level of uncovered demand. Considering that June 9th is during the cold season described in Chapter 4.2, it is reasonable to assume that this will not cause remarkable discomfort for the end users.

7.3 System Dispatch in Prosumpy

In the annual dispatch of the initial system in Scenario 0, a remarkable amount of unmet demand is detected. As anticipated, the annual unmet demand is reduced after the optimization. However, the reduction is limited to 2 kWh and is persistent for all the scenarios. The additional batteries in Scenario 1 and 2 decrease the uncovered demand, but the reduction after optimization is persistent. This reveals that load shifting mostly affects the uncovered demand caused by load peaks. By shifting loads, the peaks are reduced to be within the limit of the inverter, and the demand is covered. The limited reduction in annual uncovered demand is also caused by the number of days where the optimization model fails to fulfill the constraints. When this happens, the initial load

profiles are used in the system dispatch. Hence, the battery is depleted at the end of the day, and the system is unable to cover the demand on the following day. By cutting load to prevent model failure, the total annual uncovered demand would be remarkably reduced in all the scenarios. The amount of shifted load is remarkably decreased in Scenario 1 compared to Scenario 0. However, there is a slight increase from Scenario 1 to Scenario 2. This is caused by the reduction in days when the optimization model fails. The number of days with optimized load profiles is increased in Scenario 2. Hence, the amount of shifted load is increased despite the additional battery capacity.

7.4 Cost Comparison for Staff Court Electrification Approaches

For the electrification of the Staff Court, the possibility of implementing a new system consisting of PV panels, batteries, and an inverter is explored in Chapter 5.5. The estimated cost for the system is estimated to 8500 USD, and it was decided not to move forward with the project due to insufficient funds. However, the new system proposal includes unlikely high usage times for the appliances, resulting in higher costs. The overall cost will be reduced by opting for a system with a more suitable capacity for its intended use. However, this is not an option for Eco Moyo. Their knowledge is limited, and they are limited to the offer from the local company.

Alternatively, the cost of extending the existing system is only 7% of the estimated expense of installing a new system. However, with the extended system, the high-power appliances must be used in the Staff Room due to the cable's capacity. Based on the power rating of the high-power appliances in the Staff Room, it is evident that the cost of implementing a cable with a higher capacity to power appliances in the Staff Court would be significantly lower than purchasing a new system. As of today, most of the high-power appliances are used in the Staff Room, without causing remarkable disutility for the users. Hence, the extension of the cable is not necessary for the moment. However, the simulations of Scenario 0 show that the extension caused notable uncovered demand, even when considering user flexibility in form of load shifting. However, most of the uncovered demand is during the season with limited PV production. By adapting to seasonal variations, the uncovered demand can be reduced.

The extension of the system with an additional battery, as simulated in Scenario 1, gives an additional cost of about 14% of the price of implementing a new system. Further, the cost of implementing two additional batteries, as simulated in Scenario 2, corresponds to a total cost of close to 21% of implementing a new system. As discussed in Chapter 7.2, adding additional batteries lead to a reduction in the occurrence of model failure. Hence, there is a decrease in the number of days when load shifting alone fails to meet the demand. However, the optimization model developed in this thesis only includes load shifting within the same day, and other types of DR can also contribute to meeting the demand. The results show that the days of model failure usually occur during periods when the PV production is limited. Extra battery capacity will not cover the demand on such days, and the consumer must adapt in this season regardless of the battery capacity. Observations during the fieldwork revealed that the degree of user flexibility at Eco Moyo is high. The teachers and staff are used to a limited power supply and adapting their consumption to the seasonal variations.

7.5 Graphical User Interface

The design of the GUI draft, presented in Chapter 6.5, includes different functionalities to improve the flexibility of end user consumption behavior. However, the interface should have been implemented as an application for an enhanced user experience. Based on the provided GUI design proposal, all the functionalities are implemented as buttons, and the teachers responded positively to this approach. Nevertheless, the main dashboard of the interface should provide more valuable information. This can be achieved with widgets presenting the current weather of the day, weekly weather forecast, the actual SoC, and the percentage of energy utilization, among other relevant information. It is essential to acknowledge that the GUI is currently in its initial draft stage, based on feedback from the end users at Eco Moyo, without GUI design experience. Hence, this interface may not implement crucial factors related to the user experience design.

Following, the batteries' actual SoC is impossible to visualize with the available data from ShineDesign. The accessible SoC is given as four different levels from 0 to 100%. Nonetheless, this may be solved by changing the default settings of the data logger of the inverter. Due to the absence of accurate SoC, the implementation of the theoretical-trends-functionality is not included in the GUI at this time. Additionally, the input demand to the optimization model is significantly increased due to examining flexibility with several appliances. Hence, a daily load profile with additional appliances and modeled PV production is used as input to the GUI to describe the importance of flexibility in the extended system. Ideally, the optimization model should also take short-term weather forecasts as input for calculating the PV production and purpose optimal consumption behavior based on the production of the day ahead. As a result, the end user flexibility increases, and the user experience will significantly improved.

As highlighted in related research in Chapter 3.4, obtaining early-stage user feedback on GUI design is crucial. The ultimate goal is to enhance the user's experience and engagement with the system. Additionally, allowing users to customize the GUI based on their individual needs and curiosity, creates opportunities for increased interest in the software. This enables users to personalize their experience and choose the functionalities they wish to visualize within the application. At Eco Moyo, the teachers' engagement with the system varies. To address this, the app could offer a standard set of functionalities, allowing users to add additional features from a menu. With this possibility, the teachers can gain a greater awareness of their energy usage, enhance their understanding of user flexibility, and ultimately increase their interest and knowledge of the system.

7.6 Energy Flexibility in Rural Off-Grid Systems

As discussed in Chapter 3.3, there is a lack of research regarding DR in off-grid systems. The simulations in this thesis show that DR is an essential tool to secure reliable energy access in rural areas. Hence, user flexibility plays a crucial role in the challenges of these systems. In remote areas, access to reliable electricity is limited, and the ability to adapt and optimize energy consumption is essential. The results of this thesis show that load shifting is an effective strategy for DR to cover the demand in rural off-grid systems. By adjusting the timing of high-power appliances, such as kettles and irons, the users can align their energy consumption with available power generation from intermittent sources, such as PV power. However, consumers are also reliant on adaption to seasonal variations to cover the demand. This flexibility enables them to make the most of their limited energy resources.

The optimization model developed in this thesis is easily adjustable to other rural off-grid systems. By modifying the system parameters in Pyomo and the input parameters in RAMP, it can be used to investigate flexibility in similar systems. The model also allows for the assessment of various scenarios with additional storage and production capacity.

8 Conclusions

This master's thesis investigates flexibility in rural off-grid microgrids, based on a case of the solar and battery off-grid system at Eco Moyo Education Centre in Kenya. The main objectives are to develop an optimization model to decide the optimal scheduling of flexible loads by minimizing the disutility cost of load shifting. Additionally, an early-stage GUI, developed in Python, for end user communication to incentivize user flexibility. One of the main findings of the thesis is that DR in terms of load shifting is an effective strategy to cover unmet demand in rural off-grid systems, in addition to adapting to seasonal variations. A GUI can be used to incentivize such flexibility by increasing the interaction between the microgrid and the users.

Three different scenarios are simulated to investigate how additional battery capacity affects the load shifting and disutility of the consumer when extending the system. The first scenario considers the existing system, and the results show that there is uncovered demand after optimizing the load profiles. The optimization model fails to fulfill the constraints for several days, resulting in no load shifting even when there is uncovered demand or the battery is depleted at the end of the day. However, most of these days are during periods when the PV production is limited. By adapting to such seasonal variations, the uncovered demand can be remarkably reduced. Simulations show that the demand can be covered for some days simply by limiting fan usage in the evening on days with limited power generation. By load shifting and adapting to seasonal variations, the existing system can supply the additional buildings at a cost of 7% of implementing a new system. As consumers in rural areas are used to adapting their consumption due to limited power supply, this is not assumed to cause notable disutility for the users. Scenario 1 and 2 consider the existing system with one and two additional batteries. The simulations reveal that the additional battery capacity reduces the number of days when the optimization model is unable to fulfill the constraints. As expected, the initial uncovered demand is decreased with additional batteries. However, the reduction in uncovered demand due to load shifting is persistent in all the scenarios. Hence, load shifting mostly affects the uncovered demand caused by load peaks exceeding the system's capacity. By including the additional batteries, the disutility of the users is decreased. However, the cost increases to 14% and 21% of implementing a new system, with one and two additional batteries, respectively. The user experience will be enhanced, but the lack of financial resources at Eco Moyo plays an important role in the decision.

Additionally, the GUI developed for end user communication will incentivize user flexibility and increase the user's experience and overall engagement with the system. The GUI proposal is designed with different functionalities implemented as buttons to increase the end user's understanding of the system, as the current inverter display is challenging to understand for non-technical staff. Furthermore, the GUI contributes to covering the demand when extending the existing system at Eco Moyo. However, the interface should ideally be implemented as an application, with different widgets in the main dashboard, such as weather forecasts, actual SoC, and percentage of energy usage. The application should also allow users to add additional features from a menu. With this possibility, the teachers can gain a greater awareness of their energy usage, enhance their understanding of user flexibility, and ultimately increase their interest and knowledge of the system.

Overall, this thesis contributes to valuable insight into energy flexibility in rural off-grid systems. As the developed optimization model is easily adjustable, it can also be used to investigate flexibility in similar systems. It can be extended to include other forms of user flexibility, like load cutting or curtailment of loads. The GUI must be implemented in a user-friendly manner to ensure usability for end users. Additional features can be incorporated, including weather forecasts, accurate SoC, and the ability for users to customize the dashboard to their preferences.

Bibliography

[1] 'Transforming our world: The 2030 agenda for sustainable development', United Nations, Tech. Rep., 2015.

[2] United Nations (UN), Department of Economic and Social Affairs (DESA), 'The Sustainable Development Goals Report 2022', Tech. Rep., 2022, p. 64. [Online]. Available: https://unstats.un.org/sdgs/report/2022/The-Sustainable-Development-Goals-Report-2022.pdf (visited on 22nd May 2023).

[3] 'Kenya National Electrification Strategy: Key Highlights 2018', The World Bank, Tech. Rep., 2018. [Online]. Available: https://pubdocs.worldbank.org/en/413001554284496731/Kenya-National-Electrification-Strategy-KNES-Key-Highlights-2018.pdf.

[4] International Trade Adminstration, *Kenya - Energy-Electrical Power Systems*, en, 2022. [Online]. Available: https://www.trade.gov/country-commercial-guides/kenya-energy-electrical-power-systems (visited on 28th Nov. 2022).

[5] 'Impact of VAT and Import Duty on the Stand-Alone Solar Sector in Kenya', Africa Clean Energy Technical Assistance Facility, Tech. Rep., Apr. 2021.

[6] *A unique school in rural Kenya*, 2022. [Online]. Available: https://www.ecomoyo.com/students.

[7] S. O. Ottesen and A. Tomasgard, 'A stochastic model for scheduling energy flexibility in buildings', *Energy*, vol. 88, pp. 364–376, 2015, ISSN: 0360-5442. DOI: https://doi.org/10.1016/j.energy.2015.05.049. [Online]. Available: https://www.sciencedirect.com/science/article/pii/S0360544215006301.

[8] M. Bakken and R. E. Dihle, 'Flexibility in Solar and Battery Off-Grid Systems - Case Study Eco Moyo in Kenya', NTNU, Trondheim, Specialization Project, Dec. 2022.

[9] IRENA, *Innovation landscape brief: Renewable mini-grids*, Abu Dhabi, 2019.

[10] N. Mahdavi Tabatabaei, E. Kabalci and N. Bizon, Eds., *Microgrid Architectures, Control and Protection Methods* (Power Systems), en. Springer International Publishing, 2020, 10.1007/978-3-030-23723-3, ISBN: 978-3-030-23722-6. (visited on 26th Nov. 2022).

[11] H. Louie, *Off-Grid Electrical Systems in Developing Countries*, en. Springer International Publishing, 2018, ISBN: 978-3-319-91890-7. DOI: 10.1007/978-3-319-91890-7. (visited on 27th Nov. 2022).

[12] Y. B. Aemro, P. Moura and A. T. de Almeida, 'Design and Modeling of a Standalone DC-Microgrid for Off-Grid Schools in Rural Areas of Developing Countries', *Energies*, vol. 13, no. 23, 2020, ISSN: 1996-1073. DOI: 10.3390/en13236379.

[13] E. Planas, J. Andreu, J. I. Gárate, I. M. d. Alegría and E. Ibarra, 'AC and DC technology in microgrids: A review', *Renewable and Sustainable Energy Reviews*, vol. 43, pp. 726–749, 2015, ISSN: 1364-0321. DOI: https://doi.org/10.1016/j.rser.2014.11.067.

[14] Dricus De Rooij, *What is a gel battery?* [Online]. Available: https://sinovoltaics.com/learning-center/storage/gel-battery/ (visited on 3rd Dec. 2022).

[15] IRENA, *Innovation Outlook: Renewable Mini-grids*, Abu Dhabi, 2016.

[16] Christiana Honsberg and Stuart Bowden, *Battery Capacity.* [Online]. Available: https://www.sciencedirect.com/topics/engineering/battery-capacity (visited on 3rd Dec. 2022).

[17] N. Kularatna, '2 - Rechargeable battery technologies: An electronic engineer's view point', in *Energy Storage Devices for Electronic Systems*, Boston: Academic Press, 2015, pp. 29–61, ISBN: 978-0-12-407947-2.

[18] *What is renewable energy?*, en, Publication Title: United Nations. [Online]. Available: https://www.un.org/en/climatechange/what-is-renewable-energy (visited on 26th Nov. 2022).

[19] *Solar Position*, Publication Title: pvlib. [Online]. Available: https://pvlib-python.readthedocs.io/en/stable/reference/solarposition.html (visited on 8th Dec. 2022).

[20] B. Lumby, *Utility-Scale Solar Photovoltaic Power Plants: A Project Developer's Guide.* Washingtion D.C.: International Finance Corporation, 2015.

[21] E. Tarigan, 'Azimuth Angle Impact on Specific Energy Output of Rooftops PV System in Surabaya, Indonesia', in *2022 9th International Conference on Information Technology, Computer, and Electrical Engineering (ICITACEE)*, 2022, pp. 25–28. DOI: 10.1109/ICITACEE55701.2022.9923975.

[22] A. Khaligh and O. C. Onar, *Energy Harvesting: Solar, Wind, and Ocean Energy Conversion Systems*, 1st ed. CRC Press, 2010, ISBN: 978-1-315-21813-7.

[23] F. Schmid and F. Behrendt, 'Optimal sizing of Solar Home Systems: Charge controller technology and its influence on system design', *Sustainable Energy Technologies and Assessments*, vol. 45, p. 101 198, 2021, ISSN: 2213-1388. DOI: https://doi.org/10.1016/j.seta.2021.101198.

[24] N. Mukisa, M. S. Manitisa, P. Nduhuura, E. Tugume and C. K. Chalwe, 'Solar home systems adoption in Sub-Saharan African countries: Household economic and environmental benefits assessment', *Renewable Energy*, vol. 189, pp. 836–852, 2022, ISSN: 0960-1481. DOI: https://doi.org/10.1016/j.renene.2022.03.029.

[25] *Introduction to energy system flexibility*. [Online]. Available: https://www.nationalgrideso.com/document/189851/download (visited on 10th Feb. 2023).

[26] O. M. Babatunde, J. L. Munda and Y. Hamam, 'Power system flexibility: A review', *Energy Reports*, vol. 6, pp. 101–106, 2020, ISSN: 2352-4847. DOI: https://doi.org/10.1016/j.egyr.2019.11.048.

[27] Y. Chen, P. Xu, J. Gu, F. Schmidt and W. Li, 'Measures to improve energy demand flexibility in buildings for demand response (DR): A review', *Energy and Buildings*, vol. 177, pp. 125–139, 2018, ISSN: 0378-7788. DOI: https://doi.org/10.1016/j.enbuild.2018.08.003.

[28] H. Sæle, A. Morch, M. Degefa and I. Oleinikova, 'Assessment of flexibility in different ancillary services for the power system', Oct. 2020. DOI: 10.1109/EEM49802.2020.9221996.

[29] H. Li, Z. Wang, T. Hong and M. A. Piette, 'Energy flexibility of residential buildings: A systematic review of characterization and quantification methods and applications', en, *Advances in Applied Energy*, vol. 3, p. 100 054, Aug. 2021, ISSN: 2666-7924. DOI: 10.1016/j.adapen.2021.100054. [Online]. Available: https://www.sciencedirect.com/science/article/pii/S2666792421000469 (visited on 3rd Feb. 2023).

[30] P. D. Lund, J. Lindgren, J. Mikkola and J. Salpakari, 'Review of energy system flexibility measures to enable high levels of variable renewable electricity', en, *Renewable and Sustainable Energy Reviews*, vol. 45, pp. 785–807, May 2015, ISSN: 1364-0321. DOI: 10.1016/j.rser.2015.01.057. [Online]. Available: https://www.sciencedirect.com/science/article/pii/S1364032115000672 (visited on 3rd Feb. 2023).

[31] F. Elghitani and W. Zhuang, 'Aggregating a Large Number of Residential Appliances for Demand Response Applications', *IEEE Transactions on Smart Grid*, vol. 9, no. 5, pp. 5092–5100, 2018. DOI: 10.1109/TSG.2017.2679702.

[32] X. Wang, H. Wang and S.-H. Ahn, 'Demand-side management for off-grid solar-powered microgrids: A case study of rural electrification in Tanzania', *Energy*, vol. 224, p. 120 229, 2021, ISSN: 0360-5442. DOI: https://doi.org/10.1016/j.energy.2021.120229.

[33] M. Tostado-Véliz, H. M. Hasanien, R. A. Turky, Y. O. Assolami, D. Vera and F. Jurado, 'Optimal home energy management including batteries and heterogenous uncertainties', *Journal of Energy Storage*, vol. 60, p. 106 646, 2023, ISSN: 2352-152X. DOI: https://doi.org/10.1016/j.est.2023.106646. [Online]. Available: https://www.sciencedirect.com/science/article/pii/S2352152X23000439.

[34] *Utility in Economics Explained: Types and Measurement*, English, May 2022. [Online]. Available: https://www.investopedia.com/terms/u/utility.asp (visited on 5th Jun. 2023).

[35] Etti Baranoff, P. L. Brockett and Y. Kahane, *Risk Management for Enterprises and Individuals*, English. Saylor Foundation, 2009, ISBN: 978-0-9823618-0-1.

[36] 'Overview of optimization', in *Process Integration*, ser. Process Systems Engineering, M. M. El-Halwagi, Ed., vol. 7, ISSN: 1874-5970, Academic Press, 2006, pp. 285–314. DOI: https://doi.org/10.1016/S1874-5970(06)80012-3. [Online]. Available: https://www.sciencedirect.com/science/article/pii/S1874597006800123.

[37] A. Grandjean, J. Adnot and G. Binet, 'A review and an analysis of the residential electric load curve models', *Renewable and Sustainable Energy Reviews*, vol. 16, no. 9, pp. 6539–6565, 2012, ISSN: 1364-0321. DOI: https://doi.org/10.1016/j.rser.2012.08.013.

[38] F. Lombardi, S. Balderrama, S. Quoilin and E. Colombo, 'Generating high-resolution multi-energy load profiles for remote areas with an open-source stochastic model', *Energy*, vol. 177, pp. 433–444, 2019, ISSN: 0360-5442. DOI: https://doi.org/10.1016/j.energy.2019.04.097.

[39] F. Riva, F. Gardumi, A. Tognollo and E. Colombo, 'Soft-linking energy demand and optimisation models for local long-term electricity planning: An application to rural India', *Energy*, vol. 166, pp. 32–46, 2019, ISSN: 0360-5442. DOI: https://doi.org/10.1016/j.energy.2018.10.067.

[40] S. Mandelli, M. Merlo and E. Colombo, 'Novel procedure to formulate load profiles for off-grid rural areas', *Energy for Sustainable Development*, vol. 31, pp. 130–142, 2016, ISSN: 0973-0826. DOI: https://doi.org/10.1016/j.esd.2016.01.005.

[41] A. J. Conejo, J. M. Morales and L. Baringo, 'Real-Time Demand Response Model', *IEEE Transactions on Smart Grid*, vol. 1, no. 3, pp. 236–242, 2010. DOI: 10.1109/TSG.2010.2078843.

[42] N. Gatsis and G. B. Giannakis, 'Cooperative multi-residence demand response scheduling', in *2011 45th Annual Conference on Information Sciences and Systems*, 2011, pp. 1–6. DOI: 10.1109/CISS.2011.5766245.

[43] Y. Rajbhandari, A. Marahatta, A. Shrestha *et al.*, 'Load prioritization technique to guarantee the continuous electric supply for essential loads in rural microgrids', *International Journal of Electrical Power & Energy Systems*, vol. 134, p. 107 398, 2022, ISSN: 0142-0615. DOI: https://doi.org/10.1016/j.ijepes.2021.107398. [Online]. Available: https://www.sciencedirect.com/science/article/pii/S0142061521006372.

[44] M. H. Miraz, M. Ali and P. S. Excell, 'Adaptive user interfaces and universal usability through plasticity of user interface design', *Computer Science Review*, vol. 40, p. 100 363, 2021, ISSN: 1574-0137. DOI: https://doi.org/10.1016/j.cosrev.2021.100363. [Online]. Available: https://www.sciencedirect.com/science/article/pii/S1574013721000034.

[45] Jeffrey Rubin, Dana Chisnell and Jared Spool, *Handbook of Usability Testing: How to Plan, Design, and Conduct Effective Tests, 2nd Edition*. West Sussex, United Kingdom: John Wiley & Sons, May 2008, ISBN: 978-0-470-18548-3.

[46] M. H. Miraz, M. Bhuiyan and M. E. Hossain, *Impacts of Culture and Socio-Economic Circumstances on Users' Behavior and Mobile Broadband Technology Diffusion Trends*, _eprint: 1708.02798, 2017.

[47] S. Helman, M. A. Terry, T. Pellathy *et al.*, 'Engaging clinicians early during the development of a graphical user display of an intelligent alerting system at the bedside', *International Journal of Medical Informatics*, vol. 159, p. 104 643, 2022, ISSN: 1386-5056. DOI: https://doi.org/10.1016/j.ijmedinf.2021.104643. [Online]. Available: https://www.sciencedirect.com/science/article/pii/S1386505621002690.

[48] B. A. Johnsson and B. Magnusson, 'Towards end-user development of graphical user interfaces for internet of things', *Future Generation Computer Systems*, vol. 107, pp. 670–680, 2020, ISSN: 0167-739X. DOI: https://doi.org/10.1016/j.future.2017.09.068.

[49] H. Lieberman, F. Paternò, M. Klann and V. Wulf, 'End-User Development: An Emerging Paradigm', in *End User Development*, H. Lieberman, F. Paternò and V. Wulf, Eds., Dordrecht: Springer Netherlands, 2006, pp. 1–8, ISBN: 978-1-4020-5386-3. DOI: 10.1007/1-4020-5386-X_1. [Online]. Available: https://doi.org/10.1007/1-4020-5386-X_1.

[50] H. Çimen, N. Bazmohammadi, A. Lashab, Y. Terriche, J. C. Vasquez and J. M. Guerrero, 'An online energy management system for AC/DC residential microgrids supported by non-intrusive load monitoring', *Applied Energy*, vol. 307, p. 118 136, 2022, ISSN: 0306-2619. DOI: https://doi.org/10.1016/j.apenergy.2021.118136. [Online]. Available: https://www.sciencedirect.com/science/article/pii/S0306261921014136.

[51] B. E. Sedhom, M. M. El-Saadawi, M. S. E. Moursi, M. A. Hassan and A. A. Eladl, 'IoT-based optimal demand side management and control scheme for smart microgrid', *International Journal of Electrical Power & Energy Systems*, vol. 127, p. 106 674, 2021, ISSN: 0142-0615. DOI: https://doi.org/10.1016/j.ijepes.2020.106674. [Online]. Available: https://www.sciencedirect.com/science/article/pii/S0142061520342198.

[52] H. Samanta, A. Bhattacharjee, M. Pramanik, A. Das, K. D. Bhattacharya and H. Saha, 'Internet of things based smart energy management in a vanadium redox flow battery storage integrated bio-solar microgrid', *Journal of Energy Storage*, vol. 32, p. 101 967, 2020, ISSN: 2352-152X. DOI: https://doi.org/10.1016/j.est.2020.101967. [Online]. Available: https://www.sciencedirect.com/science/article/pii/S2352152X20318028.

[53] J. A. A. Silva, J. C. López, C. P. Guzman, N. B. Arias, M. J. Rider and L. C. P. d. Silva, 'An IoT-based energy management system for AC microgrids with grid and security constraints', *Applied Energy*, vol. 337, p. 120 904, 2023, ISSN: 0306-2619. DOI: https://doi.org/10.1016/j.apenergy.2023.120904. [Online]. Available: https://www.sciencedirect.com/science/article/pii/S0306261923002684.

[54] W. F. Holmgren, C. W. Hansen and M. A. Mikofski, 'Pvlib python: A python package for modeling solar energy systems', *Journal of Open Source Software*, vol. 3, no. 29, p. 884, 2018, Publisher: The Open Journal. DOI: 10.21105/joss.00884. [Online]. Available: https://doi.org/10.21105/joss.00884.

[55] *SARAH-2 Solar Radiation Data*, en. [Online]. Available: https://joint-research-centre.ec.europa.eu/pvgis-photovoltaic-geographical-information-system/pvgis-data-download/sarah-2-solar-radiation-data_en (visited on 27th Mar. 2023).

[56] *PV Modeling*. [Online]. Available: https://pvlib-python.readthedocs.io/en/stable/reference/pv_modeling.html (visited on 8th Dec. 2022).

[57] A. P. Dobos, 'PVWatts Version 5 Manual', Sep. 2014. DOI: 10.2172/1158421. [Online]. Available: https://www.osti.gov/biblio/1158421.

[58] N. Narayan, Z. Qin, J. Popovic-Gerber, J.-C. Diehl, P. Bauer and M. Zeman, 'Stochastic load profile construction for the multi-tier framework for household electricity access using off-grid DC appliances', *Energy Efficiency*, vol. 13, no. 2, pp. 197–215, Feb. 2020, ISSN: 1570-6478. DOI: 10.1007/s12053-018-9725-6. [Online]. Available: https://doi.org/10.1007/s12053-018-9725-6.

[59] M. L. Bynum, G. A. Hackebeil, W. E. Hart *et al.*, *Pyomo - Optimization Modeling in Python*, Third Edition. Springer Optimization and Its Applications, vol. 67, ISBN: 978-3-030-68928-5.

[60] S. Quoilin, K. Kavvadias, A. Mercier, I. Pappone and A. Zucker, 'Quantifying self-consumption linked to solar home battery systems: Statistical analysis and economic assessment', *Applied Energy*, vol. 182, pp. 58–67, 2016, ISSN: 0306-2619. DOI: https://doi.org/10.1016/j.apenergy.2016.08.077.

[61] *Selenium*. [Online]. Available: https://pypi.org/project/selenium/ (visited on 11th Apr. 2023).

[62] *Eco Moyo Education Centre*. [Online]. Available: https://www.ecomoyo.com (visited on 12th Dec. 2022).

[63] K. T. Lervik and A. M. Waitz, 'Techno-Economic Analysis of Rural Microgrid at Eco Moyo Education Centre in Kenya', eng, Accepted: 2022-10-07T17:33:40Z, M.S. thesis, NTNU, 2022. [Online]. Available: https://ntnuopen.ntnu.no/ntnu-xmlui/handle/11250/3024775 (visited on 25th Nov. 2022).

[64] Kenya Meteorological Department, 'Climate Outlook for the "Long Rains" (March-May) 2023 Season and Review of the October-December 2022 "Short Rains" Season', Ministry of Environment and Forestry, Nairobi, Kenya, Tech. Rep., Jan. 2023, p. 16. [Online]. Available: https://meteo.go.ke/sites/default/files/forecast/seasonal-forecast/MAM_2023_Forecast.pdf (visited on 24th May 2023).

[65] *Kilifi Annual Weather Averages*, en. [Online]. Available: https://www.worldweatheronline.com/kilifi-weather/coast/ke.aspx (visited on 24th May 2023).

Appendix

A GCL-M8/72H Monocrystalline Module

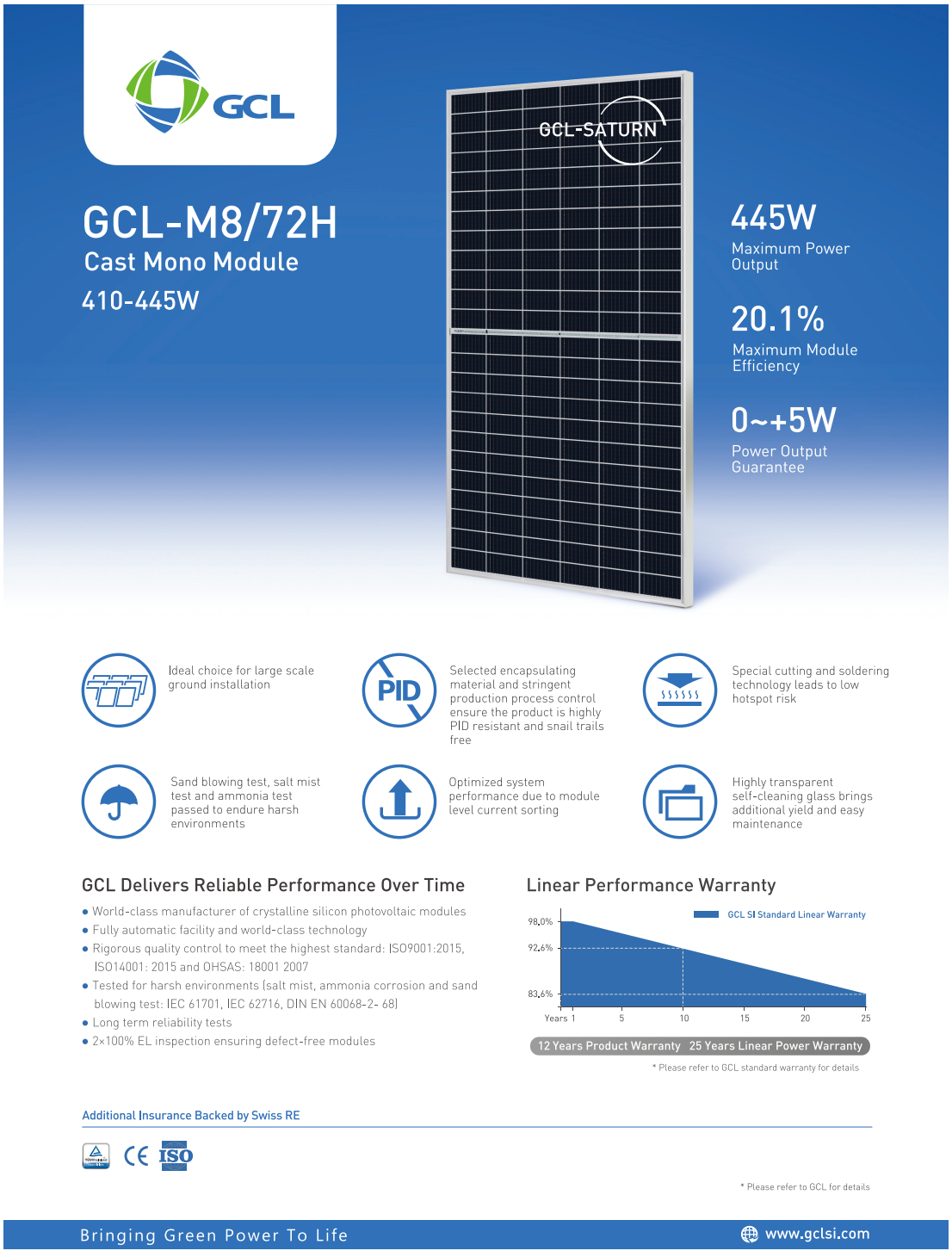

GCL-M8/72H

Cast Mono Module

410-445W

Electrical Specification (STC*)

Maximum Power	Pmax(W)	410	415	420	425	430	435	440	445
Maximum Power Voltage	Vmp(V)	39.39	39.72	40.04	40.37	40.72	41.08	41.40	41.75
Maximum Power Current	Imp(A)	10.41	10.45	10.49	10.53	10.56	10.59	10.63	10.66
Open Circuit Voltage	Voc(V)	47.58	47.86	48.13	48.40	48.69	48.99	49.25	49.55
Short Circuit Current	Isc(A)	10.92	10.96	11.00	11.04	11.07	11.10	11.14	11.17
Module Efficiency	(%)	18.6	18.8	19.0	19.2	19.5	19.7	19.9	20.1
Power Output Tolerance	(W)	0~+5							

* Irradiance 1000W/m², Module Temperature 25°C, Air Mass 1.5

Electrical Specification (NOCT*)

Maximum Power	Pmax (W)	305.34	308.95	312.57	316.22	319.88	323.55	327.25	330.96
Maximum Power Voltage	Vmp (V)	36.70	37.00	37.30	37.60	37.90	38.20	38.50	38.80
Maximum Power Current	Imp (A)	8.32	8.35	8.38	8.41	8.44	8.47	8.50	8.53
Open Circuit Voltage	Voc(V)	44.30	44.60	44.80	45.00	45.30	45.50	45.70	46.00
Short Circuit Current	Isc (A)	8.83	8.86	8.89	8.92	8.95	8.98	9.01	9.04

* Irradiance 800W/m², Ambient Temperature 20°C, Wind Speed 1m/s

Mechanical Data

Number of Cells	144 Cells (6×24)
Dimensions of Module L*W*H (mm)	2108×1048×35mm (82.99×41.26×1.38 inches)
Weight (kg)	25.6 kg
Glass	High transparency solar glass 3.2mm (0.13 inches)
Backsheet	White
Frame	Silver, anodized aluminium alloy
J-Box	IP68 Rated
Cable	4.0mm² (0.006 inches²), Portrait: 300/300mm (11.81 inches)
Number of diodes	3
Wind/ Snow Load	2400Pa/ 5400Pa*
Connector	MC Compatible

* For more details please check the installation manual of GCLSI

Temperature Ratings

Nominal Operating Cell Temperature (NOCT)	44±2°C
Temperature Coefficient of Isc	+0.06%/°C
Temperature Coefficient of Voc	-0.30%/°C
Temperature Coefficient of Pmax	-0.39%/°C

Maximum Ratings

Operational Temperature	-40~+85°C
Maximum System Voltage	1500V DC
Max Series Fuse Rating	20A

Optional

Connector:	☐ Original MC4

Packaging Configuration

Module per box	30 pieces
Module per 40' container	600 pieces

Module Dimension

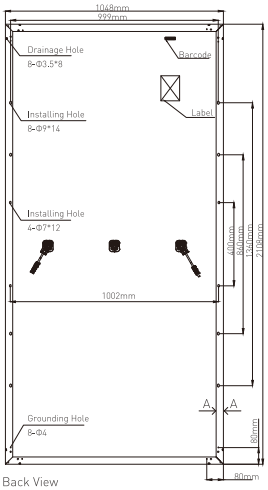

Back View

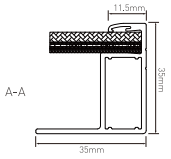

I-V Curve at Different Temperature (445W)

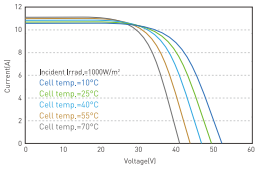

I-V/P-V Curve at Different Irradiation (445W)

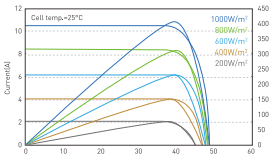

CAUTION: READ INSTALLATION MANUAL BEFORE USING THE PRODUCT

GCL

Contact Us for More Information

website: www.gclsi.com email: gclsisales@gclsi.com

Bringing Green Power To Life

GCL-EN-M8/72H-N-2019-V3.0

B Growatt PV Off-Grid Inverter

Datasheet	SPF 3500 ES	SPF 5000 ES
Battery Voltage	48VDC	
Battery Type	Lithium/Lead-acid	
INVERTER OUTPUT		
Rated Power	3500VA/ 3500W	5000VA/ 5000W
Parallel Capability	Yes, 6 units maximum	
AC Voltage Regulation (Battery Mode)	230VAC ± 5% @ 50/60Hz	
Surge Power	7000VA	10000VA
Efficiency (Peak)	93%	
Waveform	Pure sine wave	
Transfer Time	10ms typical, 20ms Max	
SOLAR CHARGER		
Maximum PV Array Power	4500W	6000W
MPPT Range @ Operating Voltage	120VDC ~ 430VDC	
Number of Independent MPP Trackers/ Strings Per MPP Tracker	1/1	
Maximum PV Array Open Circuit Voltage	450VDC	
Maximum Solar Charge Current	80A	100A
AC CHARGER		
Charge Current	60A	80A
AC Input Voltage	230 VAC	
Selectable Voltage Range	170-280 VAC (For Personal Computers) ; 90-280 VAC (For Home Appliances)	
Frequency Range	50Hz/60Hz (Auto sensing)	
PHYSICAL		
Protection Degree	IP20	
Dimension (W/H/D)	330/485/135mm	330/485/135mm
Net Weight	11.5kgs	12kgs
OPERATING ENVIRONMENT		
Humidity	5% to 95% Relative Humidity(Non-condensing)	
Altitude	<2000m	
Operating Temperature	0°C - 55°C	
Storage Temperature	-15°C - 60°C	

C Tubular Gel Battery

TECHNICAL SPECIFICATION - Tubular Gel Battery

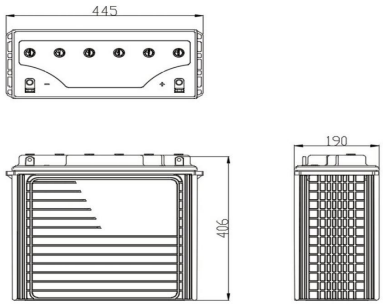

Product Features :-

1. Robust Tubular with High pressure diecasted spine - rate of spine corrosion is very low as compare to AGM VRLA
2. Gelled electrolyte - no stratification and no failure due to PSOC
3. Valve regulated - no water top up during service life
4. Antimony free alloy - longer shelf life because of very low self discharge
5. Very High Design & service life as compare to than AGM VRLA
6. Good for Cyclic & Float Applications
7. Wide operating Temperature Range.

Technical Specifications

Model	Nominal Voltage	Rated Capacity 10 Hr @ 27°C (Ah)	Dimensions in mm			Filled Battery Weight [Kg] [±3%]	Terminal Type
			Length [± 3 mm]	Width [± 3 mm]	Height [± 3 mm]		
CE150GG [12 V 150 AH @ C20]	12	135	445	190	406	48	L
CE200GG [12 V 200 AH @ C20]	12	180	445	190	406	61.5	L

Electrical Parameters & Charging Profile

Battery Specified Capacity Test @ 27 °C						
	C20 @10.5V	C10 @10.5V	C7 @10.5V	C5 @10.5V	C3 @10.5V	C1 @10.5V
CE150GG [12 V 150 AH @ C20]	150	135	124	112	97	68
CE200GG [12 V 200 AH @ C20]	200	180	166	150	129	90
Ah & Wh Efficiency						
Ah Efficiency	>96%		Wh Efficiency	>84%		

- Poly Components Material :- Polypropylene Co polymer
- Color :- Blue
- Testing Parameters :- IS 13369:2005, IEC 60896-21 & IEC 61427-1

Charging Profile

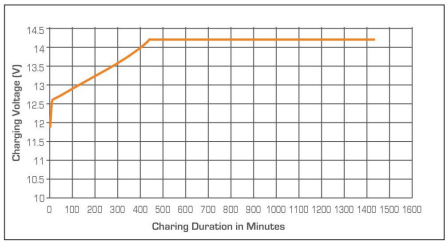

Self Discharge Characteristics @ Different Temperature

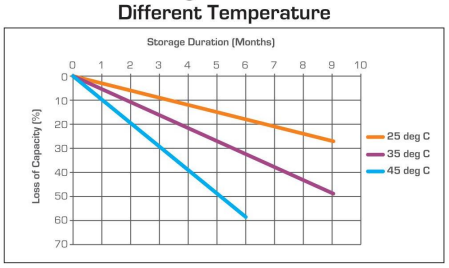

State of Charge Measure of Open-circuit Voltage @ 27°C

State of Charge	Specific Gravity	Voltage
100%	NA	13.1V
75%	NA	12.75V
50%	NA	12.45V
25%	NA	12.1
0%	NA	11.9V

Discharging Characteristics at various rates @ 27°C

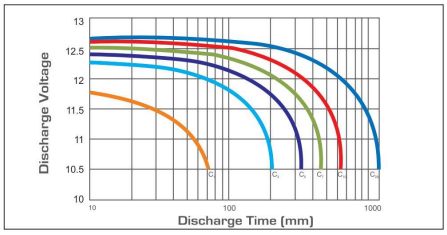

Service (Float) Life and Temperature

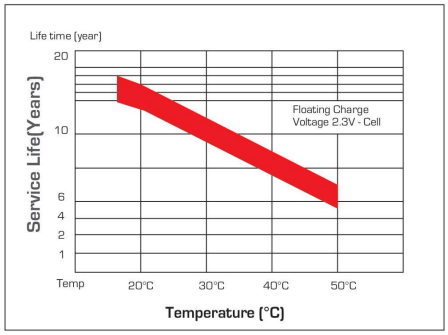

Expected Capacity vs Temperature

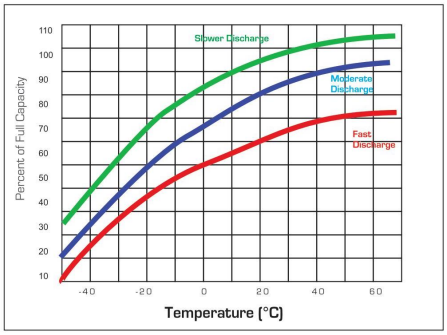

Eastman Battery Manufacturing Certified by Vincotte for

ISO 9001 CERTIFIED VINÇOTTE

ISO 14001 ENVIRONMENTAL MANAGEMENT VINÇOTTE

OHSAS 18001 CERTIFIED VINÇOTTE

Specific Gravity & Self Discharge w.r.t. Temperature

CHARGING TEMPERATURE COMPENSATION	Add	Subtract
	0.005 volt per cell for every 1°C below 25°C 0.0028 volt per cell for every 1°F below 77°F	0.005 volt per cell for every 1°C above 25°C or 0.0028 volt per cell for every 1°F above 77°F
OPERATIONAL DATA	Operating Temperature	Self Discharge
	-4°F to 131°F (-20°C to +55°C). At temperatures below 32°F (0°C) maintain a state of charge greater than 60%.	As per discharge Graph

Expected Life

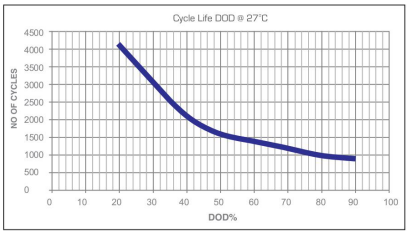

Charging Instructions

Charger Voltage Settings (at 77° F/ 25°C)			
System Voltage	12V	24V	48V
Maximum Charge Current	0.2C10		
Maximum Absorption Phase Time (hours)	4		
Absorption Voltage	14.2	28.4	56.8
Float Voltage	13.8	27.6	55.2
Equalization Voltage	14.8	29.6	59.2
Do not install or charge batteries in a sealer or non- ventilated compartment. Constant under or overcharging will damage the battery and shorten its life as with any battery.			
Periodic Charge	Provide a periodic freshening charge to maintain a SOC greater than the threshold of 70%		

Eastman Gel battery testing procedure adhere IEC , CE & UL 94 test standards

Comparison in between Chloride Tubular Gel & AGM Gel VRLA

S.No	Parameter	Chloride Tubular GEL	AGM GEL VRLA
1	Plate Technology	Tall Tubular Plate	Flat Pasted Plate
2	Electrolyte	Electrolyte in-between Gel	Electrolyte in- between AGM
3	Water Loss	Negligible	Negligible
4	Self Discharge	Very Low <2.0%	Very Low <2.0%
5	Life Cycle w.r.t DOD	1000 Cycle @ 80% DOD	450 Cycle @ 80%DOD
6	Water Top up	No water top throughout Life	No water top throughout Life
7	Plastic Material	PPCP	PPCP material & ABS material
8	Battery Technology	Valve Regulated Technology	Valve Regulated Technology
9	Separator	PVC	AGM
10	Life w.r.t Application	Excellent performance on cyclic application	Not good for cyclic application
11	Acid Stratification	NO	No
12	Discharge Current	Low Range	Wide Range
13	Charging setting	Required special set point for chargers	Required special set point for charges
14	Operating Temperature	Wide Temperature Operating range	Temperature Operating range is limited
15	Spillage	Spill-proof	Spill-proof

Terminal Configuration :-
Terminal Type :- L
Terminal Height :- 25 mm
Torque Value :- 8-10 N.m
Bolt Type :- M8

Vent Plug Type :-
M18 with vent valve &
flame arrestor assembly

EASTMAN AUTO & POWER LTD.
572, Udyog Vihar Phase 5, Gurgaon - 122016, Haryana, India | +91 124 4627900 | sales@eastmanglobal.com
www.eaplworld.com

D Price Estimate for the Extension of the System

The price estimate for the extension of the system is presented in Table D.37, and the total cost is 82,120 KES.

Table D.37: Detailed description of the price estimate for extension of the existing system at Eco Moyo.

Description	**Qty.**	**Unit price [KES]**	**Total price [KES]**
TWE 2.5 (price/m)	50	250	12,500
DB 6 way complete	1	5,300	5,300
2.5 red cable (roll)	1	5,500	5,300
2.5 black cable (roll)	1	5,500	5,500
2.5 yellow cable (roll)	1	5,500	5,500
1.5 red cable	-	3,400	3,400
1.5 black cable	-	3,400	3,400
Twin socket	6	420	2,520
Twin pattress box	6	100	600
Single socket	6	250	1,500
Single pattress box	6	70	420
Switch 2 gang	6	240	1,440
Hanging holder	6	260	1,560
Angle holder	6	140	840
Tape	4	75	300
LED bulbs 7 W	12	200	2,400
Junction box	7	70	490
Pipes h/g	25	220	5,500
Bends	10	45	450
Installation labour	-	-	23,000

E Optimization Results

E.1 Scenario 0

Table E.38: Initial and new time windows after optimization in Scenario 0.

Date	Uncovered demand	Appliance	Number	Building	Initial Window	New Window
17.01	6.075 Wh	Drill	1	Staff Room	11:15 - 13:15	11:45 - 13:45
24.01	13.58 Wh	Printer	1	Staff Room	10:00 - 10:30	09:45 - 10:15
30.01	14.08 Wh	Drill	1	Staff Room	10:00 - 12:00	09:30 - 11:30
20.02	61.90 Wh	Kettle	1	Staff Room	14:30 - 14:45	14:45 - 15:00
21.02	127.9 Wh	Kettle	1	Staff Room	14:15 - 14:30	14:00 - 14:15
23.02	10.57 Wh	Kettle	1	Staff Room	16:30 - 16:45	16:15 - 16:30
17.03	99.40 Wh	Kettle	1	Staff Room	14:45 - 15:00	15:00 - 15:15
22.04	0.000 Wh	Fan	1	Office Building	10:45 - 16:45	10:30 - 16:30
01.05	0.000 Wh	Kettle	1	Staff Room	15:00 - 15:15	14:45 - 15:00
22.05	15.15 Wh	Kettle	1	Staff Room	16:30 - 16:45	16:00 - 16:15
24.05	0.000 Wh	Fan	1	Staff Room	12:30 - 18:30	10:30 - 16:30
		Fan	3	Staff Court	16:15 - 22:15	16:00 - 22:00
03.06	41.57 Wh	Kettle	1	Staff Room	16:15 - 16:30	16:30 - 16:45
12.06	138.9 Wh	Kettle	1	Staff Room	14:15 - 14:30	14:00 - 14:15
15.06	0.000 Wh	Kettle	1	Staff Room	15:45 - 16:00	15:00 - 15:15
06.07	0.000 Wh	Fan	1	Staff Room	12:30 - 18:30	12:00 - 18:00
		Fan	1	Staff Room	12:15 - 18:15	12:00 - 18:00
		Fan	1	Office Building	11:00 - 17:00	10:30 - 16:30
07.07	0.000 Wh	Fan	1	Staff Room	12:15 - 18:15	11:30 - 17:30
		Fan	1	Staff Room	12:45 - 18:45	11:30 - 17:30
		Kettle	1	Staff Room	16:15 - 16:30	12:45 - 13:00
		Drill	1	Staff Room	07:30 - 09:30	07:45 - 09:45
		Fan	1	Office Building	10:45 - 16:45	09:30 - 15:30
		Fan	1	Office Building	11:15 - 17:15	13:30 - 19:30
		Fan	3	Staff Court	16:15 - 22:15	11:30 - 17:30
		Fan	3	Staff Court	16:15 - 22:15	13:30 - 19:30
03.09	6.900 Wh	Printer	1	Office Building	16:15 - 16:45	16:00 - 16:30
29.09	22.65 Wh	Printer	1	Office Building	16:15 - 16:45	16:30 - 17:00
11.10	90.08 Wh	Drill	1	Staff Room	13:15 - 15:15	12:45 - 14:45
20.10	247.3 Wh	Kettle	1	Staff Room	14:15 - 14:30	14:00 - 14:15
23.10	15.32 Wh	Printer	1	Office Building	10:00 - 10:30	09:45 - 10:15
26.10	126.8 Wh	Kettle	1	Staff Room	14:45 - 15:00	15:00 - 15:15
08.11	118.7 Wh	Kettle	1	Staff Room	14:45 - 15:00	15:00 - 15:15
18.11	126.6 Wh	Kettle	1	Staff Room	14:45 - 15:00	15:00 - 15:15
19.11	8.575 Wh	Fan	1	Office Building	11:15 - 17:15	10:45 - 16:45
26.11	111.9 Wh	Kettle	1	Staff Room	14:45 - 15:00	15:00 - 15:15
08.12	121.6 Wh	Kettle	1	Staff Room	15:00 - 15:15	15:15 - 15:30

Table E.39: Dates of optimization failure in Scenario 0 due to battery depletion.

Date	Uncovered demand	Battery Start
03.02	33.84 Wh	43.75%
24.04	2730 Wh	42.44%
26.04	4703 Wh	24.74%
30.04	3175 Wh	20.00%
02.05	128.4 Wh	20.97%
06.05	944.2 Wh	34.21%
12.05	2545 Wh	30.38%
19.05	5318 Wh	20.00%
25.05	2071 Wh	20.00%
26.05	505.4 Wh	20.00%
05.06	1075 Wh	20.00%
09.06	6557 Wh	20.14%
19.06	841.6 Wh	20.00%
23.06	837.2 Wh	20.00%
01.07	4917 Wh	20.00%
16.07	2010 Wh	26.06%
19.08	692.5 Wh	35.29%
11.09	471.4 Wh	38.44%
05.10	1721 Wh	26.22%
06.10	2478 Wh	20.00%
09.11	4815 Wh	28.03%
16.11	3434 Wh	25.66%

Table E.40: Dates of optimization failure in Scenario 0 due to insufficient SoC at the end of the day (no uncovered demand).

Date	Battery Start	Battery End
29.04	48.54%	13.59%
09.05	28.50%	0.9127%
18.05	27.94%	10.30%
04.06	20.54%	2.920%
16.06	20.62%	11.19%
18.06	25.26%	9.228%
22.06	28.42%	13.45%
26.06	25,61%	18.68%
30.06	31,68%	14.56%
02.07	20.00%	14.40%
10.07	32.11%	11.75%
13.10	32.73%	9.243%

E.2 Scenario 1

Table E.41: Initial and new time windows after optimization in Scenario 1.

Date	Uncovered demand	Appliance	Number	Building	Initial Window	New Window
17.01	6.075 Wh	Drill	1	Staff Room	11:15 - 13:15	11:45 - 13:45
24.01	13.58 Wh	Printer	1	Staff Room	10:00 - 10:30	09:45 - 10:15
30.01	14.08 Wh	Drill	1	Staff Room	10:00 - 12:00	09:30 - 11:30
03.02	0,000 Wh	Fan	3	Staff Court	16:00 - 22:00	14:00 - 20:00
		Fan	3	Staff Court	16:15 - 22:15	16:00 - 22:00
20.02	61.90 Wh	Kettle	1	Staff Room	14:30 - 14:45	14:45 - 15:00
21.02	127.9 Wh	Kettle	1	Staff Room	14:15 - 14:30	14:00 - 14:15
23.02	10.58 Wh	Kettle	1	Staff Room	16:30 - 16:45	16:15 - 16:30
17.03	99.40 Wh	Kettle	1	Staff Room	14:45 - 15:00	15:00 - 15:15
22.05	15.15 Wh	Kettle	1	Staff Room	16:30 - 16:45	16:00 - 16:15
03.06	41.58 Wh	Kettle	1	Staff Room	16:15 - 16:30	16:30 - 16:45
12.06	138.9 Wh	Kettle	1	Staff Room	14:15 - 14:30	14:00 - 14:15
03.09	6.900 Wh	Printer	1	Office Building	16:15 - 16:45	16:00 - 16:30
29.09	22.65 Wh	Printer	1	Office Building	16:15 - 16:45	16:30 - 17:00
11.10	90.08 Wh	Drill	1	Staff Room	13:15 - 15:15	12:45 - 14:45
20.10	247.3 Wh	Kettle	1	Staff Room	14:15 - 14:30	14:00 - 14:15
23.10	15.33 Wh	Printer	1	Office Building	10:00 - 10:30	09:45 - 10:15
26.10	126.8 Wh	Kettle	1	Staff Room	14:45 - 15:00	15:00 - 15:15
08.11	118.7 Wh	Kettle	1	Staff Room	14:45 - 15:00	15:00 - 15:15
18.11	126.6 Wh	Kettle	1	Staff Room	14:45 - 15:00	15:00 - 15:15
19.11	8.575 Wh	Fan	1	Office Building	11:15 - 17:15	10:45 - 16:45
26.11	111.9 Wh	Kettle	1	Staff Room	14:45 - 15:00	15:00 - 15:15
08.12	121.6 Wh	Kettle	1	Staff Room	15:00 - 15:15	15:15 - 15:30

Table E.42: Dates of optimization failure in Scenario 1 due to battery depletion.

Date	Uncovered demand	Battery Start
24.04	497.9 Wh	43.39%
26.04	2471 Wh	39.79%
30.04	1486 Wh	31.14%
12.05	312.6 Wh	30.38%
19.05	3961 Wh	44.31%
26.05	59.04 Wh	28.16%
05.06	371.0 Wh	22.31%
09.06	4325 Wh	36.11%
19.06	227.8 Wh	20.00%
23.06	390.8 Wh	20,00%
01.07	3197 Wh	31.41%
06.10	2032 Wh	20.00%
09.11	2583 Wh	42.42%
16.11	1202 Wh	40.53%

Table E.43: Dates of optimization failure in Scenario 1 due to insufficient SoC at the end of the day (no uncovered demand).

Date	Battery Start	Battery End
02.05	34.79%	16.86%
06.05	47.34%	11.51%
25.05	34.82%	0.2627%
22.06	27.15%	15.17%
02.07	20.00%	15.52%
16.07	40.85%	1.987%
19.08	48.23%	13.80%
11.09	50.75%	15.77%
05.10	40.97%	4.579%

E.3 Scenario 2

Table E.44: Initial and new time windows after optimization in Scenario 2.

Date	Uncovered demand	Appliance	Number	Building	Initial Window	New Window
17.01	6.075 Wh	Drill	1	Staff Room	11:15 - 13:15	11:45 - 13:45
24.01	13.58 Wh	Printer	1	Staff Room	10:00 - 10:30	09:45 - 10:15
30.01	14.08 Wh	Drill	1	Staff Room	10:00 - 12:00	09:30 - 11:30
20.02	61.90 Wh	Kettle	1	Staff Room	14:30 - 14:45	14:45 - 15:00
21.02	127.9 Wh	Kettle	1	Staff Room	14:15 - 14:30	14:00 - 14:15
23.02	10.58 Wh	Kettle	1	Staff Room	16:30 - 16:45	16:15 - 16:30
17.03	99.40 Wh	Kettle	1	Staff Room	14:45 - 15:00	15:00 - 15:15
22.05	15.15 Wh	Kettle	1	Staff Room	16:30 - 16:45	16:00 - 16:15
03.06	41.58 Wh	Kettle	1	Staff Room	16:15 - 16:30	16:30 - 16:45
12.06	138.9 Wh	Kettle	1	Staff Room	14:15 - 14:30	14:00 - 14:15
03.09	6.900 Wh	Printer	1	Office Building	16:15 - 16:45	16:00 - 16:30
29.09	22.65 Wh	Printer	1	Office Building	16:15 - 16:45	16:30 - 17:00
11.10	90.08 Wh	Drill	1	Staff Room	13:15 - 15:15	12:45 - 14:45
20.10	247.3 Wh	Kettle	1	Staff Room	14:15 - 14:30	14:00 - 14:15
23.10	15.33 Wh	Printer	1	Office Building	10:00 - 10:30	09:45 - 10:15
26.10	126.8 Wh	Kettle	1	Staff Room	14:45 - 15:00	15:00 - 15:15
08.11	118.7 Wh	Kettle	1	Staff Room	14:45 - 15:00	15:00 - 15:15
11.11	300.1 Wh	Kettle	1	Staff Room	14:30 - 14:45	14:45 - 15:00
18.11	126.6 Wh	Kettle	1	Staff Room	14:45 - 15:00	15:00 - 15:15
19.11	8.575 Wh	Fan	1	Office Building	11:15 - 17:15	10:45 - 16:45
26.11	111.9 Wh	Kettle	1	Staff Room	14:45 - 15:00	15:00 - 15:15
08.12	121.6 Wh	Kettle	1	Staff Room	15:00 - 15:15	15:15 - 15:30

Table E.45: Dates of optimization failure in Scenario 2 due to battery depletion.

Date	Uncovered demand	Battery Start
26.04	239.4 Wh	49.82%
30.04	228,1 Wh	35.34%
12.05	25,08 Wh	53.59%
19.05	1720 Wh	40.20%
09.06	2093 Wh	46.76%
01.07	938.7 Wh	43.04%
06.10	1530 Wh	20.41%
09.11	351.1 Wh	52.02%

Table E.46: Dates of optimization failure in Scenario 2 due to insufficient SoC at the end of the day (no uncovered demand).

Date	Battery Start	Battery End
24.04	52.83%	12.95%
25.05	45.68%	16.88%
26.05	20.00%	2.892%
05.06	35.11%	13.75%
19.06	34.58%	14.96%
22.06	25.98%	16.00%
23.06	20.00%	0.4149%
02.07	20.00%	16.27%
16.07	50.71%	18.32%
16.11	50.44%	7.688%

F Python Script for the Optimization Model

```
import pyomo.environ as pyo
import pandas as pd
from pyomo.opt import SolverFactory
from init_optimize import initBaseLoad, initLoadProfiles, initPV

def optimizeLoadProfile(startDate, batteryPercentage, loadList):


    '''------------- Appliance input from excel -------------'''

    appliances = pd.read_csv('InputFiles/appliances.csv', sep=";", dtype = None,
    ↪  index_col = 1)
    ratedPower = appliances['Power']
    userTime = appliances['User Time']
    userCost = appliances['User Cost']
    building = appliances['Building']

    '''------------- Initialize Parameters -------------'''

    n_inv = 0.93
    n_bat = 0.9
    timestep = 0.25
    batCapacity = ((4+1)*200*12)/1000
    invCapacity = (3500 * 0.25)/1000
    maxT = 96

    baseLoad = initBaseLoad(startDate)
    loadProfiles, windowStart, numItems = initLoadProfiles(loadList, startDate)
    pv = initPV(startDate)
    num_a = len(loadProfiles)

    '''-----Declaration of sets-----'''

    A = list(range(0, num_a))
    T = list(range(0, maxT))

    initLoad = {}
    load_profiles = {}
    for t in T:
        initLoad[t] = baseLoad[t] + sum(load_profiles[a,t] for a in A)
        for a in A:
            load_profiles[a,t] = loadProfiles[a][t]


    '''-----Creating Pyomo Model-----'''

    model = pyo.ConcreteModel()

    #Declaration of sets
    model.T               = pyo.Set(initialize = T)
    model.A               = pyo.Set(initialize = A)

    #Declaration of parameters
    model.ratedPower      = pyo.Param(model.A, initialize = ratedPower)
    model.userTime        = pyo.Param(model.A, initialize = userTime/15)
    model.baseLoad        = pyo.Param(model.T, initialize = baseLoad)
```

```
model.batteryPercentageStart = pyo.Param(initialize = batteryPercentage)
model.num_items       = pyo.Param(model.A, initialize = numItems)
model.loadProfiles    = pyo.Param(model.A, model.T, initialize =
↪  load_profiles)
model.pv              = pyo.Param(model.T, initialize = pv * timestep)
model.n_inv           = pyo.Param(initialize = n_inv)
model.n_bat           = pyo.Param(initialize = n_bat)
model.batCapacity     = pyo.Param(initialize = batCapacity )
model.timestep        = pyo.Param(initialize = timestep)
model.invCapacity     = pyo.Param(initialize = invCapacity)
model.building        = pyo.Param(model.A, initialize = building, within =
↪  pyo.Any)
model.t_start         = pyo.Param(model.A, initialize = windowStart)
model.X               = pyo.Param(model.A, initialize = userCost)
model.t_end           = pyo.Param(initialize = maxT - 1)

#Declaration of variables
model.demand          = pyo.Var(model.A, model.T, within =
↪  pyo.NonNegativeReals)
model.d               = pyo.Var(model.A, model.T, within = pyo.Binary)
model.store2inv       = pyo.Var(model.T, within = pyo.NonNegativeReals)
model.pv2inv          = pyo.Var(model.T, within = pyo.NonNegativeReals)
model.pv2store        = pyo.Var(model.T, within = pyo.NonNegativeReals)
model.res_pv          = pyo.Var(model.T, within = pyo.NonNegativeReals)
model.inv2load        = pyo.Var(model.T, within = pyo.NonNegativeReals)
model.SOC             = pyo.Var(model.T, within = pyo.NonNegativeReals,
↪  bounds = (0, model.batCapacity))
model.cost            = pyo.Var(model.A, model.T, within =
↪  pyo.NonNegativeReals)
model.t_moved         = pyo.Var(model.A, model.T,  within =
↪  pyo.NonNegativeReals)

'''----- Objective function -----'''

def cost(model):
    return sum(sum((model.X[a] * model.t_moved[a,t]) for t in model.T) for a
    ↪  in model.A) + sum(model.res_pv[t] for t in model.T)
model.OBJ = pyo.Objective(rule = cost, sense = pyo.minimize)


'''----- Constraints -----'''

def applianceDaily(model, a):
    i = list(range(1, int(maxT - model.userTime[a] + 1)))
    return sum(model.d[a,j] for j in i) == 1
model.constraint_3b = pyo.Constraint(model.A, rule = applianceDaily)

def calculateDemand(model, a, t):
    if (t <= model.userTime[a] - 2):
        i = list(range(0,t + 1))
        return model.demand[a,t] == sum(model.ratedPower[a] * model.d[a,j] *
        ↪  model.num_items[a] for j in i)
    else:
        start = int(t - model.userTime[a] + 1)
        i = list(range(start, t + 1))
        return model.demand[a,t] == sum(model.ratedPower[a] * model.d[a,j] *
        ↪  model.num_items[a]  for j in i)
```

```
model.constraint_3cd = pyo.Constraint(model.A, model.T, rule =
↪  calculateDemand)

def calculateMove(model, a, t):
    return model.t_moved[a, t] == model.d[a,t] * abs((model.t_start[a] - t) *
    ↪  model.num_items[a])
model.constraint_3e = pyo.Constraint(model.A, model.T, rule = calculateMove)

def noCut(model, a, t):
    return sum(sum(model.demand[a,t] for a in model.A) for t in model.T) ==
    ↪  sum(sum(model.loadProfiles[a,t] for a in model.A) for t in model.T)
model.constraint_3f = pyo.Constraint(model.A, model.T, rule = noCut)

def balanceInverter(model, t):
    return model.inv2load[t] == (model.store2inv[t] + model.pv2inv[t]) *
    ↪  model.n_inv
model.constraint_3g = pyo.Constraint(model.T, rule = balanceInverter)

def balancePV(model, t):
    return model.pv[t] == model.pv2store[t] + model.pv2inv[t] +
    ↪  model.res_pv[t]
model.constraint_3h = pyo.Constraint(model.T, rule = balancePV)

def totalLoad(model, t):
    return model.inv2load[t] == (model.baseLoad[t] + sum(model.demand[a, t]
    ↪  for a in model.A)) * (0.25/1000)
model.constraint_3i = pyo.Constraint(model.T, rule = totalLoad)

def capacityInv(model, t):
    return model.inv2load[t] <= model.invCapacity * model.n_inv
model.constraint_3j = pyo.Constraint(model.T, rule = capacityInv)

def maxpv2store(model, t):
    return model.pv2store[t] <= model.batCapacity
model.constraint_3k = pyo.Constraint(model.T, rule = maxpv2store)

def batCharge(model, t):
    if t == 0:
        return model.SOC[t] == model.batteryPercentageStart *
        ↪  model.batCapacity
    else:
        return model.SOC[t] == model.SOC[t-1] + model.pv2store[t] *
        ↪  model.n_bat - model.store2inv[t]
model.constraint_3lm = pyo.Constraint(model.T, rule = batCharge)

def batCapacityMax(model, t):
    if t == model.t_end:
        return model.SOC[t] >= model.batCapacity * 0.2
    else:
        return model.SOC[t] <= model.batCapacity
model.constraint_3no = pyo.Constraint(model.T, rule=batCapacityMax)


'''----- Solving the model -----'''

SolverFactory('glpk').solve(model)
```

G Python Script for GUI Backend: Automatic Download of Real-Time Data

```
import os
import time
import pytesseract
import configparser
import pandas as pd
from PIL import Image
from io import BytesIO
from datetime import datetime
from selenium import webdriver
import matplotlib.pyplot as plt
from selenium.webdriver.support.ui import WebDriverWait
from selenium.webdriver.support import expected_conditions as EC
from selenium.webdriver.chrome.options import Options

def download_from_shineDesign():
    #Path to the chromedriver
    path_chromedriver = 'GUI/chromedriver'

    #Including the path in the system
    os.environ['PATH'] += os.pathsep + path_chromedriver

    #Check if today's file already is downloaded and delete it
    today = datetime.today().strftime('%Y-%m-%d')
    file_name =
    ↪  'Downloaded files from shine/NZH3BFA024 storage data - {today}_{today}.xls'

    if os.path.exists(file_name):
        os.remove(file_name)

    #The username and password is stored in config.ini to keep it confidential
    config = configparser.ConfigParser()
    config.read('GUI/config.ini')
    username = config.get('credentials', 'username')
    password = config.get('credentials', 'password')

    #The url of the server
    url = "https://server.growatt.com/login.do"

    #Want to run the code without seeing the window ("headless" mode)
    options_chrome = Options()
    options_chrome.add_argument("--headless")

    #Create the path where the file is to be downloaded
    download_path = 'GUI/Downloaded files from shine'
    preferance = {"download.default_directory": download_path}
    options_chrome.add_experimental_option("prefs", preferance)

    #Creating a driver in Chrome and open the url
    driver = webdriver.Chrome(executable_path=path_chromedriver,
    ↪  chrome_options=options_chrome)

    #Maximize the window
    driver.maximize_window()
```

```
#Open the url
driver.get(url)

#Filling out the username and password and click on the sign in button
uname = driver.find_element("id", "account")
uname.send_keys(username)

time.sleep(2)

pword = driver.find_element("id", "password")
pword.send_keys(password)

time.sleep(2)

#Find the code image element and extract the code value from it
find_code_element = driver.find_element("id", "validateCode")

#While loop to prevent error while reading the validation code
code_value = None
while not code_value:
    code_image_data = find_code_element.screenshot_as_png
    code_image = Image.open(BytesIO(code_image_data))
    code_value = pytesseract.image_to_string(code_image).strip()

    if not code_value or len(code_value) != 3:
        find_code_element.click()
        code_image_data = find_code_element.screenshot_as_png
        time.sleep(1)
        code_value = None
    else:
       #Fill in the value of the code
       code = driver.find_element("id", "vCode")
       code.send_keys(code_value)

#Find the sign-in button and click
sign_in = WebDriverWait(driver,
↪  5).until(EC.presence_of_element_located(("id", "btnLoginSub")))
sign_in.click()

#Find plant button
plant = WebDriverWait(driver,
↪  5).until(EC.presence_of_element_located(("css selector",
↪  "a.ts_menu.ts_man[href='plant.do']")))
plant.click()

#Find device list element
device_list = WebDriverWait(driver,
↪  5).until(EC.presence_of_element_located(("xpath",
↪  "//span[@class='i18n_device_devManage']")))
device_list.click()

time.sleep(2)

#Find storage button
storage = driver.find_element("xpath",
↪  "//span[@class='i18n_device_storage']")
storage.click()
```

```
    time.sleep(2)

    #Find the element with the name NZH3BFA024
    element = driver.find_element("xpath", "//tr[@id='plantStorage_NZH3BFA024']")

    #The element cannot be clicked on by using driver.find_element(). The method
    ↪  below creates a mouse object and double click on the row by using
    ↪  JavaScript
    driver.execute_script("var evt = document.createEvent('MouseEvents');" +
                          "evt.initMouseEvent('dblclick',true,true,window,0,0,"
                          "0,0,0,false,false,false,false,0,null);" +
                          "arguments[0].dispatchEvent(evt);", element)

    #Find the new window with the data and switch frame
    new_window = WebDriverWait(driver,
    ↪  5).until(EC.presence_of_element_located(("id", 'storageHistoryDialog')))
    driver.switch_to.frame(new_window)

    #Find the export button and click
    export = WebDriverWait(driver, 5).until(EC.element_to_be_clickable(("id",
    ↪  'exportStorageHis')))
    export.click()

    time.sleep(2)

    #Close the driver
    driver.close()
```

H Python Script for GUI Frontend: Design in Tkinter

```
import tkinter as tk
import matplotlib.pyplot as plt
from PIL import Image, ImageTk
from datetime import datetime
from download_from_shine import plot_production_demand, download_from_shineDesign

#Parameters for the battery, kettle, iron, drill and inverter
bat_capacity    = 4*200*12  #Wh
bat_n           = 0.9
power_kettle    = 2200      #W
usertime_kettle = 1/6       #h
power_iron      = 2000      #W
usertime_iron   = 0.5       #h
power_drill     = 500       #W
usertime_drill  = 0.5       #h
inv_n           = 0.93
inv_max         = 3500      #W

#Reference for the currently open frame to later close the frame if another
↪  button is clicked
current_frame = None

'''This function includes data processing of the real-time data'''
file_name_production, file_name_soc, soc,  demand, pv = plot_production_demand()
#Button 1
```

```
def show_production_and_demand():

    global current_frame

    #Close the previous current frame is it exists
    if current_frame:
        current_frame.destroy()

    #Get the data from plot_production_demand_platform_2()
    file_name_production, file_name_soc, soc, demand, pv =
    ↪  plot_production_demand()

    #Open and create a Tkinter object for the image
    load_image = Image.open(file_name_production)
    image_object = ImageTk.PhotoImage(load_image)

    #Frame for visualizing the production and demand
    production_frame = tk.Frame(root, bg='#FFFFFF', highlightthickness=0)
    production_frame.pack(expand=True, fill='both', side='right')

    #Update the reference for the current frame
    current_frame = production_frame

    #Give the image a label
    image_label = tk.Label(production_frame, image=image_object,
    ↪  highlightthickness=0, bg='#FFFFFF')
    image_label.image = image_object
    image_label.pack()

    #Calculating the percentage of demand of the max capacity of the inverter
    demand_now      = demand[-1]
    percentage_use  = (demand_now/inv_max)*100 #%

    #Make a Tkinter text object and insert the text
    prod_text = tk.Text(production_frame, font=('Helvetica', (16)), height=1,
    ↪  highlightthickness=0, bg='#FFFFFF')
    prod_text.tag_configure('center', justify='center')
    prod_text.insert(tk.END,
    ↪  'The percentage of used capacity is: {:.2f}%'.format(percentage_use),
    ↪  'center')
    prod_text.pack(pady=10)

    #Make the text non-editable
    prod_text.configure(state='disabled')

    #Button for closing the new window
    close = tk.Button(production_frame, text='Close',
    ↪  command=production_frame.forget, bg='#FFFFFF',
    ↪  highlightbackground='#FFFFFF')
    close.pack()


#Button 2

def show_state_of_charge():

    global current_frame
```

```
    #Close the previous current frame is it exists
    if current_frame:
        current_frame.destroy()

    #Get the data from plot_production_demand_platform_2()
    file_name_production, file_name_soc, soc, demand, pv =
    ↪  plot_production_demand()

    #Open and create a Tkinter object for the image
    load_image = Image.open(file_name_soc)
    image_object = ImageTk.PhotoImage(load_image)

    #Frame for visualizing the production and demand
    soc_frame = tk.Frame(root, bg='#FFFFFF', highlightthickness=0)
    soc_frame.pack(expand=True, fill='both', side='right')

    #Update the reference for the current frame
    current_frame = soc_frame

    #Give the image a label
    image_label = tk.Label(soc_frame, image=image_object, highlightthickness=0,
    ↪  bg='#FFFFFF')
    image_label.image = image_object
    image_label.pack()

    #Find the current level of SoC in percent
    soc_now  = soc[-1]                                  #%

    #Make a Tkinter text object and insert the text
    soc_text = tk.Text(soc_frame, font=('Helvetica', (16)), height=1,
    ↪  highlightthickness=0, bg='#FFFFFF')
    soc_text.tag_configure('center', justify='center')
    soc_text.insert(tk.END,
    ↪  'The level of the battery in percent is: {}%'.format(soc_now), 'center')
    soc_text.pack(pady=10)

    #Make the text non-editable
    soc_text.configure(state='disabled')

    #Button for closing the new window
    close = tk.Button(soc_frame, text='Close', bg='#FFFFFF',
    ↪  command=soc_frame.destroy, highlightbackground='#FFFFFF')
    close.pack(pady=10)


#Button 3, 4 and 5

def high_power_appliances(appliance):

    global current_frame

    #Close the previous current frame is it exists
    if current_frame:
        current_frame.destroy()

    #Get the data from plot_production_demand_platform_2()
```

```
file_name_production, file_name_soc, soc,  demand, pv =
↪  plot_production_demand()

#Find the last tracked demand and soc
demand_now = demand[-1]      #W
soc_now = soc[-1]            #%

#Energy available in the battery
bat_available = bat_capacity * bat_n * soc_now

if appliance == 'iron':
    #The energy of using the iron
    energy_iron = power_iron * usertime_iron #Wh

    if bat_available > energy_iron and demand_now + power_iron < inv_max *
    ↪  inv_n:
        text = 'You can use the iron without any problem right now! \n'
        'The total percent of used capacity including the iron: {:.2f}% '
        .format(((demand_now + power_iron)/inv_max)*100)


    else:
        text =
        ↪  'Sorry, there is not enough capacity for you to use the iron now...'
        'Try again in 15 minutes!'


elif appliance == 'kettle':
    #The energy of using the kettle
    energy_kettle = power_kettle * usertime_kettle #Wh

    if bat_available > energy_kettle and demand_now + power_kettle < inv_max
    ↪  * inv_n:
        text = 'You can use the kettle without any problem right now! \n'
        'The total percent of used capacity including the kettle: {:.2f}% '
        .format(((demand_now + power_kettle)/inv_max)*100)

    else:
        text =
        ↪  'Sorry, there is not enough capacity for you to use the kettle now... '
        'Try again in 15 minutes!'


elif appliance == 'drill':
    #The energy of using the kettle
    energy_drill = power_drill * usertime_drill #Wh

    if bat_available > energy_drill and demand_now + power_drill < inv_max *
    ↪  inv_n:
        text = 'You can use the drill without any problem right now! \n'
        'The total percent of used capacity including the drill: {:.2f}% '
        .format(((demand_now + power_drill)/inv_max)*100)

    else:
        text =
        ↪  'Sorry, there is not enough capacity for you to use the drill now... '
        'Try again in 15 minutes!'
```

```
    #Making the frame and the text
    text_frame = tk.Frame(root, bg='#FFFFFF', highlightthickness=0)
    text_frame.pack(side='right', expand=True, fill='both')

    appliance_text = tk.Text(text_frame, font=('Helvetica', (16)), height = 2,
    ↪  bg='#FFFFFF', highlightthickness=0)
    appliance_text.tag_configure('center', justify='center')
    appliance_text.insert(tk.END, '{}'.format(text), 'center')
    appliance_text.pack(pady=10)

    #Make the text non-editable
    appliance_text.configure(state='disabled')

    #Update the reference for the current frame
    current_frame = text_frame

    #Button for closing the new window
    close = tk.Button(text_frame, text='Close', command=text_frame.destroy,
    ↪  bg='#FFFFFF', highlightbackground='#FFFFFF')
    close.pack(pady=10)


#Button 6

def show_trends():

    global current_frame

    #Close the previous current frame is it exists
    if current_frame:
        current_frame.destroy()

    text = 'This is the trends of the period: '

    #Making the frame and the text
    text_frame = tk.Frame(root, bg='#FFFFFF', highlightthickness=0)
    text_frame.pack(side='right', expand=True, fill='both')



    trend_text = tk.Text(text_frame, font=('Helvetica', (16)), height = 2,
    ↪  bg='#FFFFFF', highlightthickness=0)
    trend_text.tag_configure('center', justify='center')
    trend_text.insert(tk.END, '{}'.format(text), 'center')
    trend_text.pack(pady=10)

    #Make the text non-editable
    trend_text.configure(state='disabled')

    #Update the reference for the current frame
    current_frame = text_frame

    #Button for closing the new window
    close = tk.Button(text_frame, text='Close', command=text_frame.destroy,
    ↪  bg='#FFFFFF', highlightbackground='#FFFFFF')
    close.pack(pady=10)
```

```
#Turn off plots in console
plt.ioff()

#Download real time data each time the code is running
download_from_shineDesign()


#Creating the main window
root = tk.Tk()
root.title("ECO MOYO GUI")

#Background color
#root.configure(bg='#F0FFF0')  #Green
root.configure(bg='#FFFFFF')   #White

#Set font
font_title  = ('Helvetica', 36, 'bold')
font_date   = ('Helvetica', 14)
font_button = ('Helvetica', 20)

#Label for the title
label_title = tk.Label(root, text='Eco Moyo GUI', font=font_title, bg='#FFFFFF',
↪  fg='#669900')
label_title.pack(pady=15)

#Current date of today
date =  datetime.today().strftime('%B %d, %Y')
date = 'July 7th, 2023'

#Label for the date
label_date = tk.Label(root, text=date, font=font_date, bg='#FFFFFF',
↪  fg='#669900')
label_date.pack()

#Make canvas
canvas = tk.Canvas(root, width=600, height=500, highlightthickness=0,
↪  bg='#FFFFFF')
canvas.pack()

#Logo
load_logo = Image.open('GUI/logo.jpg')
logo = ImageTk.PhotoImage(load_logo)

label_logo = tk.Label(root, image=logo, bg='#FFFFFF')
label_logo.place(relx=0.9, rely=0.0, anchor='ne')

#Making button 1 for production and demand
button_1 = tk.Button(canvas, text='Solar production and demand of today',
↪  font=font_button, command=show_production_and_demand,
↪  highlightbackground='#FFFFFF')
#Size and place of the button
button_1.config(padx=20, pady=10)
button_1.place(relx=0.5, rely=0.15, anchor='center')

#Making button 2 for state of charge
button_2 = tk.Button(canvas, text='Show the battery capacity', font=font_button,
↪  command=show_state_of_charge, highlightbackground='#FFFFFF')
```

```
#Size and place of the button
button_2.config(padx=20, pady=10)
button_2.place(relx=0.5, rely=0.30, anchor='center')

#Making button 3 for iron
button_3 = tk.Button(canvas, text='Usage of iron', font=font_button,
↪  command=lambda: high_power_appliances('iron'), highlightbackground='#FFFFFF')
#Size and place of the button
button_3.config(padx=20, pady=10)
button_3.place(relx=0.5, rely=0.45, anchor='center')

#Making button 4 for kettle
button_4 = tk.Button(canvas, text='Usage of kettle', font=font_button,
↪  command=lambda: high_power_appliances('kettle'),
↪  highlightbackground='#FFFFFF')
#Size and place of the button
button_4.config(padx=20, pady=10)
button_4.place(relx=0.5, rely=0.6, anchor='center')

#Making button 5 for drill
button_5 = tk.Button(canvas, text='Usage of drill', font=font_button,
↪  command=lambda: high_power_appliances('drill'),
↪  highlightbackground='#FFFFFF')
#Size and place of the button
button_5.config(padx=20, pady=10)
button_5.place(relx=0.5, rely=0.75, anchor='center')

#Making button 6 for theoretic trends for the period
button_6 = tk.Button(canvas, text='Theoretical trends and consumption behavior',
↪  font=font_button, command=show_trends, highlightbackground='#FFFFFF')
#Size and place of the button
button_6.config(padx=20, pady=10)
button_6.place(relx=0.5, rely=0.9, anchor='center')


root.mainloop()
```

NTNU
Norwegian University of
Science and Technology

Solar Energy Without Borders
Solenergi Uten Grenser